UCSF

UC San Francisco Electronic Theses and Dissertations

Title

Biochemical characterization of 4.5S RNA's role in the Ffh-FtsY GTPase cycle

Permalink

https://escholarship.org/uc/item/0xz5q56d

Author

Peluso, Paul S

Publication Date

2001

Peer reviewed|Thesis/dissertation

eScholarship.org Powered by the California Digital Library
University of California

Biochemical Characterization of 4.5S RNA's Role in the Ffh-FtsY GTPase Cycle

by

Paul S. Peluso

DISSERTATION

Submitted in partial satisfaction of the requirements for the degree of

DOCTOR OF PHILOSOPHY

in

Biochemistry

in the

GRADUATE DIVISION

of the

UNIVERSITY OF CALIFORNIA SAN FRANCISCO

[redacted]

Date University Librarian

Degree Conferred: ....

This thesis is dedicated to my parents, John and Patricia Peluso.

Acknowledgements

There are so many people to thank, especially when you have been a graduate student for as long as I have. Unfortunately the space and time will never permit me to do proper justice to this task. At the outset, I will have to apologize if there is anyone that I have forgotten to mention.

First I would like to thank my advisor, Peter Walter, for a lively tenure in his lab. I thank him for giving me a great deal of freedom to explore the areas which became the bulk of this thesis work. I am especially grateful for his patience and uncanny ability not to take things "too personally" during the entire time and our many discussions. The fact that we could have a terrible argument on one day and he could come back to me with the keys to his house for two weeks of house-sitting is a true testament to this. Above all, I will try to never lose sight of what you always place the most emphasis on – to always think about the biological importance of the questions at hand. I should also take this time to say a word of thanks to your family, Patricia, Gabbi, and Sylvia for many wonderful times outside of the lab.

I was fortunate to have two other surrogate advisors from which I learned a great deal during the course of my graduate work. Art Johnson and Dan Herschlag were very helpful sources from which I learned a fair amount

concerning fluorescence spectroscopy and enzyme kinetics, respectively. I feel very fortunate to have been able to work closely with both of them. I would also like to thank Art's lab for putting on a "Spectroscopy 101" clinic for me during the early stages of the fluorescence work. To Dan, I can put it best by saying that you bring the concept of a discussion to a whole new level.

In addition to Peter and Dan, I would also like to thank at this time the other members of my thesis committee, Carol Gross, Tim Mitchison, and Alan Frankel. To all five individuals, I would like to apologize for the "marathon sessions" to which I have subjected you all. I must admit the 3+ hour meetings were perhaps a bit too much. I have really appreciated all for your patience, input, enthusiasm, and guidance especially in bringing it all together at the end. I would also like to thank Carol and Alan for their moral support after one meeting in particular where I was left a little "frazzled".

When I started working in Peter's lab, we were initially in HSE9 where we shared space with Bruce Albert's, Marc Kirschner's and John Watson's labs. I will always remember this time fondly because of all the wonderful, intense, fun-loving people who worked together in this space. From the other labs I would like to thank Dave, Elly, Steve, Pascal, Andre, Ray, Michele, Becky, Yixian, Chris, Karen, Jack, and Raffi for many wonderful discussions concerning science, sports, opera, food, and life in general.

I was initially in the "outcasts" room where members of both the Walter and Kirschner labs shared benches. I consider myself very lucky to have been able to share a bay with two very wonderful people, Dieter Zopf and Tina Lee. Dieter, you are an amazing biochemist. You taught me a lot concerning SRP and protein biochemistry, not to mention dealing with adversity. Tina, you were always willing to hear about my "footprinting" results, even when the data looked really bad and I wasn't explaining it with much coherence. I would also like to thank you for getting me hooked onto to Miles Davis' music and Hama-Ko sushi.

Having been a member of the Walter lab for almost ten years, you inevitably meet a lot of people. It would be best to approach this from a chronological fashion. When I first started in the lab, there were already many "Walter lab veterans" who made those first couple of years very special. I would especially like to thank Jodi Nunari for being a great colleague, teacher, and above all a great friend. When I was at my typical low points she would always be there to whip up the excitement. Of course there was also Dieter, Harris (the "slickster"), Josh, Byron, Steve, Doug, Davis, Jeff, Caroline, Kent, Sarah, Chi, and Maho. I have enjoyed sharing scientific discussions, breaking bread, and sharing a beer or two with all of you. Josh you were like a big brother in those early days. I will never forget those crazy late nights of beer drinking and cigar smoking. I would especially like to thank Davis for many interesting scientifc discussions and for introducing me to some truly crazy Chinese delicacies. To Kent, Caroline, and Chi, I would just like to take the time to thank you all for your wonderful friendship and moral support over the years, not to mention the many wonderful late night dinners we shared.

In the recent years I have been fortunate to have shared a bay with Chris, Isabella, Carmela, and Sarah. What can I say, you all made the working environment an interesting place. I enjoyed the many discussions, bizarre topics, and crazy joking shared among you all.

Two other wonderful people I would like to take this time to thank are MaryVic and Teresa. You both are constantly doing many wonderful things for us in the Walter lab. I would also like to thank you both for always having the ability to make me stop and find appreciation for the good things in life when my mood would have otherwise directed me to do the exact opposite.

I have had the opportunity to work closely with many wonderful colleagues in the lab. Doug, Bob, and Ted were all excellent scientists to work alongside as we were trying to figure out how SRP54 and the receptor did their thing. Doug thank you for giving me a better understanding of what "RTFM" is really all about. I would also like to thank Sho-ou for her patience and help with the last phase of the work.

Finally, I must say a very special note of thanks to Silke for all of the wonderful work you have done with me on the Ffh project. You are a great colleague, protein biochemist, beer-drinking force to be reckoned with, and above all a wonderful friend. I will try and make it up to the city for many more sushi meals in the future, for certain.

There are many wonderful people at UCSF who enable things to proceed very smoothly. I would like to thank Sue, Teresa, Rachel, and Julianne for taking care of all those "little things" which aren't so little when you stop and think about it.

I have made many friends here at UCSF. I feel like I have adopted a whole new family here in the Bay Area over the last 10 years. Wallace, Arshad, Kayvan, Andy, Ramon, Hernan, Cara, and Kevin have all been like brothers since we all started grad school together those many years ago. I will never forget those late nights of ad hoc pasta dinners and bridge playing. Andy you redefined the meaning of "counting cards" for me. Wallace, what can I say, you are one amazing guy in terms of your passion for all that is important to you, namely things like science, food, books, and music. I hope you and Jennifer always enjoy life to the fullest. I will never forget all those fun times we had in SF. The same holds for you Arshad. You and Karen were always there to share a laugh, a movie and a meal, not necessarily in that order. And Karen, I must not forget to especially thank you for helping me prepare for my orals by sitting and listening to numerous reiterations of my introduction. My exam committee should also be thanking you, come to think of it. In the final years of grad school, I was lucky to be sharing an apartment complex with Cara, Hernan, Andy, and Kayvan. Cara and Hernan, you were both wonderful roomates. Meanwhile, I would like to thank Kayvan for putting up with me much the same way Sienfeld had to deal with Kramer, especially my erratic late night antics in the last year.

I have been fortunate to interact with many various circles of friends here at UCSF. Foremost, I would like to thank Heather, Kathleen, Alan, and Jim for many fun filled evenings of food, movies and card games. Alan, you always were a fun opponent with whom to debate the merits of modern atonal music. I will one day get you hooked on the music of Berio and Varese. Heather and Kathleen, you have been wonderful sources of encouragement over these many years. The many Thanksgiving dinners will always be fond memories for me. I also would like to thank Jen, Maki, Javier, Tom, and Mike for many wonderful sushi outings and Iron Chef watching. Maki you have been a very dear friend over these past years and I have come to feel as if you are a sister to me. Thank you for always putting up with my crazy antics.

From the move to the tenth floor, I was able to meet many wonderful people from the Mitchison and Vale labs. I would especially like to take the time to thank Jim H., Cindy, Pete, Nora, Bernice, Sarita, Mimi, and Ann for those many coffee/smoking/record buying/food breaks which arise over the space of 5 some years. And to members of the Agard lab: Shiela, Alan, and Erin for providing me with those precious moments of "blowing off steam". Jim Hartman, Sarah Mutka, and Martha Arnaud have been a great group to commiserate with over the ups and downs of grad school. Many a "coffee" run has been useful for providing a better perspective on life. Jim, I will never forget the "black and tan" made with Guiness and "Bud Lite". Mimi, what can I say, you have always been there to shock a jolt of life into me at any given moment. You and Joel are two very wonderful people who I will never forget from the UCSF experience.

This last year of finishing up has been a crazy one while juggling work in a new place and trying to write up at the same time. I would like to thank Steffen for his patience, which I am sure has been stretched to its maximum. I would also like to thank Maanasa and Duc for putting up with my sometimes "frazzled" nature. You guys have been a joy to work with over these last two years. And lastly, to all my friends at Zyomyx, you have made the last year of finishing up a very exciting one both in and out of the lab.

I would like to thank two very wonderful people whom I have had the pleasure to become friends with over the last seven years. There is this small sushi bar near the corner of Cole and Carl called Hama-Ko Sushi which is run by

Tetsuo and Junko Kashiyama. In addition to having the best sushi in town, I feel like this place is almost a second home to me.

I would like to finally take some time to thank my family for their support over the years. My mom and dad have always supported whatever I have set out to do throughout my life. Their love, understanding, support, and encouragement has always been an inspiration to me, especially during those bad times. The hardest thing about living in the Bay Area is the distance it places between us. I miss you very much and always look forward to the times when I can fly back east for a visit. To my brother John and his wife Diane, I would like to thank you for your constant support and encouragement. You two have always been there to lift my spirits when I was at my low points. John, you can always find a way to give me a new perspective on a bad situation. Thanks for your common sense. Diane, what can I say, your cookies and cakes were always a welcome surprise in the Walter lab. You became quite popular with everyone here. I hope I can spend more time with you guys as well as Noel and Jack in the future. That way the kids will get to no me as more than the crazy uncle from the bay area.

AMERICAN
ASSOCIATION FOR THE
ADVANCEMENT OF
SCIENCE

Permissions Letter

Ref # 01-2121

DATE: Monday, October 01, 2001

TO: Paul Peluso
University of California
Department of Biochemistry & Biophysics
San Francisco, CA 94143

FROM: Karen Lentz, Permissions Assistant
RE: Your request for permission dated 09/28/01

Regarding your request, we are pleased to grant you non-exclusive, non-transferable permission, but limited to print and microform formats only, and provided that you meet the criteria below. Such permission is for one-time use and therefore does not include permission for future editions, revisions, additional printings, updates, ancillaries, customized forms, any electronic forms, braille editions, translations, or promotional pieces. We must be contacted for permission each time such use is planned. This permission does not apply to figures / artwork that are credited to non-AAAS sources. This permission does not include the right to modify AAAS material.

Print the required copyright credit line on the first page that the material appears: "Reprinted (abstracted/excerpted) with permission from [FULL REFERENCE CITATION]. Copyright [YEAR] American Association for the Advancement of Science." Insert the appropriate information in place of the capitalized words.

Permission is limited to the number of copies specified in your request or your first printing.

AAAS must publish the full paper prior to use of any text.

AAAS does not supply photos or artwork. Use of the AAAS material must not imply any endorsement by the American Association for the Advancement of Science. This permission is not valid for the use of the AAAS and/or SCIENCE logos.

Thank you for writing. If you have any questions please call me at (202) 326-6765 or write to me via fax at (202) 682-0816. For international calls, +1 is the country code for the United States.

Headquarters: 1200 New York Avenue NW, Washington, DC 20005 USA

Permission is valid for use of the following AAAS content only:
Peluso, et al., Role of 4.5S RNA in Assembly of the Bacterial Signal Recognition Particle with Its Receptor. Science 288, 1640 (2000).

ABSTRACT

Biochemical Characterization of 4.5S RNA's Role in the Ffh-FtsY GTPase Cycle

Paul S. Peluso

The targeting of proteins to the endoplasmic reticulum by the signal recognition particle (SRP) and its receptor is an evolutionarily conserved process. In *Escherichia coli,* this process is mediated by the Ffh/4.5S RNA ribonucleoprotein complex and the FtsY protein. Ffh and FtsY form a specific subclass of GTPase proteins. These novel GTPases form a complex during the protein targeting cycle wherein both proteins not only hydrolyze GTP but also function to stimulate each other's GTPase activity. While much has been learned concerning the functional roles of these two GTPases in the targeting cycle, the exact role that 4.5S RNA plays had been relatively unclear at the start of this thesis work. In Chapter 3, a fluorescence assay is described which enabled us to quantify the interaction between Ffh and FtsY. Using this assay, we identified a novel role for 4.5S RNA with respect to the interaction between Ffh and FtsY. 4.5S RNA, as will be further described, acts in a catalytic fashion, to enhance both the assembly and disassembly of the Ffh-FtsY complex. Also, from an in depth enzymatic characterization of the GTPase cycle, as described in Chapter 4, we identified an additional step in the enzymatic pathway where 4.5S RNA appears to be acting. From these studies we postulate that 4.5S RNA can somehow act to enhance the rate at which conformational changes occur in the Ffh-FtsY complex which have a direct impact on the catalytic activity of the complex. Taken together, this data suggests that 4.5S RNA may function in some manner to

control the GTPase activity of the complex perhaps in conjunction with other effector molecules which take part in the targeting reaction. Finally, in addition to identifying a mechanistic role for 4.5S RNA, this thesis work has set up a biochemical framework for future mechanistic studies of the Ffh-FtsY GTPase cycle.

Peter Walter 10/22/01

Table of Contents

Chapter 1

Introduction..1

Chapter 2

Chemical Probing of 4.5S RNA - Protein Interactions................59

Chapter 3

Role of 4.5S RNA in Assembly of the Bacterial
Signal Recognition Particle with its Receptor..........................100

Chapter 4

Kinetics of the Ffh/4.5S RNP•FtsY GTPase Complex:
The Role of the 4.5S RNA..120

Appendix A

Fluorescence Studies to Monitor Ffh/4.5S RNP
Interactions With the Ribosome...173

Appendix B

Fluorescence Studies Probing Nucleotide Binding
And Release by Ffh and FtsY...193

List of Figure

Chapter 1

Figure 1-1..44

Figure 1-2..46

Figure 1-3..48

Figure 1-4..50

Figure 1-5..52

Figure 1-6..54

Figure 1-7..56

Figure 1-8..58

Chapter 2

Figure 2-1..85

Figure 2-2..87

Figure 2-3..89

Figure 2-4..91

Figure 2-5..93

Figure 2-6..95

Figure 2-7..97

Figure 2-8..99

Chapter 3

Figure 3-1..116
Figure 3-2..117
Figure 3-3..118
Figure 3-4..119

Chapter 4

Figure 4-1..158
Figure 4-2..160
Figure 4-3..162
Figure 4-4..164
Figure 4-5..166
Figure 4-6..168
Figure 4-7..170
Figure 4-8..172

Appendix A

Figure A-1..184
Figure A-2..186
Figure A-3..188
Figure A-4..190
Figure A-5..192

Appendix B

Figure B-1..207
Figure B-2..209
Figure B-3..211
Figure B-4..213
Figure B-5..215
Figure B-6..217
Figure B-7..219

Chapter 1. Introduction

Cells maintain organized compartments and target proteins to the ER via N-terminal signal sequences

Cells, possessing hundreds of proteins with specific functions, need to maintain a high degree of organization. Cells achieve this by having specialized compartments, called organelles, which are separated by phospholipid membranes. Within these organelles, proteins perform their specialized activities. Cells, therefore, require mechanisms to sort proteins, which are synthesized by ribosomes in the cytoplasm, to their correct location whether it be a specific organelle, the plasma membrane, or the extracellular space. One major cellular pathway for the sorting and/or secretion of many proteins begins with the targeting of these proteins to the endoplasmic recticulum, or ER.

The targeting of proteins to the ER presents a number of challenges for the cell. First, specificity must be maintained to ensure that only the correct proteins are targeted to the ER. Secondly, since proteins typically fold into highly charged and stable structures, their passage through the hydrophobic ER membrane would seem especially difficult. Cells have evolved targeting mechanisms for dealing with these inherent problems.

In the early 1970s, Blobel and Sabatini hypothesized that proteins were localized to the ER via a specific amino acid sequence element within the translating nascent chain (Blobel and Sabatini, 1971).Taking their cue from immulnolgists' findings that the *in vitro* synthesis of the IgG light chain resulted a larger form of the protein possessing a novel N-terminal extension (Brownlee et al., 1972; Milstein et al., 1972; Swan et al., 1972), Blobel and Dobberstein went on to support this model using cell free translation systems (Blobel and Dobberstein, 1975). Since this earlier work our understanding of the molecular bases of signal sequence mediated targeting to the ER has advanced enormously (Walter, 1996).

ER targeting sequences are perhaps best characterized by their overall hydrophobicity. While signal sequences are rather degenerate with respect to their length and amino acid composition, all typically contain a hydrophobic core of approximately 10 amino acids (von Heijne, 1983; von Heijne, 1985). The other hallmark feature of signal sequences is the presence of positively charged amino acids at the N-terminus (von Heijne and Abrahmsen, 1989). In order to utilize these signal sequences, cells need machinery to recognize them and mediate the targeting process . This machinery was identified in the signal recognition particle, or SRP (Walter and Blobel, 1981a; Walter and Blobel, 1981b; Walter et al., 1981).

SRP and its receptor mediate signal sequence dependent protein targeting

Mammalian SRP is a cytoplasmic complex consisting of 6 proteins and an RNA molecule (Walter and Blobel, 1982), which is responsible for targeting proteins to the ER (Walter and Johnson, 1994). Using wheat germ translational extracts, and membranes derived from dog pancreatic tissue, SRP was purified as the targeting activity that specifically recognizes ribosomes bearing nascent chains which have N-terminal signal sequence (Walter and Blobel, 1980). Upon forming a complex with the ribosome nascent chain, SRP causes an arrest in translation allowing time for the complex to be targeted to the membrane (Walter and Blobel, 1981a; Walter and Blobel, 1981b). At the membrane, the translational arrest is relieved and co-translational translocation of proteins through the ER membrane ensues (Walter and Blobel, 1981b).

As shown in Figure 1, mammalian SRP consists of a 317 nucleotide RNA (the SRP RNA) (Walter and Blobel, 1982) and 6 protein components designated by their molecular masses (Walter et al., 1981). The ability to disassemble and reconstitute SRP from purified components facilitated the dissection of SRP's various activities (Walter and Blobel, 1983). By selective NEM treatment of the several of the protein components within the particle, several of the subunits could be assigned a specific activities (Siegel and Walter, 1988b). The SRP54 component was found to mediate recognition of the ribosome-nascent chain complex while the SRP68 and SRP72 subunits were shown to facilitate protein translocation at the membrane by some as yet unknown mechanism. By treatment of SRP with a specific nuclease, the removal of a subdomain containing a portion of SRP RNA complexed with SRP9 and SRP14 led to inactivation of the SRP's translational arrest activity (Siegel and Walter, 1986). Moreover, addition of pure SRP9 and SRP14 proteins could not restore the activity (Siegel and Walter, 1986) suggesting that the missing RNA element was also required for translational arrest. SRP19 was found to assist the assembly of SRP54 into the particle (Lingelbach et al., 1988).The SRP RNA, meanwhile, provided a scaffold with 4 distinct structural domains (designated by Roman numerals I-IV in Figure 1) to which each of the proteins could be mapped (Siegel and Walter, 1988a).

A receptor for SRP was isolated from membranes through affinity chromatography using an SRP-linked matrix (Gilmore et al., 1982a; Gilmore et al., 1982b; Meyer et al., 1982). The SRP receptor consists of two subunits, designated SRα and SRβ, which form a tight heterodimeric complex (Gilmore et al., 1982a; Gilmore et al., 1982b). SRβ possesses a transmembrane domain and displays biochemical properties that are consistent with it being an integral membrane protein (Lauffer et al., 1985; Miller et al., 1995; Tajima et al., 1986). SRα, on the other hand, is peripherally associated with the membrane, presumably through its interaction with SRβ (Lauffer et al., 1985).

The SEC61 complex was later shown by genetic and biochemical studies to provide the channel through which the nascent chain translocates across the ER membrane (Deshaies and Schekman, 1989; Deshaies and Schekman, 1990; Sanders et al., 1992). This complex directly interacts with the ribosome as evidenced from biochemical studies and EM visualization (Beckmann et al., 1997; Kalies et al., 1994). The translocon provides an aqueous channel through which proteins pass into the ER. The acqueous properties of this channel has been elegantly demonstrated by electro-physiological and fluorescence spectroscopic techniques (Crowley et al., 1994; Crowley et al., 1993; Simon and Blobel, 1991; Simon et al., 1989).

The SRP targeting pathway as depicted in Figure 2, therefore, provides solutions to the inherent problems associated with protein targeting. SRP imparts specificity to the process by only recognizing the correct cytoplasmic ribosome-nascent chain complexes that possess signal sequences. SRP's ability to arrest translation by the ribosome prevents the growing nascent chain from becoming too long to the point where it folds into a stable structure which would be unable to pass through the SEC61 complex's channel. The subsequent co-translational insertion of the proteins through the aqueous interior of the SEC61 complex handles the problem of getting charged proteins across the hydrophobic membrane.

The SRP targeting pathway is evolutionarily conserved

The SRP-mediated protein-targeting pathway is evolutionarily conserved from mammalian to prokaryotic cells (Luirink and Dobberstein, 1994; Walter, 1996; Walter and Johnson, 1994). From the cloned sequences of SRP54 and SRα, a simpler SRP system was identified in *E. coli*. Homologues for the SRP54 and SRα proteins were identified in Ffh and FtsY, respectively (Bernstein et al., 1989). As shown in Figure 3, the *E. coli* 4.5S RNA was observed to share homology with the domain IV of the mammalian SRP RNA (Poritz et al., 1988).

Shortly after this simpler *E. coli* SRP system was identified via the observed homologies, subsequent genetic and biochemical studies validated the existence of this *E. coli* SRP pathway. Ffh and 4.5S RNA were found tightly bound together in a complex as would be expected for an SRP homologue (Poritz et al., 1990). In addition, genetic disruptions for each of the three genes resulted in growth defects with impaired protein secretory activity (Luirink et al., 1994; Phillips and Silhavy, 1992; Ribes et al., 1990; Seluanov and Bibi, 1997). Moreover, *in vitro* and *in vivo* studies have directly demonstrated that Ffh/4.5S RNP and FtsY mediated protein targeting to membranes (de Gier et al., 1996; Macfarlane and Muller, 1995; Powers and Walter, 1997; Valent et al., 1995; Valent et al., 1998). Even more recently bacterial geneticists have isolated alleles of 4.5SRNA in genetic screens that utilize an integral membrane protein substrate which had not been previously used (Tian et al., 2000).

The Ffh/4.5S RNP and FtsY components became an ideal model system for studying the biochemical properties of the SRP-SRP receptor interaction. When the work in this thesis was begun, we hoped to take advantage of the obvious benefits offered by the *E. coli* system. All of the components, both wild type and mutant forms, can be over-expressed in *E. coli* and readily purified in large quantities. We expected Ffh and FtsY to serve as a model biochemical system for understanding the SRP54-SRα interaction .

The modular domain architecture of SRP54/Ffh and SRα/FtsY make them ideal molecular matchmakers

From their amino acid sequences, both SRP54/Ffh and SRα/FtsY can be schematically depicted as each having three discrete domains. As shown in

Figure 4, both proteins share common N and G domains. However, each protein also possesses its own unique domain. SRP54/Ffh possess a C-terminal M-domain, which is so named because of its atypical abundance in methionine residues (Bernstein et al., 1989). Meanwhile, SRα/FtsY contains a unique N-terminal extension which has been designated the A-domain. This name reflects the fact that this domain is highly acidic in its amino acid composition. As will be described in more detail below, SRP54/Ffh and SRα/FtsY use these specialized domains in order to interact with their respective cargo molecules, namely the ribosome nascent chain complexes and the protein translocon, respectively. In light of this domain architecture, SRP54/Ffh and SRα/FtsY have come to be viewed as "molecular matchmakers" (Walter, 1996).

SRP54/Ffh and SRα/FtsY share identical NG-domains

SRP54/Ffh and SRα/FtsY possess similar GTPase, or G-domains, which define them as a unique sub-family of GTPases. Structurally, the NG-domains from Ffh and FtsY were found have the same overall fold (Freymann et al., 1997; Montoya et al., 1997). The N-domain portion was found to be a 4 α-helix bundle for both proteins. Moreover, both GTPases possess a unique insertion element specific to this GTPase sub-class. This element, which consists of 2 α-helices and 2 β –strands, has been termed the insertion box domain, or IBD (Moser et al., 1997). From nucleotide binding, which employed fluorescent substrates, the IBD was suggested to mediate the atypical fast release of nucleotides which is unique to this class of GTPases (Montoya et al., 1997; Moser et al., 1997). Comparisons of crystal structures of nucleotide-free and GDP-bound forms of Ffh further supported this notion (Freymann et al., 1997; Freymann et al., 1999).

Unlike the classical Ras-like GTPases, SRP54/Ffh and SRα/FtsY have relatively weak affinities for nucleotides and can be isolated in their nucleotide-free states (Freymann et al., 1997; Montoya et al., 1997). Due to these weak affinities, a UV-crosslinking approach was initially employed in order to estimate the binding affinities of these proteins for nucleotides (Miller et al., 1994; Miller et al., 1993). As will be detailed in Appendix 1, we and others have employed fluorescent nucleotide analogues and spectroscopic techniques in order to quantify the kinetics of nucleotide binding and release for Ffh and FtsY (Jagath et al., 1998; Moser et al., 1997). With these experiments we have been able to directly quantify the rapid rates with which these proteins release GTP and GDP. In the crystal structures of the nucleotide-free forms of the two NG-domains, residues within this IBD were found to form salt bridges with residues that would normally be in contact with the nucleotide (Freymann et al., 1997; Freymann et al., 1999; Montoya et al., 1997). These salt bridges would stabilize the empty state and presumably be the driving force for nucleotide release.

Perhaps the most distinguishing feature of this GTPase subfamily, however, is the fact that both proteins form a complex with unique GTPase properties. Both SRP54/Ffh and SRα/FtsY function both as GTPases and GTPase Activating Proteins, or GAPs within the SRP54•SRα or Ffh•FtsY complexes. This was originally observed from biochemical studies focusing on the SRP54/SRP RNA^{GTP}•SRα^{GTP}complex. In these studies, the complex exhibited higher GTPase activity than either component alone, suggesting that at least one of the components was serving as a GAP protein (Miller et al., 1993). This stimulation of the GTPase activity was subsequently observed for the *E. coli* homologues as well (Miller et al., 1994).

Using the *E. coli* components as a model system, a better detailed understanding of the unique enzymatic properties of this complex has been obtained. Studies with the Ffh/4.5S $\mathrm{RNP}^{\mathrm{GTP}} \bullet \mathrm{FtsY}^{\mathrm{GTP}}$ complex have been able to assign GTPase and GAP activities to both proteins within the complex. A mutant form of FtsY with specificity to XTP was utilized to distinguish each active site within the complex (Powers and Walter, 1995). In these studies, both proteins were demonstrated to hydrolyze substrate after formation of the complex. Moreover, each protein acts as a GAP for the other when in its nucleotide triphosphate state. An inherent biochemical symmetry is therefore found within this novel complex of two GTPases.

SRα/FtsY has a unique A-domain for membrane interactions

The N-terminal acidic domain of FtsY is crucial for its interaction with the membrane. Deletion of the first 47 amino acids of the A-domain, yields an FtsY which is unable to associate with the membrane and promote *in vitro* protein targeting. Yet, this truncated FtsY can hydrolyze GTP and GAP Ffh to a similar extent as the full length protein (Powers and Walter, 1997). Genetic studies have also demonstrated a membrane association role for the A-domain. A generic transmembrane motif can be substituted for this acidic domain resulting in a fully functional mutant FtsY protein (Zelazny et al., 1997). SRα, as shown in Figure 4 possesses a larger A-domain which most likely reflects the fact that SRα also must interact with an SRβ subunit (Young et al., 1995).

SRP54/Ffh possesses an M-domain which specifically interacts with SRP RNA and signal sequences

The M-domain of SRP54 provides the link to both signal sequences and the SRP RNA as suggested originally by its amino acid sequence composition. The M-domain was predicted to contain distinct amphipathec α-helices that possesses an unusually large number of methionine residues. These helices were suggested to form a hydrophobic pocket that is lined with "methionine bristles" (Bernstein et al., 1989). It was reasoned that the unbranched and highly flexible methionines would be able to accommodate the variety of signal sequences found in nature (von Heijne, 1983; von Heijne, 1985). Two of the α-helices were found to possess a large net positive charge and possess a number of highly conserved arginine residues. These helices seemed the best candidate for the SRP RNA binding domain (Römisch et al., 1989).

Biochemical studies supported the idea that the M-domain bound specifically to both the signal sequences and the SRP RNA. Photo-crosslinking studies supported the idea that the M-domain was interacting directly with the signal sequence (Lütcke et al., 1992; Zopf et al., 1990). In addition, proteolytically generated M-domain can be reconstituted into SRP in place of full length SRP54. Although unable to mediate targeting, this reconstituted SRP can still interact specifically with ribosomes that are bearing signal sequences (Zopf et al., 1993). Lastly, an extensive deletion analysis using the *Bacillus subtilisis* Ffh protein demonstrated the predicted helix-turn-helix motif within the M-domain to be the RNA binding domain (Kurita et al., 1996). In fact, several of the conserved arginine residues within this motif were found to be required for RNA binding (Kurita et al., 1996).

X-ray crystallographic studies have provided us with structures which are consistent with these functional models (Keenan et al., 1998). In this crystal structure, the predicted amphipathic α-helices form a hydrophobic pocket which is lined with many of the conserved methionine residues. In addition, a large loop structure was found adjacent to the binding pocket which could pack over the signal sequence like a clamp. On the other side of the M-domain was found a helix-turn-helix domain displaying a highly positively charged surface that would make a suitable RNA binding site.

This RNA binding site has been recently confirmed by a crystal structure of the M-domain/domain IV complex (Batey et al., 2000). In this structure, extensive contacts between the helix-turn-helix and the conserved bases of domain IV are shown to contribute to the specific binding between Ffh and 4.5S RNA. Moreover, the structure nicely validates data from mutagenesis and chemical footprinting experiments, which identified specific amino acids and RNA bases as being critical in the formation of the Ffh/4.5S RNP (Kurita et al., 1996; Lentzen et al., 1996; Wood et al., 1992).

The most intriguing feature of this structure is the close proximity of the RNA to the signal sequence binding site (Batey et al., 2000). Perhaps the RNA provides a portion of the signal sequence binding face within SRP. The negative charges from the RNA's phosphate backbone would complement the conserved positive charges of the signal sequence. This opens the possibility that the RNA might directly interact with the signal sequence and/or serve as a sensor for signal sequence occupancy within the M-domain (Walter et al., 2000). A crystal structure of this complex with a bound signal sequence peptide will be required in order to validate these predictions.

Domain-Domain Cross-talk occurs within both SRP54/Ffh and SRα/FtsY

As one might expect, the domains of SRP54/Ffh and SRα/FtsY are not independently acting modules which have no direct influence upon each other. Rather, there is biochemical communication between the respective domains within each protein. Many examples of domain cross-talk have been observed which suggest that the M-domain and A-domain cooperate with the NG-domains to regulate function within Ffh and FtsY respectively.

Within SRP54/Ffh, signal sequence occupancy in the M-domain and nucleotide binding by the NG-domains are thought to influence each other.

Originally, NEM-alkylation of the cysteine(s) within the NG-domain of SRP54 interfered with SRP54's ability to associate with ribosome-nascent chain complexes (Siegel and Walter, 1988b). This was further supported by the observation that specific mutations within the N-domain could impair ribosome nascent chain binding by SRP54 (Newitt and Bernstein, 1997). Conversely, M-domain binding to signal sequences seemed to antagonize the function of the NG-domain. From *in vitro* studies, signal sequence peptides appeared to block GTP cross-linking to Ffh's G-domain and to inhibit hydrolysis of the Ffh-FtsY complex (Miller et al., 1994; Miller et al., 1993). This led to the notion that signal sequence binding stabilized a nucleotide free-state in Ffh.

Nucleotide crosslinking studies in the context of the ribosome-nascent chain complex, however, showed the situation to be more complicated. Ribosome-nascent chain complexes were found to enhance cross-linking of GTP to SRP54 (Bacher et al., 1996). This suggested that SRP54's affinity for GTP was actually enhanced by the ribosome-nascent chain complex. These seemingly contradictory results could reflect differences in SRP54 conformation when it binds to signal sequences in the presence and absence of ribosomes. It is not unreasonable to expect the ribosome to affect the conformational state of SRP54 and influence SRP54's activity.

SRP RNA has also been implicated as playing a role in the cross-talk between the M- and NG-domains. From *in vitro* proteolysis studies, signal sequences were found to destabilize the NG-domain making it more susceptible to proteolysis. Meanwhile, binding of SRP RNA was shown to have an antagonistic effect on this destabilization (Zheng and Gierasch, 1997). This opens further the speculation that SRP RNA somehow plays an active role as a sensor for signal sequence occupancy within the M-domain. This model is further supported by the crystal structure positioning the RNA in close proximity to the putative signal sequence binding pocket (Batey et al., 2000; Walter et al., 2000).

With respect to FtsY , recent evidence has emerged which suggests that the A-domain affects the GTPase activity of FtsY. Biochemical studies have shown that anionic lipids positively affect the GTPase activity of FtsY (de Leeuw et al., 2000). Potential lipid interacting sites within the A-domain have been implicating in mediating this modulatory effect (de Leeuw et al., 2000). This is somewhat surprising in light of the fact that the A-domain can be replaced by a generic transmembrane domain without completely impairing FtsY's role in protein secretion within the cell (Zelazny et al., 1997). Perhaps this modulatory cross-talk is not absolutely required for FtsY function. The functional relevance of this interaction to the SRP targeting pathway awaits further study.

The GTPase domains of SRP and the SRP-receptor play critical roles in protein targeting process

As seen for many important cellular processes, SRP-dependent protein targeting requires GTP as a co-factor (Connolly and Gilmore, 1989; Gilmore, 1988; Hoffman and Gilmore, 1988). SRP54, SRα, and SRβ all contain GTPase domains whose functions are critical to the SRP pathway (Bernstein et al., 1989;

Connolly and Gilmore, 1989; Miller et al., 1995; Römisch et al., 1989). From results obtained using both the eukaryotic and prokaryotic systems, a basic model has been suggested for how GTP is utilized as a co-factor. The SRP54/Ffh and SRα/FtsY GTPases are believed to play a central role in the SRP-mediated targeting process. This notion is supported by several observations. First, SRP reconstituted with an SRP54 that is missing its GTPase domain can interact with ribosome-nascent chain complexes but is unable to facilitate membrane targeting (Zopf et al., 1993). Second, as SRP54 and SRα are the only GTPases maintained in *E. coli*, their interaction must be essential to the SRP pathway (Walter, 1996). The simplest model suggests that the GTP-dependent interaction between SRP54/Ffh and SRα/FtsY directly drives the targeting process and the release of the signal sequence by SRP at the membrane (Connolly and Gilmore, 1989). GTP hydrolysis by the complex subsequently enables recycling of SRP and SRα to promote further targeting rounds within the cell (Connolly et al., 1991). This idea follows directly from *in vitro* mammalian targeting assays wherein the non-hydrolyzable GTP analogue, 5'guanylylimidodiphosphate (GppNHp), was used as a co-factor. In these assays, SRP was capable of mediating only one round of targeting. In the absence of GTP hydrolysis, SRP became stuck at the membrane presumably in a tight complex with the receptor (Connolly et al., 1991).

Because of its fast release rate for nucleotides, the SRP54/Ffh GTPase utilizes a nucleotide loading factor in order to maintain in its GTP-bound state. From the crosslinking studies mentioned before, the ribosome-nascent chain complex is thought to provide this function presumably by slowing down the release rate (Bacher et al., 1996). This would keep SRP54 in its GTP-bound form long enough to interact with SRα and facilitate the targeting process.

From the symmetry seen between SRP54 and SRα one would expect SRα to have its own GTP loading factor. Potentially, a similar GTP loading activity could also exist at the membrane for SRα/FtsY either in the form of membrane lipids (de Leeuw et al., 2000) or some other protein component of the translocation machinery. This, in turn, would keep SRα/FtsY in a prolonged GTP-bound state for interaction with SRP54/Ffh. Although at present a *bona fide* loading factor has not been identified for SRα/FtsY.

While *E. coli* does not possess a homologue to SRβ, all eukaryotic SRP pathways utilize a third GTPase in the β-subunit of the SRP receptor. From its primary amino acid sequence, SRβ is more closely related to Arf-like GTPases than to the SRP54/SRα sub-family (Miller et al., 1995). While less is known concerning SRβ's affinity for nucleotides, it does bind GTP as evidenced from ^{32}P-GTP crosslinking studies (Miller et al., 1993). Moreover, genetic studies in *S. cerevisiae* have demonstrated that an active SRβ GTPase domain is required for the SRP secretory pathway (Ogg et al., 1998).

A role for the SRβ GTPase has recently been suggested from experiments in the mammalian system (Bacher et al., 1999). SRβ, in its GTP bound state, was shown to interact with ribosomes. Moreover, upon binding to SRβ, ribosomes were found to reduce SRβ's affinity for GTP. SRβ would then appear to provide a communication link between the SRP receptor and the ribosome. This would provide a second major interaction critical foor the SRP-SRP receptor targeting process.

From these various results a simple model can be proposed for how the three GTPases work to facilitate protein targeting. As shown in Figure 5, SRP would initially become loaded with GTP upon interacting with a ribosome that bears a signal sequence. Meanwhile, SRα and SRβ would be at the membrane presumably associated with the translocon and locked into their respective GTP-bound states. The combined effect of the SRβ-ribosome and SRP54-SRα interaction would facilitate proper docking of only the correct ribosome-nascent chains which possess signal sequences. Meanwhile, the SRP components would recycle for subsequent targeting rounds after GTP hydrolysis and/or nucleotide release.

A recent model (Figure 6) has been put forth which suggests that SRβ mediates the initial targeting of ribosomes to the translocon (Bacher et al., 1999). Following ribosome-stimulated GTP hydrolysis by SRβ , SRα is able to scan for the presence of SRP within the ribosome-nascent chain complex. If SRα is able to interact with SRP, proper docking of the ribosome with the nascent chain being handed off to the SEC61 complex can ensue. This would ensure that only the correct ribosome nascent chains would be properly docked to the translocon.

This model, however, is unlikely from an evolutionary perspective. SRβ function is not maintained in *E. coli* where SRP-dependent targeting is mediated solely by Ffh/4.5S RNP and FtsY. While the GTP-dependent interaction between SRβ and the ribosome is somehow mechanistically integrated into the SRP-dependent targeting pathway, it is probably not the critical initial step which is suggested in Figure 6.

An alternative mechanistic model, as depicted in Figure 7, can be offered in which SRP54 and SRα mediate the primary targeting event. This ensures that only the correct ribosome-nascent chain complexes are brought to the membrane. SRβ could be functioning in a subsequent step to facilitate the proper docking of the ribosome-nascent chain to the SEC61 complex. Alternatively SRβ could serve to block ribosome contact with the SEC61 complex until the proper ribosome-nascent chains are targeted to the membrane by the SRP54-SRα interaction. This would provide an additional safeguard to maintain fidelity within the SRP-dependent targeting pathway.

A functional role for SRP RNA?

While extensive biochemical studies elucidated functional roles for all of the protein components of SRP, it was initially unclear whether SRP RNA was anything more than a structural scaffold. The existence of a simpler Ffh/4.5S RNP complex within *E. coli* strongly argued for a functional role for this highly conserved domain IV of the SRP RNA (Poritz et al., 1988). Ffh already provided the crucial functions of signal sequence recognition and SRP receptor cross-talk. Clearly 4.5S RNA must provide some functional role in order to be maintained in *E. coli*. This became the driving focus of the work in this thesis. Specifically, we wished to determine what mechanistic role 4.5S RNA was playing in the *E. coli* SRP-targeting cycle.

4.5S RNA possesses the most conserved SRP bases maintained across all phyllogeny. As shown in Figure 3, these bases are predicted from secondary structural models to be in exposed loop regions of the RNA (Poritz et al., 1988). From the chemical footprinting studies detailed in Chapter 2 of this thesis, we and others (Lentzen et al., 1996) found that many of these conserved bases were highly solvent accessible when 4.5S RNA is not bound to Ffh. When Ffh bound to the RNA, several of these bases were no longer reactive to the modifying agents suggesting that they made critical contacts with Ffh during formation of the Ffh/4.5S RNP. More importantly, the crystal structure of the M-domain-4.5S RNA complex provided structural confirmation of these footprinting results as will be discussed in further detail in Chapter 2 (Batey et al., 2000).

Interestingly, many of these conserved bases are solvent accessible even upon binding to Ffh. We were curious whether these exposed bases were interacting with other components of the SRP cycle. The most likely candidates were obviously the signal sequence, GTP/GDP, the SRP receptor, and the ribosome. From many previous observations outlined below, it was tempting to speculate that SRP RNA functionally interacted with these components either through direct interaction or indirectly through some allosteric means. When I began the work in this thesis, we knew that SRP RNA was playing an important role in the SRP-SRP receptor interaction.

SRP RNA enhances the interaction between SRP54/Ffh and SRα/FtsY

SRP RNA was found to be essential for the interaction between SRP54 and SRα. The stimulated GTPase activity of the SRP54-Srα complex was absolutely dependent on the presence of SRP RNA (Miller et al., 1993). Similar observations were made for the *E. coli* homologues as well. In the absence of 4.5S RNA, Ffh and FtsY also failed to exhibit stimulated GTPase activity (Miller et al., 1994). Moreover, work with these *E. coli* homologues demonstrated that binding between Ffh and FtsY was dependent on 4.5S RNA (Miller et al., 1994). It was therefore not unreasonable to speculate that 4.5S RNA might be making direct contacts with FtsY, perhaps through several of the highly conserved bases within Domain IV.

In addition to further characterizing , we wished to make a complete study of 4.5S RNA's role in the SRP functional cycle. As shown in Figure 2, the ribosome represented the last major component with which the Ffh/4.5S RNP was most likely to interact during its functional cycle. At the time this work was started, there was reason to think that the 4.5S RNA could interact directly with ribosomes.

4.5S RNA interacts with the ribosome?

Before 4.5S RNA was identified as an SRP RNA homologue, it was initially thought to serve as a modulator of the ribosome during translation. Initially identified as an abundant small cytoplasmic RNA in *E. coli*, 4.5S RNA was known to be essential for growth (Brown and Fournier, 1984). Based on the fact that reduced levels of 4.5S RNA were lethal to *E. coli*, genetic screens were developed to identify the cellular components that interacted with the RNA (Brown, 1987). Interestingly, these screens yielded components of the translation pathway. Specifically, mutant alleles of elongation factor G (EF-G), the 23S ribosomal RNA (23S rRNA), and a number of tRNA synthetases were isolated (Brown, 1987). In addition, it was observed that certain antiobiotics targeted against EF-G increased the amount of 4.5S RNA found associated with ribosomes (Brown, 1989). From these observations Brown and his collegues proposed that 4.5S RNA functioned at a specific step in the translational process, namely, translocation between the tRNA binding sites within the ribosome (Brown, 1991).

The 23S rRNA allele was interesting for an additional reason. Within this region of the 23S rRNA exists a 10 base element which is identical to one found in the most conserved region of 4.5S RNA (Brown, 1991). The allele which suppressed the deleterious 4.5S RNA levels mapped to position 1067 of this region. It had also been known that this region of the 23S rRNA provides a binding site for EF-G (Moazed et al., 1988), which had also been identified in the genetic screen. This led to speculation that 4.5S RNA directly interacts with EF-G. Since these early studies, direct interaction between EF-G and 4.5S RNA has been observed using gel shift assays (Shibata et al., 1996). However, the significance of these studies remains unclear. The *in vitro* interaction demonstrated by these studies is interesting as it would argue for a structural similarity between the respective regions of the 23S rRNA and the 4.5S RNA. However, a biologically relevant role for the interaction between EF-G and 4.5S RNA has not been demonstrated since it was initially observed. In the absence of any functional relevance, the sequence conservation between 4.5S RNA and 23S rRNA can be viewed as nothing more than a provocative coincidence at present.

Subsequent studies in *S. cerevisiae* can shed light on these earlier ribosome-4.5S RNA interactions in the framework of the SRP function. A temperature sensitive allele had been isolated for SRP19, the sec65^{ts} allele, which is lethal to yeast cells at elevated temperatures (Stirling and Hewitt, 1992). Cycloheximide suppresses this growth defect at the non-permissive temperature (Ogg and Walter, 1995). Moreover, this effect appears to be specific to cycloheximide as a second translational inhibitor, anisomycin, cannot suppress the mutation's effects. From the mechanistic actions of these drugs, a parallel can be drawn with the earlier work in *E. coli* (Brown, 1989). Cycloheximide blocks the translocation of the peptidyl-tRNA from the A to P site on the ribosome, the same translational step that was the target in the earlier 4.5S studies. Based on both the prokaryotic and eukaryotic results, it has been suggested that SRP, which operates in a co-translational manner, can only recognize the ribosome at a particular step in the translation cycle (Ogg and Walter, 1995). In the mutant *E. coli* and *S. cerevisiae* strains described above, the reduced levels of SRP would compromise its interaction with the ribosome. Any drug or mutation which maintains the ribosome in a conformation that is favorable for SRP binding would, therefore, counter these effects. This would then account for the narrow selectivity seen in the suppressor and antibiotic studies.

When the work for this thesis began, we had preliminary evidence that the Ffh/4.5S RNP was interacting with purified ribosomes. Using a fluorescenctly labeled 4.5S RNA, measurements of fluorescent anisotropy exhibited a dramatic increase upon addition of the Ffh protein to the RNA (Arthur Johnson, et al., unpublished results). The profile fit reasonably well to a tight binding curve. Extending this study further, additional changes were observed in response to the addition of ribosomes to the preformed Ffh/fluorescein-4.5S RNA complex. The addition of ribosomes resulted in a decrease in anisotropy, which also showed the hallmarks of a binding curve (Arthur Johnson, et al., unpublished results). Based on these observations, we set out to map the Ffh/4.5S RNP binding site on the ribosome in addition to probing 4.5S RNA as well in the presence of ribosomes. During the process of carrying out these studies, we subsequently discovered that the fluorescence anisotropy measurements were actually monitoring an aggregation phenomena which was of no biological relevance. The discovery of this aggregation is the focus of the data presented in Appendix A of this thesis.

A footprinting approach to uncovering 4.5S RNA's functional role

In Chapter 2 of this thesis, we employed standard RNA footprinting techniques in order to identify potential interactions between 4.5S RNA and the various other components of the SRP pathway. From the success of this approach demonstrated in the ribosome field, we were optimistic that adopting this line of investigation would prove enlightening on many levels. First, we hoped to find RNA bases which directly interacted with either Ffh, the signal sequence, GTP, GDP, ribosomes, or FtsY. Second, these footprinting techniques would also uncover conformational changes in addition to identifying direct contacts. We hoped to gain useful structural information about the Ffh/4.5S RNP during its functional cycle.

As will be discussed in greater detail in Chapter 2. The footprinting approach proved useful in mapping the Ffh contacts with 4.5S RNA. However, the footprinting efforts failed to identify any contacts or conformational changes within 4.5S RNA upon binding of the Ffh/4.5S RNP to other interacting molecules of the SRP targeting cycle. When we discovered that the fluorescein-4.5S RNA studies were monitoring a non-physiologically relevant aggregation between Ffh and 4.5S RNA (see Appendix 1), we were not surprised that our efforts to map a interactions with the ribosome met with failure. However, we were surprised at our failure to observe a footprint from FtsY. From previous work, we had expected 4.5S RNA to be in direct contact with FtsY in order to increase FtsY's affinity for Ffh.

Mechanistic and Spectroscopic Studies of the Ffh-FtsY Complex

As the footprinting studies failed to uncover any information with respect to the Ffh•FtsY interaction, we turned our attention to more fundamental enzymological questions concerning the Ffh•FtsY complex. We reasoned that a better mechanistic understanding of the Ffh•FtsY GTPase cycle was needed in order to determine how specifically 4.5S RNA was influencing this complex. We therefore modeled a reaction scheme for the Ffh/4.5S RNP•FtsY complex and set out to devise assays which would allow us to monitor each step quantitatively.

The basic reaction scheme for the Ffh/4.5S RNP•FtsY complex is depicted in Figure 8. This scheme represents the basic GTPase reaction in the absence of any other ligands normally present in the SRP pathway as shown in Figure 2. Both GTPases are assumed to hydrolyze one molecule of GTP per cycle as suggested from the results using the XTP-specific FtsY protein (Powers and Walter, 1995). As this reaction mechanism shows many steps can serve as a means of regulation. We therefore set out to develop useful assays to probe each step in turn.

In Chapter 3, a novel fluorescence assay is described which we and others have developed to monitor interactions between Ffh and FtsY (Jagath et al., 2000; Peluso et al., 2000). Taking advantage of FtsY's unique tryptophan residues, we were able to monitor binding between Ffh and FtsY through changes in FtsY's tryptophan fluorescence. With this assay we could demonstrate that Ffh could interact with FtsY in the absence of 4.5S RNA. This was supported by observations in the *Mycoplasma mycoides* system where stimulated GTPase activity was observed for the Ffh•FtsY complex even in the absence of 4.5S RNA (Macao et al., 1997). Through the work in Chapter 3, we discovered a novel catalytic role for 4.5S RNA in the formation of the Ffh•FstY complex. This finding explained the discrepancies between the results in the *M. mycoides* system with those from previous work from our lab concerning the requirement of 4.5S RNA in the Ffh•FtsY interaction (Macao et al., 1997; Miller et al., 1994).

In Chapter 4, we carried out a thorough enzymatic analysis of the Ffh•FtsY complex both in the presence and absence of 4.5S RNA. While 4.5S RNA displayed little effect on Ffh's basal nucleotide binding and hydrolysis properties, it exerted most of its influence on the Ffh•FtsY complex. This enzymatic analysis argued that binding of Ffh to FtsY was under many conditions assayed a major rate limiting factor to the GTPase activity. The data closely agreed with the equilibrium studies in Chapter 3 which had employed GppNHp in order to trap the complexes. The enhanced association rate was also seen in the context of GTP. Moreover, the existence of a conformational change leading to GTP turnover by the complex was also uncovered through this work. Paralleling its catalytic role in Ffh•FtsY association, 4.5S RNA appeared to enhance the kinetics of this conformational change.

Lastly, Appendix B describes fluorescence studies we used to monitor nucleotide binding by Ffh, Ffh/4.5S RNP, and FtsY. This work was done as part of the complete enzymatic analysis in Chapter 4. From this work, we found nucleotide association and release to be fast for these proteins relative to the classical Ras-like GTPases. These results closely agreed with those from independent work by other groups. However, as will be discussed later on in detailed, we inadvertently uncovered some problems which may arise with these fluorescence techniques.

In summary, we provided a thorough enzymatic analysis of the Ffh•FtsY complex in the hope of gaining a better understanding of 4.5S RNA's role in this functional cycle. In doing this we have uncovered a novel function for 4.5S RNA with respect to Ffh•FtsY complex formation. Second, we have provided a detailed kinetic framework and established assays to gain insight into how the Ffh•FtsY complex functions during protein targeting. We have been able to integrate the SRP RNA's role within this mechanistic context. The future challenge will be to uncover the role of the other components with respect to this framework.

References

Bacher, G., H. Lutcke, B. Jungnickel, T.A. Rapoport, and B. Dobberstein. 1996. Regulation by the ribosome of the GTPase of the signal-recognition particle during protein targeting. *Nature* 381:248-251.

Bacher, G., M. Pool, and B. Dobberstein. 1999. The ribosome regulates the GTPase of the beta-subunit of the signal recognition particle receptor. *J. Cell Biol.* 146:723-730.

Batey, R.T., R.P. Rambo, L. Lucast, B. Rha, and J.A. Doudna. 2000. Crystal structure of the ribonucleoprotein core of the signal recognition particle. *Science* 287:1232-1239.

Beckmann, R., D. Bubeck, R. Grassucci, P. Penczek, A. Verschoor, G. Blobel, and J. Frank. 1997. Alignment of conduits for the nascent polypeptide chain in the ribosome- Sec61 complex. *Science* 278:2123-2126.

Bernstein, H.D., M.A. Poritz, K. Strub, P.J. Hoben, S. Brenner, and P. Walter. 1989. Model for signal sequence recognition from amino-acid sequence of 54k subunit of signal recognition particle. *Nature* 340:482-486.

Blobel, G., and B. Dobberstein. 1975. Transfer of proteins across membranes. I. Presence of proteolytically processed and unprocessed nascent immunoglobulin light chains on membrane-bound ribosomes of murine myeloma. *J. Cell Biol.* 67:835-851.

Blobel, G., and G.G. Sabatini. 1971. *In* Biomembranes. L.A. Manson, editor. Plenum, New York. pp. 193-195.

Brown, S. 1987. Mutations in the gene for EF-G reduce the requirement for 4.5S RNA in the growth of E. coli. *Cell* 49:825-833.

Brown, S. 1989. Time of action of 4.5 S RNA in Escherichia coli translation. *J. Mol. Biol.* 209:79-90.

Brown, S. 1991. 4.5S RNA: does form predict function? *New Biol.* 3:430-438.

Brown, S., and M.J. Fournier. 1984. The 4.5S RNA Gene of *Escherichia coli* is Essential for Cell Growth. *J. Mol. Biol.* 178:533-550.

Brownlee, G.G., T.M. Harrison, M.B. Mathews, and C. Milstein. 1972. Translation of messenger RNA for immunoglobulin light chains in a cell- free system from Krebs II ascites cells. *FEBS Lett.* 23:244-248.

Connolly, T., and R. Gilmore. 1989. The signal recognition particle receptor mediates the GTP-dependent displacement of SRP from the signal sequence of the nascent polypeptide. *Cell* 57:599-610.

Connolly, T., P.J. Rapiejko, and R. Gilmore. 1991. Requirement of GTP Hydrolysis for Dissociation of the Signal Recognition Particle from Its Receptor. *Science.* 252:1171-1173.

Crowley, K.S., S. Liao, V.E. Worrell, G.D. Reinhart, and A.E. Johnson. 1994. Secretory proteins move through the ER membrane via an aqueous, gated pore. *Cell* 78:461-471.

Crowley, K.S., G.D. Reinhart, and A.E. Johnson. 1993. The signal sequence moves through a ribosomal tunnel into a noncytoplasmic aqueous environment at the ER membrane early in translocation. *Cell* 73:1101-1115.

de Gier, J.W., P. Mansournia, Q.A. Valent, G.J. Phillips, J. Luirink, and G. von Heijne. 1996. Assembly of a cytoplasmic membrane protein in Escherichia coli is dependent on the signal recognition particle. *FEBS Lett.* 399:307-309.

de Leeuw, E., K. te Kaat, C. Moser, G. Menestrina, R. Demel, B. de Kruijff, B. Oudega, J. Luirink, and I. Sinning. 2000. Anionic phospholipids are involved in membrane association of FtsY and stimulate its GTPase activity. *EMBO J.* 19:531-541.

Deshaies, R.J., and R. Schekman. 1989. SEC62 encodes a putative membrane protein required for protein translocation into the yeast endoplasmic reticulum. *J. Cell BioL.* 109:2653-2664.

Deshaies, R.J., and R. Schekman. 1990. Structural and functional dissection of Sec62p, a membrane-bound component of the yeast endoplasmic reticulum protein import machinery. *Mol. CelL. BioL.* 10:6024-6035.

Freymann, D.M., R.J. Keenan, R.M. Stroud, and P. Walter. 1997. Structure of the conserved GTPase domain fo the signal recognition particle. *Nature* 385:361-364.

Freymann, D.M., R.J. Keenan, R.M. Stroud, and P. Walter. 1999. Functional changes in the structure of the SRP GTPase on binding GDP and Mg^{2+}GDP. *Nat Struct. Biol.* 6:793-801.

Gilmore, R., and Hoffman, K.E. 1988. Guanosine Triphosphate Promotes the Post-translational Integration of Opsin into the Endoplasmic Reticulum Membrane. *The J. Biol. Chem.*. 263:4381-4385.

Gilmore, R., G. Blobel, and P. Walter. 1982a. Protein translocation across the endoplasmic reticulum. I. Detection in the microsomal membrane of a receptor for the signal recognition particle. *J. Cell Biol.* 95:463-469.

Gilmore, R., P. Walter, and G. Blobel. 1982b. Protein translocation across the endoplasmic reticulum. II. Isolation and characterization of the signal recognition particle receptor. *J. Cell Biol.* 95:470-477.

Hoffman, K.E., and R. Gilmore. 1988. Guanosine triphosphate promotes the post-translational integration of opsin into the endoplasmic reticulum membrane. *The J. Biol. Chem.* 263:4381-4385.

Jagath, J.R., M.V. Rodnina, G. Lentzen, and W. Wintermeyer. 1998. Interaction of guanine nucleotides with the signal recognition particle from Escherichia coli. *Biochemistry* 37:15408-15413.

Jagath, J.R., M.V. Rodnina, and W. Wintermeyer. 2000. Conformational changes in the bacterial SRP receptor FtsY upon binding of guanine nucleotides and SRP. *J. Mol. Biol.* 295:745-753.

Kalies, K.-U., D. Görlich, and T.A. Rapoport. 1994. Binding of ribosomes to the rough endoplasmic reticulum mediated by the Sec61p-complex. *The J. Cell Biol.* 126:925-934.

Keenan, R.J., D.M. Freymann, P. Walter, and R.M. Stroud. 1998. Crystal structure of the signal sequence binding subunit of the signal recognition particle. *Cell* 94:181-191.

Kurita, K., K. Honda, S. Suzuma, H. Takamatsu, K. Nakamura, and K. Yamane. 1996. Identification of a region of Bacillus subtilis Ffh, a homologue of mammalian SRP54 protein, that is essential for binding to small cytoplasmic RNA. *J. Biol. Chem.* 271:13140-13146.

Lauffer, L., P.D. Garcia, R.N. Harkins, L. Coussens, A. Ullrich, and P. Walter. 1985. Topology of the SRP receptor in the endoplasmic reticulum membrane. *Nature* 318:334-338.

Lentzen, G., H. Moine, C. Ehresmann, B. Ehresmann, and W. Wintermeyer. 1996. Structure of 4.5S RNA in the signal recognition particle of Escherichia coli as studied by enzymatic and chemical probing. *RNA* 2:244-253.

Lingelbach, K., C. Zwieb, J.R. Webb, C. Marshallsay, P.J. Hoben, P. Walter, and B. Dobberstein. 1988. Isolation and characterization of a cDNA clone encoding the 19 kDa protein of the signal recognition particle (SRP): expression and binding to 7SL RNA. *Nuc. Ac. Res.* 16:9431-9442.

Luirink, J., and B. Dobberstein. 1994. Mammalian and Escherichia coli signal recognition particles. *Mol. Microbiol.* 11:9-13.

Luirink, J., C.M. ten Hagen-Jongman, C.C. van der Weijden, B. Oudega, S. High, B. Dobberstein, and R. Kusters. 1994. An alternative protein targeting pathway in Escherichia coli: studies on the role of FtsY. *EMBO J.* 13:2289-2296.

Lütcke, H., S. High, K. Römisch, A. Ashford, and B. Dobberstein. 1992. The methionine-rich domain of the 54 kDa subunit of signal recognition particle is sufficient for the interaction with signal sequences. *EMBO J.* 11:1543-1551.

Macao, B., J. Luirink, and T. Samuelsson. 1997. Ffh and FtsY in a Mycoplasma mycoides signal-recognition particle pathway: SRP RNA and M domain of Ffh are not required for stimulation of GTPase activity in vitro. *Mol. Microbiol.* 24:523-534.

Macfarlane, J., and M. Muller. 1995. The functional integration of a polytopic membrane protein of Escherichia coli is dependent on the bacterial signal-recognition particle. *Eur. J. Biochem.* 233:766-771.

Meyer, D.I., E. Krause, and B. Dobberstein. 1982. Secretory protein translocation across membranes- the role of the docking protein. *Nature* 297:647-650.

Miller, J.D., H.D. Bernstein, and P. Walter. 1994. Interaction of E. coli Ffh/4.5S ribonucleoprotein and FtsY mimics that of mammalian signal recognition particle and its receptor. *Nature* 367:657-659.

Miller, J.D., S. Tajima, L. Lauffer, and P. Walter. 1995. The β-subunit of the signal recognition particle receptor is a transmembrane GTPase that anchors the α-subunit, a peripheral membrane GTPase, to the endoplasmic reticulum membrane. *J. Cell Biol.* 128:273-282.

Miller, J.D., H. Wilhelm, L. Gierasch, R. Gilmore, and P. Walter. 1993. GTP binding and hydrolysis by the signal recognition particle during initiation of protein translocation. *Nature* 366:351-354.

Milstein, C., G.G. Brownlee, T.M. Harrison, and M.B. Mathews. 1972. A possible precursor of immunoglobulin light chains. *Nat. New Biol.* 239:117-120.

Moazed, D., J.M. Robertson, and H.F. Noller. 1988. Interaction of elongation factors EF-G and EF-Tu with a conserved loop in 23S RNA. *Nature.* 334:362-364.

Montoya, G., C. Svensson, J. Luirink, and I. Sinning. 1997. Crystal structure of the NG domain from the signal-recognition particle receptor FtsY. *Nature* 385:365-368.

Moser, C., O. Mol, R.S. Goody, and I. Sinning. 1997. The signal recognition particle receptor of Escherichia coli (FtsY) has a nucleotide exchange factor built into the GTPase domain. *Proc. Natl. Acad. Sci. U.S.A.* 94:11339-11344.

Newitt, J.A., and H.D. Bernstein. 1997. The N-domain of the signal recognition particle 54-kDa subunit promotes efficient signal sequence binding. *Eur.J. Biochem.* 245:720-729.

Ogg, S.C., W.P. Barz, and P. Walter. 1998. A Functional GTPase Domain, but not its Transmembrane Domain, is Required for Function of the SRP Receptor beta-subunit. *J. Cell Biol.* 142:341-354.

Ogg, S.C., and P. Walter. 1995. SRP Samples Nascent Chains for the Presence of Signal Sequences by Interacting with Ribosomes at a Discrete Step during Translation Elongation. *Cell* 81:1075-1084.

Peluso, P., D. Herschlag, S. Nock, D.M. Freymann, A.E. Johnson, and P. Walter. 2000. Role of 4.5S RNA in assembly of the bacterial signal recognition particle with its receptor. *Science* 288:1640-1643.

Phillips, G.J., and T.J. Silhavy. 1992. The E. coli *ffh* gene is necessary for viability and efficient protein export. *Nature* 359:744-746.

Poritz, M.A., H.D. Bernstein, K. Strub, D. Zopf, H. Wilhelm, and P. Walter. 1990. An E. coli ribonucleoprotein containing 4.5S RNA resembles mammalian signal recognition particle. *Science* 250:111-1117.

Poritz, M.A., K. Strub, and P. Walter. 1988. Human SRP RNA and E. coli 4.5S RNA contain a highly homologous structural domain. *Cell* 55:4-6.

Powers, T., and P. Walter. 1995. Reciprocal Stimulation of GTP Hydrolysis by Two Directly Interacting GTPases. *Science* 269:1422-1424.

Powers, T., and P. Walter. 1997. Co-translational protein targeting catalyzed by the Escherichia coli signal recognition particle and its receptor. *EMBO J.* 16:4880-4886.

Ribes, V., K. Römisch, A. Giner, B. Dobberstein, and D. Tollervey. 1990. E. coli 4.5S RNA Is Part of a Ribonucleoprotein Particle That Has Properties Related to Signal Recognition Particle. *Cell* 63:591-600.

Römisch, K., J. Webb, J. Herz, S. Prehn, R. Frank, M. Vingron, and B. Dobberstein. 1989. Homology of the 54K Protein of signal recognition particle, docking protein, and two E. coli proteins with putative GTP-binding domains. *Nature* 340:478-482.

Sanders, S.L., K.M. Whitfield, J.P. Vogel, M.D. Rose, and R.W. Schekman. 1992. Sec61p and BiP directly facilitate polypeptide translocation into the ER. *Cell* 69:353-365.

Seluanov, A., and E. Bibi. 1997. FtsY, the prokaryotic signal recognition particle receptor homologue, is essential for biogenesis of membrane proteins. *J. Biol. Chem.* 272:2053-2055.

Shibata, T., Y. Fujii, Y. Nakamura, K. Nakamura, and K. Yamane. 1996. Identification of protein synthesis elongation factor G as a 4.5 S RNA- binding protein in Escherichia coli. *J. Biol. Chem.* 271:13162-13168.

Siegel, V., and P. Walter. 1986. Removal of the Alu structural domain from signal recognition particle leaves its protein translocation activity intact. *Nature* 320:81-84.

Siegel, V., and P. Walter. 1988a. Binding sites of the 19-kDa and 68/72-kDa signal recognition particle (SRP) proteins on SRP RNA as determined by protein-RNA "footprinting". *Proc. Natl. Acad. Sci.U.S.A.* 85:1801-1805.

Siegel, V., and P. Walter. 1988b. Each of the activities of signal recognition particle (SRP) is contained within a distinct domain: analysis of biochemical mutants of SRP. *Cell* 52:39-49.

Simon, S.M., and G. Blobel. 1991. A protein-conducting channel in the endoplasmic reticulum. *Cell* 65:371-380.

Simon, S.M., G. Blobel, and J. Zimmerberg. 1989. Large aqueous channels in membrane vesicles derived from the rough endoplasmic reticulum of canine pancreas or the plasma membrane of Escherichia coli. *Proc. Natl. Acad. Sci.U.S.A.* 86:6176-6180.

Stirling, C.J., and E.W. Hewitt. 1992. The *Saccharomyces cerevisiae SEC65* gene encodes a component of the yeast signal recognition particle with homology to human SRP19. *Nature* 356:534-537.

Swan, D., H. Aviv, and P. Leder. 1972. Purification and properties of biologically active messenger RNA for a myeloma light chain. *Proc. Natl. Acad. Sci. U.S.A.*. 69:1967-1971.

Tajima, S., L. Lauffer, V.L. Rath, and P. Walter. 1986. The signal recognition particle is a complex that contains two distinct polypeptide chains. *J. Cell Biol.* 103:1167-1178.

Tian, H., D. Boyd, and J. Beckwith. 2000. A mutant hunt for defects in membrane protein assembly yields mutations affecting the bacterial signal recognition particle and Sec machinery. *Proc. Natl. Acad. Sci. U.S.A.* 97:4730-4735.

Valent, Q.A., D.A. Kendall, S. High, R. Kusters, B. Oudega, and J. Luirink. 1995. Early events in preprotein recognition in E. coli: interaction of SRP and trigger factor with nascent polypeptides. *EMBO J.* 14:5494-5505.

Valent, Q.A., P.A. Scotti, S. High, J.W. de Gier, G. von Heijne, G. Lentzen, W. Wintermeyer, B. Oudega, and J. Luirink. 1998. The Escherichia coli SRP and SecB targeting pathways converge at the translocon. *Embo J.* 17:2504-2512.

von Heijne, G. 1983. Patterns of amino acids near signal sequence cleavage sites. *Eur. J. Biochem.* 133:17-21.

von Heijne, G. 1985. Signal sequences. The limits of variation. *J. Mol. Biol.* 184:99-105.

von Heijne, G., and L. Abrahmsen. 1989. Species-specific variation in signal peptide design. Implications for protein secretion in foreign hosts. *FEBS Lett.* 244:439-446.

Walter, P. 1996. Signal Sequence Recognition and Protein Targeting to the Endoplasmic Reticulum Membrane. *In* The Harvey Lectures, Series 91. Wiley-Liss, Inc. 115-131.

Walter, P., and G. Blobel. 1980. Purification of membrane-associated protein complex required for protein translocation across the endoplasmic reticulum. *Proc. Natl. Acad. Sci. U.S.A.* 77:7112-7116.

Walter, P., and G. Blobel. 1981a. Translocation of proteins across the endoplasmic reticulum. II. Signal recognition protein (SRP) mediates the selective binding to microsomal membranes of in vitro assembled polysomes synthesizing secretory protein. *J. Cell Biol.* 91:551-556.

Walter, P., and G. Blobel. 1981b. Translocation of proteins across the endoplasmic reticulum. III. Signal recognition protein (SRP) causes signal sequence and site specific arrest of chain elongation that is released by microsomal membranes. *J. Cell Biol.* 91:557-561.

Walter, P., and G. Blobel. 1982. Signal recognition particle contains a 7S RNA essential for protein translocation across the endoplasmic reticulum. *Nature* 299:691-698.

Walter, P., and G. Blobel. 1983. Disassembly and reconstitution of the signal recognition particle. *Cell* 34:525-533.

Walter, P., I. Ibrahimi, and G. Blobel. 1981. Translocation of proteins across the endoplasmic reticulum I. Signal Recognition Protein (SRP) binds to in vitro assembled polysomes synthesizing secretory protein. *J. Cell Biol.* 91:545-550.

Walter, P., and A.E. Johnson. 1994. Signal Sequence Recognition and Protein Targeting to the Endoplasmic Reticulum Membrane. *Ann. Rev. Cell Biol.* 10:87-119.

Walter, P., R. Keenan, and U. Schmitz. 2000. Perspectives: structural biology. SRP--where the RNA and membrane worlds meet [comment]. *Science* 287:1212-1213.

Wood, H., J. Luirink, and D. Tollervey. 1992. Evolutionary conserved nucleotides within the E. coli 4.5S RNA are required for association with p48 in vitro and for optimal function in vivo. *Nucleic Acids Res.* 20:5919-5925.

Young, J.C., J. Ursini, K.R. Legate, J.D. Miller, P. Walter, and D.W. Andrews. 1995. An amino-terminal domain containing hydrophobic and hydrophilic sequences binds the signal recognition particle receptor alpha subunit to the beta subunit on the endoplasmic reticulum membrane. *J. Biol. Chem.* 270:15650-15657.

Zelazny, A., A. Seluanov, A. Cooper, and E. Bibi. 1997. The NG domain of the prokaryotic signal recognition particle receptor, FtsY, is fully functional when fused to an unrelated integral membrane polypeptide. *Proc. Natl. Acad. Sci. U.S.A.*. 94:6025-6029.

Zheng, N., and L.M. Gierasch. 1997. Domain interactions in E. coli SRP: stabilization of M domain by RNA is required for effective signal sequence modulation of NG domain. *Mol.Cell* 1:79-87.

Zopf, D., H.D. Bernstein, A.E. Johnson, and P. Walter. 1990. The methionine-rich domain of the 54 kd protein subunit of the signal recognition particle contains an RNA binding site and can be crosslinked to a signal sequence. *EMBO J.* 9:4511-4517.

Zopf, D., H.D. Bernstein, and P. Walter. 1993. GTPase domain of the 54kD subunit of the mammalian signal recognition particle is required for protein translocation but not for signal sequence binding. *J. Cell Biol.* 120:1113-1121.

Figure 1-1: Schematic diagram of mammalian SRP. By established convention, each protein component is designated by its molecular mass. Placement of the various proteins on the SRP RNA in based on earlier footprinting work (see Siegel et al., 1988a). In addition, each protein subunit's essential SRP function is indicated right next to it. Functions for SRP54, SRP68, and SRP72 were determined from selective alkylation experiments(see Siegel et al., 1988b). Functions for SRP9 and SRP14 were determined by nuclease treatment of the particle (see Siegel et al., 1986). Finally SRP19 function was demonstrated from in vitro reconstitution studies (see Lingelbach, et al., 1988).

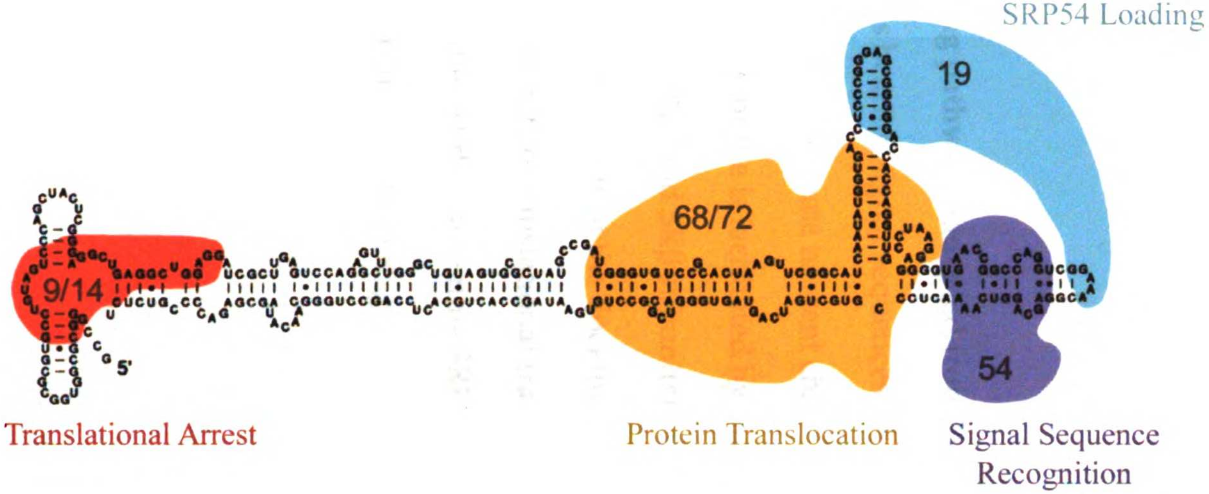
SRP54 Loading
19
68/72
9/14
54
5'
Translational Arrest
Protein Translocation
Signal Sequence Recognition

Figu

SR

Afte

tran

and

serie

SEC

char

recy

Figure 1-2: The SRP targeting pathway (adapted from Walter, 1996) Cytosolic SRP interacts with ribosomes bearing signal sequences (the dark sqiggled line). After forming a complex with the ribosome nascent chain, SRP causes a pause in translation. Targeting to the membrane is facilitated by interactions between SRP and its receptor (heterodimer of SRα and SRβ subunits). At the membrane a series of events takes place which results in the docking of the ribosome with the SEC61 complex and the subsequent co-translational translocation of the nascent chain through the ER membrane. At the same time SRP and the SRP receptor are recycled to perform multiple rounds of targeting.

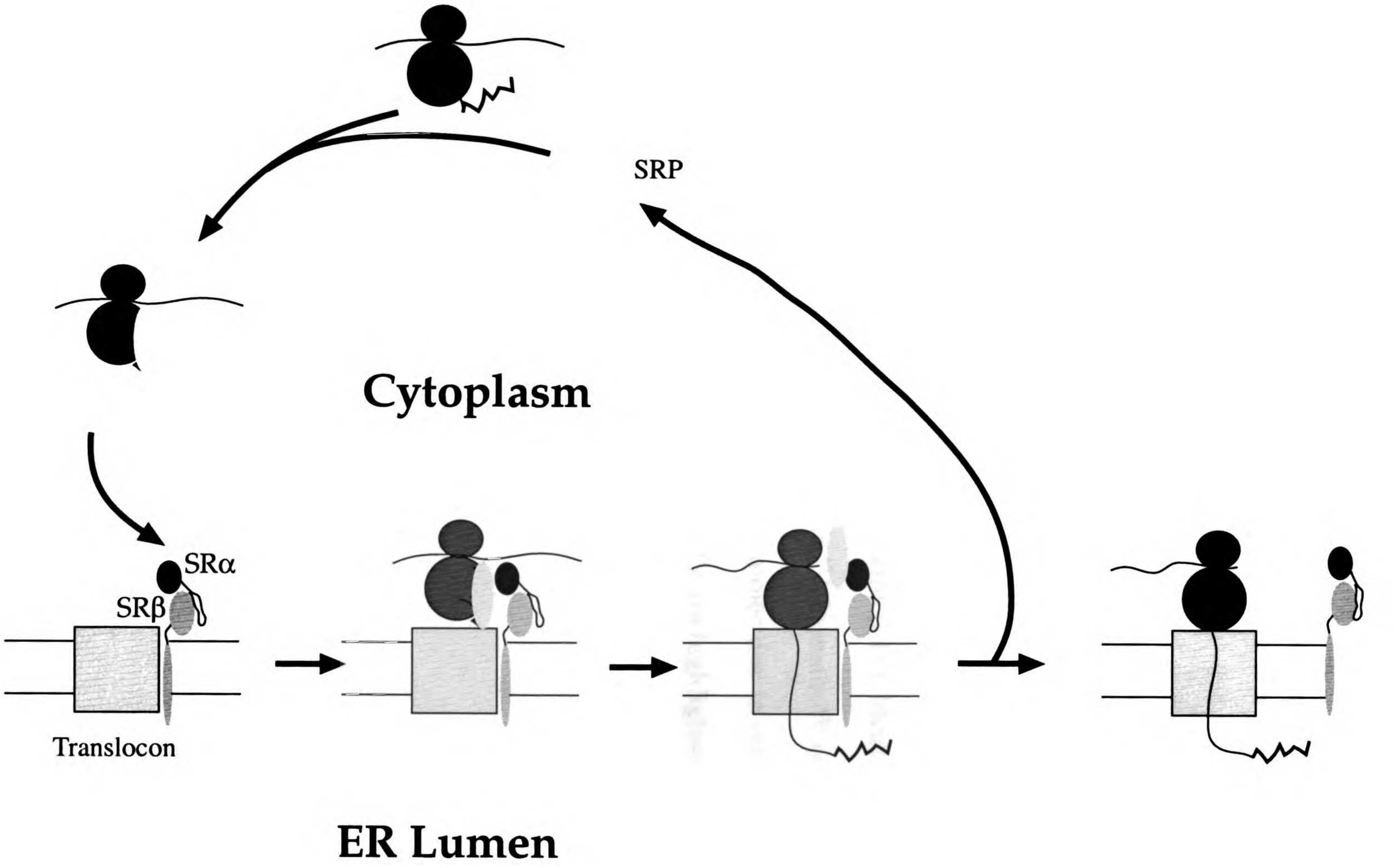
SRP
Cytoplasm
SRα
SRβ
Translocon
ER Lumen

Figure 1-3: A comparison between mammalian SRP RNA and E. coli 4.5S RNA. Mammalian SRP RNA can be subdivided into 4 domains (I-IV). Meanwhile, the *E. coli* homologue, 4.5S RNA only maintains domain IV. Domain IV is highlighted in the grey shaded region for both RNA molecules. In addition, the most evolutionarily conserved bases within domain IV are highlighted in red.

SRP RNA

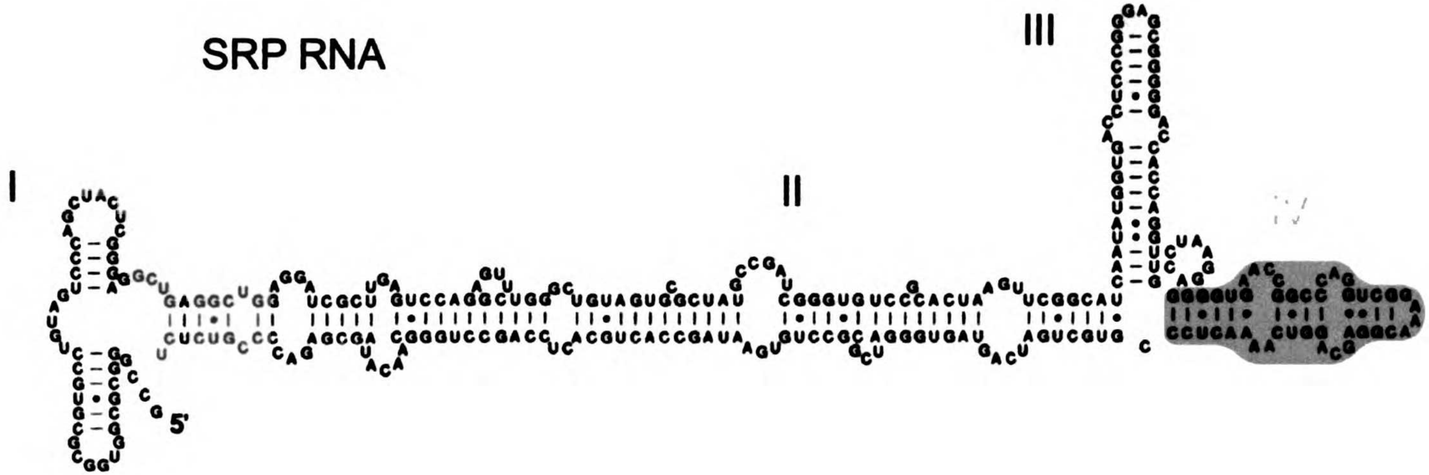

4.5S RNA

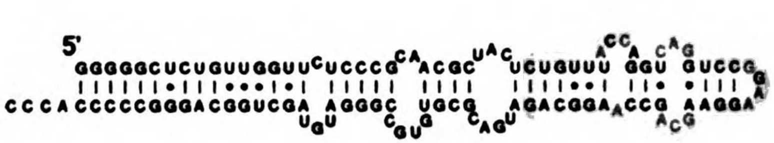

● = evolutionarily conserved residues

Fig

stru

proc

dom

path

seq

som

dom

men

Figure 1-4: Domain architecture of Ffh and FtsY. Ffh and FtsY share in common structurally identical NG-domains which are believed to mediate the targeting process through their interactions with each other. With their respective unique domains, Ffh and FtsY can interact with other components of the targeting pathway. For Ffh, the M-domain interacts with both 4.5S RNA and signal sequences. Meanwhile, FtsY's acidic A-domain enables FtsY to interact with some component of the membrane. Also note that SRα has a slightly larger A-domain. This may reflect the fact that SRα must also interact with SRβ at the membrane.

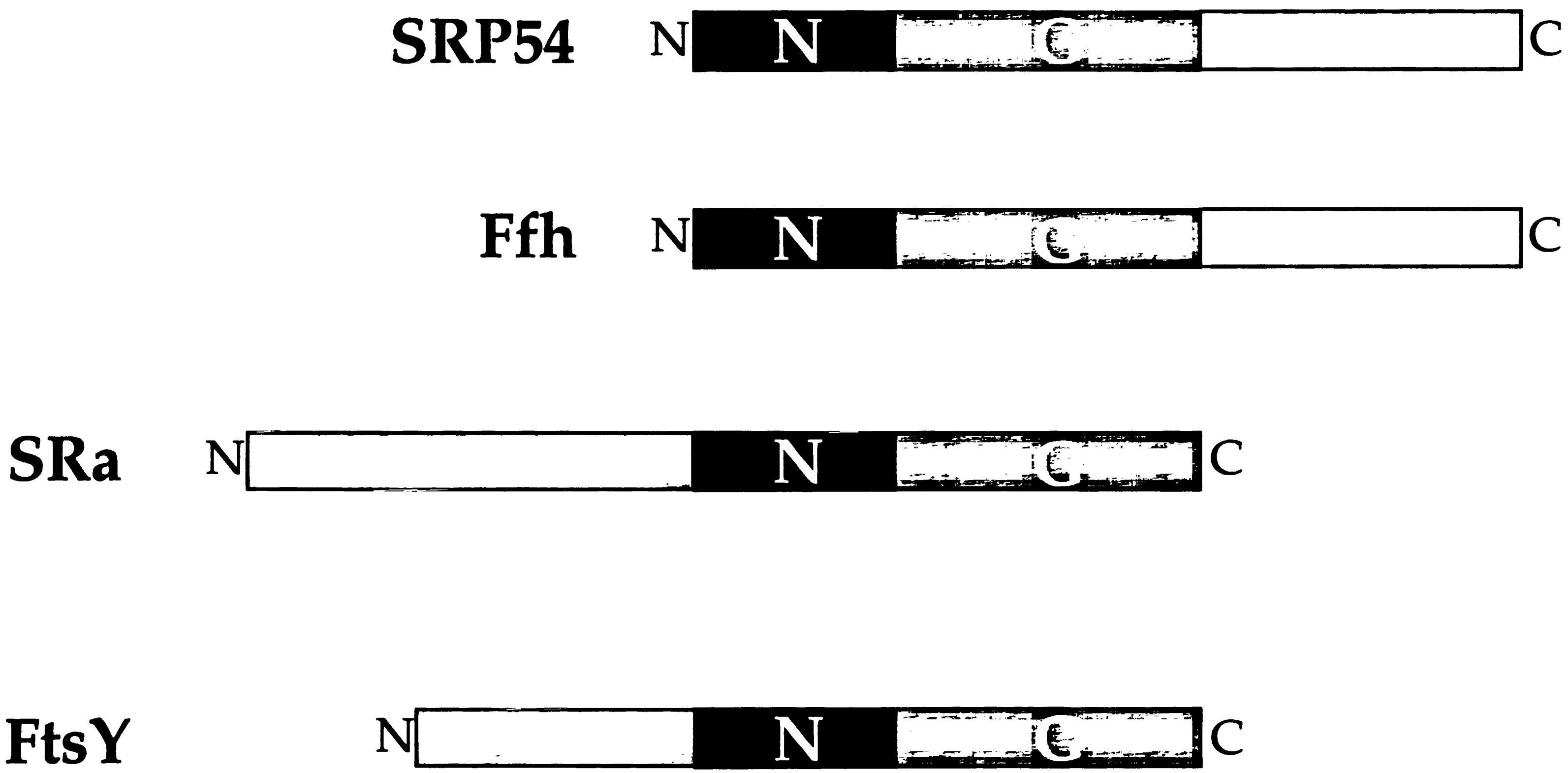
SRP54
N
N
G
C
Ffh
N
N
G
C
SRa
N
N
G
C
FtsY
N
N
G
C

Figure 1-5: The two essential interactions mediated by the SRP receptor during targeting . SRP recognizes ribosomes which are bearing signal sequences in the cytosol. This enables SRP54 to become locked into its GTP state. At the membrane, the subunits of the receptor are presumed to be locked into their corresponding GTP states. As indicated by the heavy grey arrows, two major GTP-dependent interactions are critical for protein targeting. One is between the homologous GTPases, SRP54 and SRα. Meanwhile the other is between SRβ and the ribosome. These crucial interactions somehow facilitate the docking of the ribosome nascent chain to the translocon and the concomitant recycling of SRP and the SRP receptor.

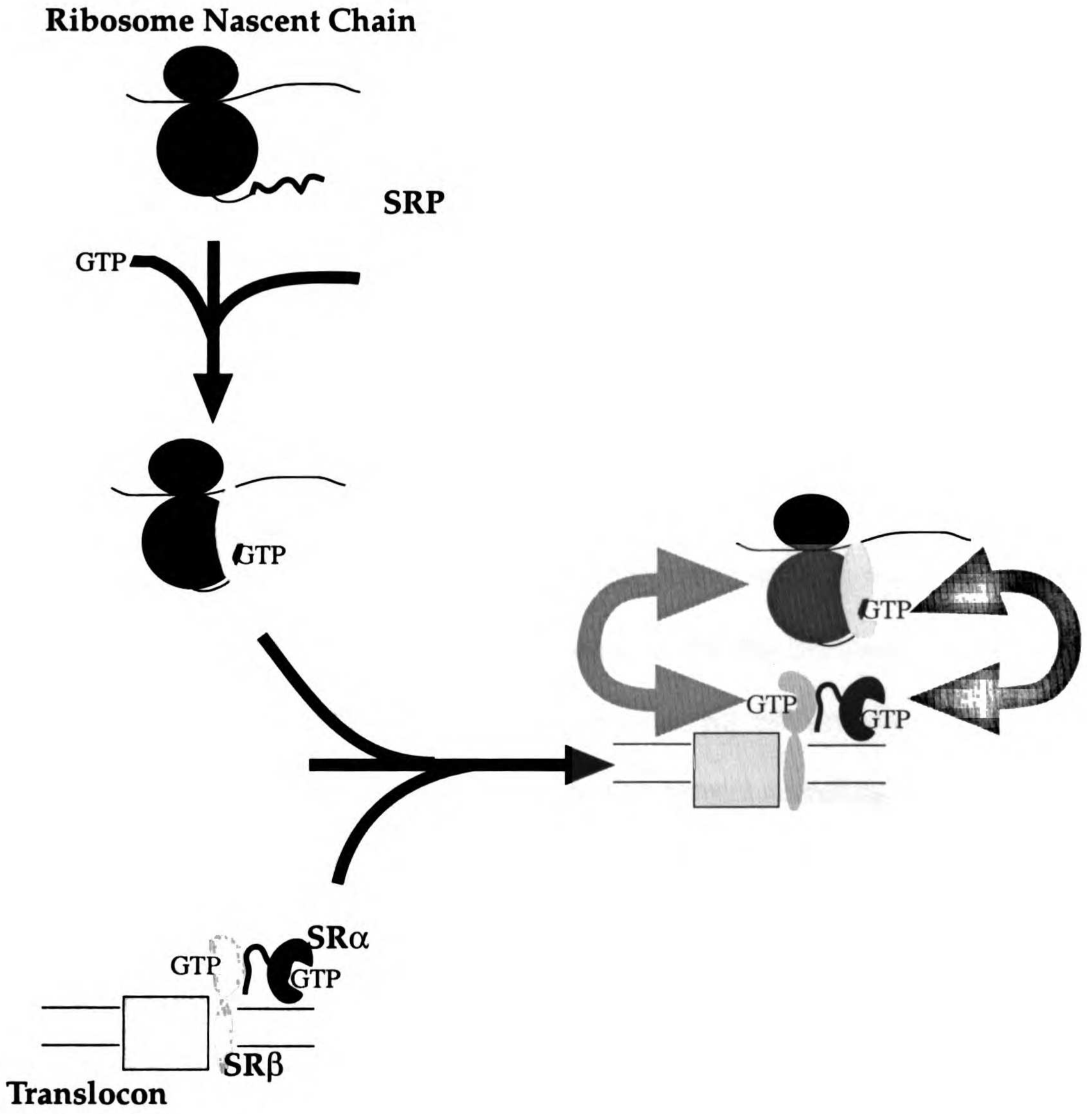
Ribosome Nascent Chain
SRP
GTP
GTP
GTP
GTP
GTP
SRα
GTP
GTP
SRβ
Translocon

Figure 1-6: How 3 GTPases function to promote targeting within the SRP pathway? (Adapted from Bacher, et al., 1999) In the cytosol, SRP forms a tight complex with a ribosome that bears a signal sequence (designated by the heavy squiggled line). Concomitant with formation of this complex, SRP54 becomes locked into its GTP-bound state. Meanwhile at the membrane, SRα and SRβ presumably become locked into their GTP bound states through their interactions with specific membrane components and/or each other. The interaction between SRβ and the ribosome is proposed to bring the ribosome nascent chain to the membrane. SRα can then scan for the presence of SRP via its interaction with SRP54. As suggested in this model, the ribosome stimulates SRβ's GTPase activity. This triggers SRα into the correct scanning conformation by enabling SRα to become loaded with GTP. SRα interacts with SRP54 resulting in stimulated GTP hydrolysis. This leads to proper docking of the ribosome nascent chain within the translocon and recycling of the SRP components. Co-translational translocation of the synthesized protein ensues.

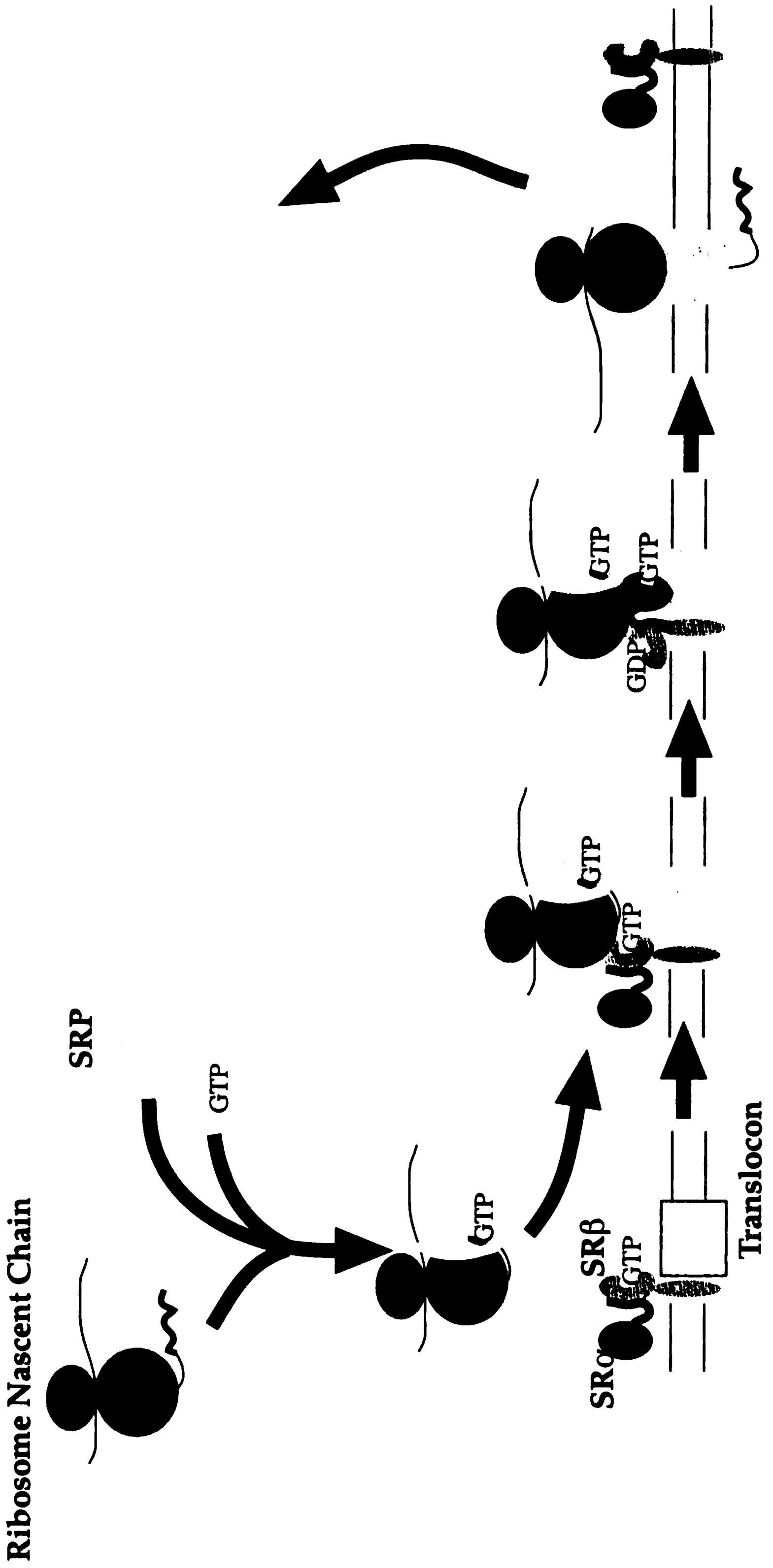
Ribosome Nascent Chain
SRP
GTP
GTP
SRα
SRβ
GTP
Translocon
GTP
GTP
GTP
GTP
GDP
GTP

Figure 1-7: An alternative model for how the three GTPases in the SRP targeting pathway might be functioning. In this model, SRP interacts with cytoplasmic ribosome-nascent chain complexes which specifically bear a signal sequence (the thick squiggled line emerging from the ribosome). SRP54 becomes locked into its GTP-bound state. Meanwhile at the membrane, SRα and SRβ are presumably locked into their respective GTP-bound states via interactions with membrane lipids and or other protein components. Targeting is initially mediated by the GTP-dependent interaction between SRP54 and SRα. Following GTP hydrolysis by both SRP54 and SRα and release of SRP from the ribosome-nascent chain complex, a conformational change would occur within the receptor heterodimer which enables SRβ to interact with the ribosome. GTP hydrolysis by SRβ enables the ribosome to properly dock with the SEC61 complex and subsequent co-translational passage of the nascent chain through the SEC61 complex ensues. In this model, SRβ could function as a barrier for the ribosome on the translocon which the ribosome actively displaces by enhancing the GTPase activity of SRβ.

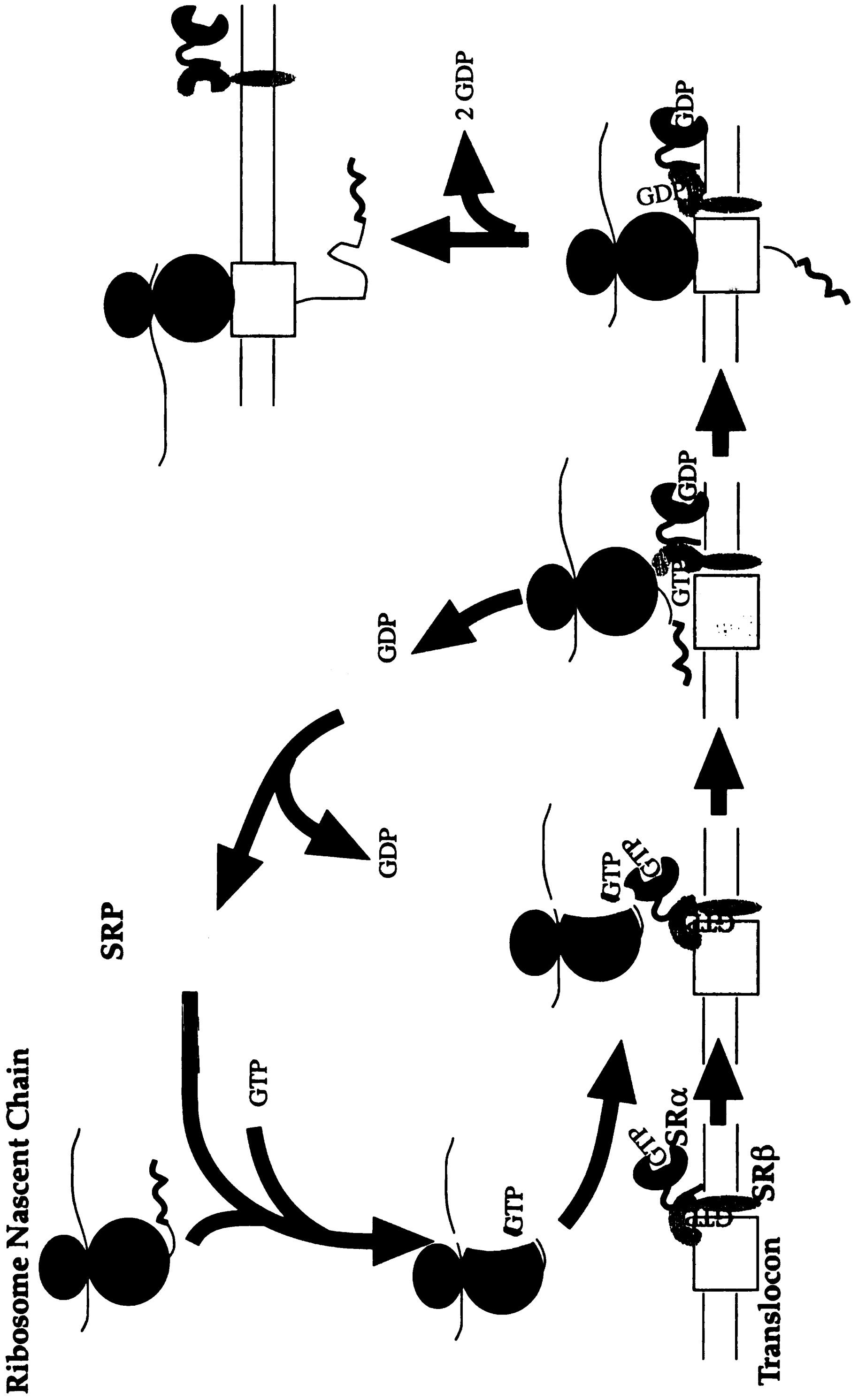
Ribosome Nascent Chain
SRP
GTP
GTP
GDP
GDP
GTP
GTP
GTP
SRα
SRβ
Translocon
GTP
GDP
GDP
GDP
2 GDP

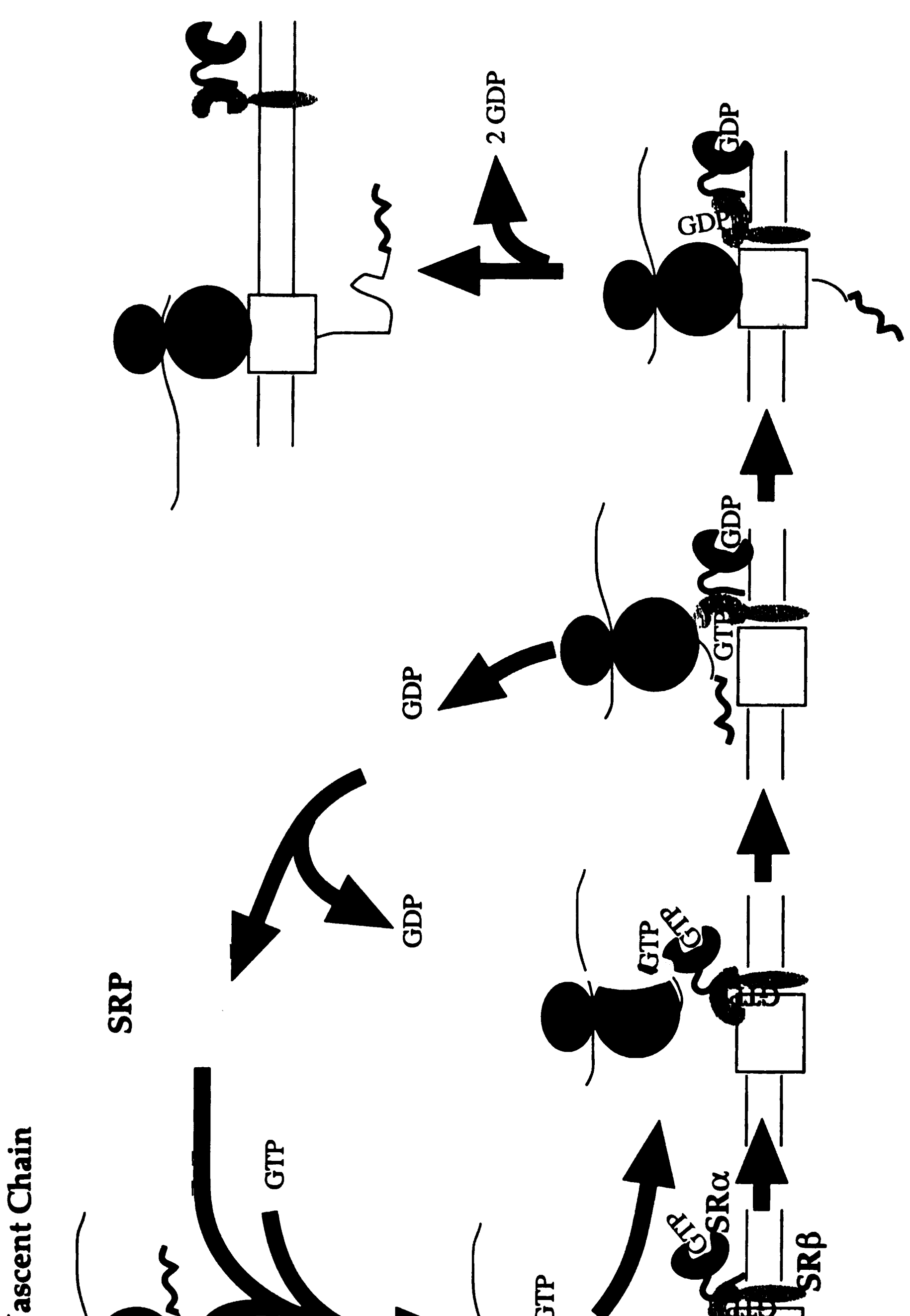
Ribosome Nascent Chain
SRP
GTP
GTP
GDP
GDP
GTP
GTP
SRα
SRβ
Translocon
GTP
GTP
GTP
GDP
GDP
GDP
2 GDP

Figure 1-8 **Model depicting a simple reaction scheme of GTP hydrolysis by the Ffh-FtsY complex.** The symmetrical model implies that both GTPases, Ffh and FtsY, each have a basal rate of hydrolysis (upper cycles, steps 1, 2 and 6 for Ffh and steps 1′, 2′, and 6′ for FtsY), and then exhibit stimulated GTP hydrolysis upon complex formation (steps 3, 4 and 5). Ffh can participate in this reaction by itself, or can be complexed with 4.5S RNA to form Ffh/4.5S RNP, a stable ribonucleoprotein (as indicated by the "± R").

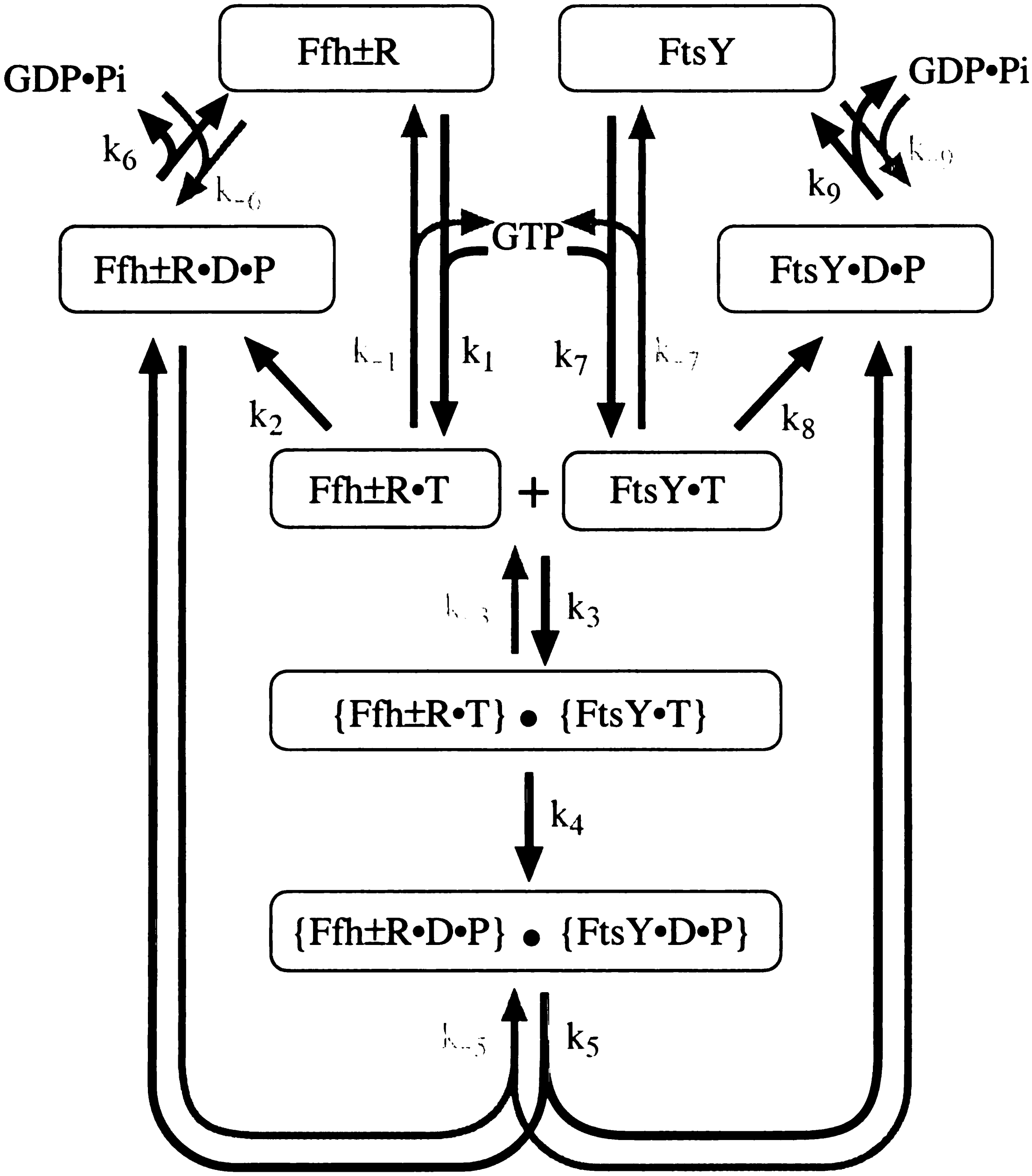

Ffh±R
FtsY
GDP•Pi
GDP•Pi
k6
k-6
k-9
k9
GTP
Ffh±R•D•P
FtsY•D•P
k-1
k1
k7
k-7
k2
k8
Ffh±R•T
+
FtsY•T
k-3
k3
{Ffh±R•T} • {FtsY•T}
k4
{Ffh±R•D•P} • {FtsY•D•P}
k-5
k5

Chapter 2. Chemical Probing of 4.5S RNA – Protein Interactions

Abstract Using standard chemical RNA footprinting methods, we have probed 4.5S RNA in order to identify bases within the RNA that play a functional role during the SRP targeting cycle. From these studies we have identified critical bases that comprise the binding site for Ffh. Upon complex formation between Ffh and 4.5S RNA, several phyllogenetically conserved bases were protected from chemical modification, suggesting they might be directly interacting with Ffh. This is in close agreement with independently obtained results using similar methods (Lentzen et al., 1996). In addition, crystal structures of the free 4.5S RNA (Jovine, et al., 2000) as well as a crystal structure of the M-domain-4.5S RNA domain IV complex (Batey et al., 2000) corroborate our footprinting results. Additionally, we probed 4.5S RNA in the presence of other interacting components from the SRP pathway: ribosomes, FtsY, GTP, GDP and signal sequence peptides. However these footprinting experiments failed to identify any RNA elements which might be critical for interaction with these various components.

Introduction

In many biochemical processes carried out by RNA-protein complexes, the RNA components have been found to carry out interesting functional roles. Examples of this include the RNA component of RNAseP (Guerrier-Takada et al., 1983), group I self-splicing introns (Kruger et al., 1982), and even the ribosomal RNA (Noller et al., 1992). We were interested in determining whether SRP RNA played an active functional role in the SRP targeting cycle.

In previous work, different RNA modification patterns were observed on the mammalian SRP RNA when it was probed in a polysome-associated state versus a membrane-bound state (Andreazzoli and Gerbi, 1991). From these findings it seemed likely that the SRP RNA was interacting with other components of the SRP cycle, the obvious candidates being the ribosome-nascent chain complex and the SRP receptor. We wished to extend this analysis in a more refined purified system with the hope of identifying specific interactions between the RNA and these other components.

We chose to biochemically probe this question in *E. coli* for several reasons. First, large quantities of pure Ffh, 4.5S RNA, ribosomes, and FtsY were easily obtainable. Second, the Ffh/4.5S RNP represents the most phylogenetically conserved core portion of SRP and mediates the crucial interactions of the SRP targeting pathway. Thus, we assumed that the *E. coli* system would serve as a paradigm for understanding the role of domain IV of the SRP RNA.

The initial motivation for these experiments came from preliminary fluorescence studies that argued for the existence of a high affinity interaction between Ffh/4.5S RNP and ribosomes. Addition of salt-washed ribosomes to a Ffh/3'-fluorescein-4.5S RNP was found to cause a dramatic change in the dye's fluorescence anisotropy. The change in fluorescence anisotropy when analyzed as a function of ribosome concentration suggested a very tight affinity, on the order of 10^{-9} M. Moreover, this interaction did not require the ribosomes to be in a translating state. This argued for the existence of a specific site on the ribosome for the binding of the Ffh/4.5S RNP, which we hoped to map experimentally. Therefore, we set out to determine whether 4.5S RNA played a major role in the interaction between Ffh/4.5S RNP and the ribosome, perhaps through 4.5S RNA-rRNA contacts.

At the time this project was started, we also knew that 4.5S RNA enhanced the interaction between Ffh and FtsY as monitored by GTPase activity and affinity resin binding (Miller et al., 1994). Similar observations had been made in the mammalian system as well suggesting that this was a conserved function of SRP RNA (Miller et al., 1993). We felt that perhaps 4.5S RNA was directly interacting with FtsY in order to increase the apparent affinity between the two proteins.

Finally, we wished to ask if small ligands such as signal sequences and nucleotides had a structural impact on 4.5S RNA. Probing these small ligand interactions seemed rather straightforward in this purified biochemical system. We hoped that probing all of these interacting components with respect to 4.5S RNA might give us insights into what mechanistic role, if any, 4.5S RNA was playing during the SRP-dependent protein targeting cycle.

Our strategy for identifying critical functional regions of 4.5S RNA was to employ RNA foot-printing techniques. Using base-specific chemicals that modify RNA in a way which can be readily detected by primer extension analysis, bases important for critical interactions can be identified (Moazed et al., 1986).These techniques had proven useful in the past as it had uncovered the binding sites for various ribosomal proteins (Powers et al., 1988; Stern et al., 1988a; Stern et al., 1988b; Stern et al., 1988c), elongation factors (Moazed et al., 1988), and the tRNAs on the ribosome (Moazed and Noller, 1989). We also performed hydroxy radical probing experiments on the 4.5S RNA with the hope of complementing our base specific probing studies. This technique has proven useful in yielding high resolution structural information about RNA molecules (Latham and Cech, 1989).

From this work, we were able to identify RNA bases critical for interaction between Ffh and 4.5S RNA. These results are in close agreement with RNA probing experiments independently carried out by others (Lentzen et al., 1996). Moreover, a recent crystal structure of the M-domain-4.5S RNA domain IV complex provides a structural picture which clearly explains our observations at the molecular level (Batey et al., 2000). Many of the protected bases are found in this structure to make close contacts with amino acid residues of the M-domain.

While we have been able to map the binding site of Ffh on 4.5S RNA, our chemical probing studies failed to identify any changes in 4.5S RNA in response to other components of the SRP-targeting pathway. Neither FtsY nor ribosomes caused a change in the modification pattern on 4.5S RNA. In addition, small molecule ligands such as signal sequences and nucleotides failed to affect the RNA's conformation as evidenced by the chemical probing results. In summary, our studies provided a detailed picture of the Ffh binding site but failed to extend a functional role for 4.5S RNA within the context of the Ffh/4.5S RNP functional cycle.

Materials and Methods

Cloning of a 4.5S RNA $^{3'5'\,del}$ template for *in vitro* transcription

The following primers were used to generate a T7 RNA Polymerase based transcription template which produced a shortened 4.5S RNA containing only bases 23-101 ($4.5^{3'5'del}$). The RNA was shortened in order to facilitate primer extension analysis during the footprinting studies. The construct was made by performing PCR on plasmid pSN1 (ref) using the following primers, 5'-GGAATTCTAATACGACTCACTCACTATAGGGCAA-3' and 5'-GGGAAAGGATCCCCAGCTACATCCCGG-3'. The PCR fragment was digested with EcoRI and BamHI and ligated into the corresponding sites within pUC19. The construct produced, pPSP1, was verified by sequencing.

In vitro transcription and gel isolation of the 5'3'deletion 4.5S RNA ($4.5S\ RNA^{3'5'del}$)

For each reaction, 10 μg of template, pPSP1, was linearized with BamHI prior to the transcription reaction. The buffer conditions for the transcription reaction were as follows: 40 mM Tris•HCl, pH 8.1, 22 mM $MgCl_2$, 5 mM DTT, 2mM spermidine, 50 μg/ml BSA. Each of the NTPs were at 4 mM. RNAsin and pyrophosphatase were present at 1200 units and 0.2 units respectively. T7 RNA Polymerase (0.1 mg) was used in each reaction. The reaction was incubated at 37°C for 1 hour.

Gel Purification of the in vitro transcript

The transcripts were purified on a 0.25 M citric acid, pH 3.5, 8 M Urea, 10% polyacrylamide gel which was run in 0.25 M citric acid, pH 3.5 running buffer. The acid urea gels were the best means of completely denaturing the RNA and isolating the correct transcript by gel purification. The RNA was located on the gel using UV shadowing. The appropriate gel slab was cut out, crushed, and soaked in 500 μl of 0.3 M sodium acetate, pH 6.5, 0.2% SDS, and 5 mM EDTA and 500 μl of water saturated phenol. The aqueous phase was extracted with 3 times with an equal volume of phenol and 3 times with an equal volume of chloroform/isoamyl alcohol (1:29 vol/vol) mixture. The RNA was ethanol precipitated overnight. After centrifugation, the pellet was washed in 75% ethanol and resuspended in ddH_2O. The RNA concentration was determined by measuring the sample's absorbance at 260 nm and using the following extinction coefficient: 1 A_{260} = 40 μg/ml.

Base Specific Chemical Probing of the 4.5S RNA

Chemical probing reactions were performed as previously described (refs). Typically 1 μM (about 2 μg) of 4.5S $RNA^{3'5'del}$ was probed per reaction in a 100 μl volume. Ffh was typically present in 4-fold molar excess over the RNA. Initial footprinting experiments with Ffh were performed in the following buffer conditions: 50 mM Hepes, pH 7.5, 250 mM KOAc, 5mM $Mg(OAc)_2$, and 0.01% Nikkol. Addition of either 20 μl of DMS (1:10 diluted in ethanol) or 20 μl of kethoxal (diluted in ethanol typically 1:250) initiated the chemical modification reactions, which were performed at 25°C for 30 minutes. For the DMS probing, the reactions were stopped with 1.0 M Tris acetate, pH 7.5 , 1.0 M β-mercaptoethanol, and 1.5 M sodium acetate prior to organic extractions. Modified RNA was then extracted 3 times with phenol and 3 times with a chloroform/isoamyl alcohol mixture (1:29 vol/vol). The RNA was precipitated in ethanol overnight. After pelleting the RNA in a microcentrifuge, the pellet was routinely washed with 75% ethanol. For the primer extension reactions, typically 0.5 - 1.0 pmoles of RNA was analyzed per reaction. For probing reactions involving nucleotides, signal sequences, FtsY, or ribosomes, the following buffer condition was used: 50 mM Hepes, pH 7.5, 50 mM KOAc, 2 mM $Mg(OAc)_2$, and 0.01% Nikkol.

Cleavage of RNA with Fe(II)-EDTA

A slight modification of the method described by (Latham and Cech, 1989). was used to probe the 4.5S $RNA^{3'5'del}$ in the absence and presence of Ffh. Reaction volumes were typically 25 µl. On the edges of the reaction tubes above the samples were spotted 1 µl of each of the following reagents: 50 mM $Fe(NH_4)_2(SO_4)_2$, 100 mM EDTA, 250 mM ascorbate, and 2.5% H_2O_2. The tubes were centrifuged in a microfuge to mix the droplets with the rest of the sample and initiate the modification reaction. The samples were incubated at 4°C for 10 minutes. The samples were then extracted three times with water-saturated phenol followed by three extractions with chloroform/isoamyl alcohol mixture (1:29 vol/vol). One tenth volume of 3 M NaOAc was added to the samples followed by precipitation of the RNA with 2.5 volumes of ethanol. The RNA pellets were washed with 75% ethanol. The RNA was then resuspended in a suitable concentration for primer extension analysis as described below.

Labeling of the Primer for Primer Extensions

For primer extension analysis of 4.5S RNA, the following oligonucleotide was used: 5′-CCAGCTACATCCCGGCA-3′. Typically, 20 pmoles of the oligonucleotide was labeled on the 5′ end with T4 polynucleotide kinase. Labeling conditions was done for 1 hour at 37°C in the following buffer conditions: 100 mM Tris•HCl, pH 8.0, 30 mM magnesium chloride, 10 mM DTT. [γ^{32}P] ATP (20 μCi) was typically used in each reaction. The labelled oligonucleotide was typically separated from the unincorporated label by gel exclusion chromatography using a NAP-5 column (Pharmacia) equilibrated with 10 mM sodium phosphate, pH 7.0.

Primer Extension Analysis

For the annealing of the ^{32}P-labelled primer to the RNA, 0.5 pmoles of primer was mixed with 0.5-1.0 pmoles of RNA in a total volume of 5 μl. The annealing was carried out in the following buffer: 50 mM Tris pH 8.3, 60 mM NaCl, 10 mM DTT. The reactions were heated to 90°C for 5 minutes and then slowly cooled to room temperature. To this was added 6 μl of the following: 1.33 mM dNTPs and 6U of reverse transcriptase in the following buffer: 17 mM Tris, pH 8.3, 20 mM

NaCl, 3.3 mM DTT, and 10 mM $Mg(OAc)_2$. The reactions were initially incubated at 37°C for 5 minutes followed by incubation at 42°C for 20 minutes. For the sequencing reactions a final concentration of 1 mM stock for each ddNTP was added to the appropriate reaction. Reactions were then analyzed on 10% polyacrylamide, 1X TBE, 8 M urea gels.

Results

Domain IV of SRP RNA

As shown in Figure 1, 4.5S RNA contains the highly conserved Domain IV of SRP RNA. This domain is characterized by two highly conserved loops, one of which is referred to as the symmetric internal loop (shown in red) and the other of which has been designated the asymmetric internal loop (shown in blue). In addition, there is sequence conservation in the tetraloop at the tip of Domain IV (shown in green). This small domain, Domain IV, represents the most evolutionarily conserved element of the SRP RNA (Poritz et al., 1988).

Binding of Ffh causes a change in the chemical modification patterns of 4.5S RNA

In order to identify important elements for Ffh binding, we performed chemical modification studies in the presence and absence of Ffh. For specific modification of adenosine and cytosine residues, we employed dimethyl sulfate, or DMS. DMS modifies the N1 of adenine and the N3 of cytidine. For guanosine residues, kethoxal was the modification reagent used because it specifically reacts with the N1 and N2 of guanine. For higher resolution probing to complement the base specific approach, we used hydroxyl radical cleavage which is directed against the RNA's phosphate backbone.

Upon binding Ffh, many conserved bases become protected from chemical modification. As shown in Figure 2, A39 and A47 become protected from modification by DMS (as indicated by the arrows). In addition, G48, G49, and G61 are blocked from modification by kethoxal (also indicated by arrows). Using the hydroxy radical probes, we also observed protected stretches of the phosphate backbone which flanked these particular bases (as indicated by the brackets).

Figure 3 shows a summary of the Ffh footprint pattern on 4.5S RNA. Additionally A68 was also observed to be protected by Ffh (see Figures 4 and 5). The protections tend to cluster into two specific regions, namely the symmetric and asymmetric internal loops as indicated by the red shading. Stretches of the phosphate backbone (the grey shaded regions) that overlap with the protected bases also appear to be shielded from hydroxyl radical cleavage upon the binding of Ffh. The correlation of the two patterns is very strong. For the most part, these footprinting results were in close agreement with a similar study carried out independently by Lentzen, et al (Lentzen et al., 1996). These results also agree well with previous mutagenesis work that implicated critical bases within 4.5S RNA for Ffh binding (Wood et al., 1992). Most of these positions, as one might expect, are the highly conserved positions.

From the modification patterns presented here, it is not clear how much of a conformational change 4.5S RNA undergoes upon interacting with Ffh. Position A63 becomes more susceptible to DMS modification upon binding Ffh as indicated by the large arrow in Figure 3 (see Figures 4 and 5 for the actual data). This would be suggestive of a slight change in the conformation of the RNA. Comparison of the NMR structure of the unbound 4.5S RNA Domain IV and the crystal structure of the M-domain/Domain IV complex reveals a dramatic conformational rearrangement in the RNA upon interaction with Ffh (Batey et al., 2000; Schmitz, 1999). A comparison of a crystal structure of 4.5S RNA domain IV with that of the complex (Jovine, et al., 2000; Batey et al., 2000), however, suggests that the RNA undergoes little conformational change upon binding the M-domain. While our modification results, particularly of the asymmetric loop for the unbound 4.5S RNA domain IV agrees closely with the two crystallographic structures, the footprinting results cannot conclusively resolve this issue.

Interestingly, many bases within 4.5S RNA were still highly reactive to DMS and kethoxal as designated by the smaller arrows in Figure 3. As many of these bases are highly conserved, we reasoned that these residues must be conserved for interaction with some other molecule other than the Ffh protein. Therefore, we next turned our attention to signal sequence peptides.

Probing signal sequence –4.5S RNA interactions

In order to probe the effects of signal sequence binding, we used signal sequence peptides as a model system. A set of two specific peptides was employed in this footprinting study. These peptides, termed the dm peptide and the R2 peptide, are derived from the signal sequence of lamB in *E. coli*. This dm peptide, serving as a negative control for these studies, has been demonstrated to be inactive as a targeting sequence both from *in vivo* and *in vitro* work (Chen et al., 1987; Emr and Silhavy, 1983). A deletion within dm peptide places a proline and a glycine close enough to each other to disrupt the α-helical structure of the peptide (McKnight et al., 1989). The r2 peptide is almost completely identical to the dm peptide, with the exception of a single point mutation where the proline has been changed to a leucine. This point mutation restores the peptides ability to adopt an α-helical conformation and restores the peptides ability to function as a signal sequence (McKnight et al., 1989) .

We knew indirectly from previous GTPase and GTP-crosslinking studies that the r2 peptide interacted with Ffh whereas the dm peptide did not (Miller et al., 1994). The r2 peptide inhibited both of these activities and appeared keep Ffh stabilized in a nucleotide-free state. Meanwhile, the dm peptide displayed no effects presumably because it does not interact with Ffh.

We therefore set out to chemically probe 4.5S RNA in the presence of Ffh with both of these peptides. As shown in Figure 4, no novel protections or modification enhancements were seen on 4.5S RNA in the presence of the r2 peptide. We initially probed with DMS because of the abundance of conserved adenines and cytidines found within domain IV of the RNA (Figure 1). As seen in Figure 5, the expected protection pattern from Ffh was obtained in these assays and served as an internal control to verify that our probing conditions were indeed working.

Oddly, some very subtle footprinting differences were observed in the presence of the peptides. As indicated by the asterix in Figure 4, bases A30, A55, A56, A63, and A76 appeared to be slightly more reactive to DMS in the presence of the peptides. These observations are interesting mainly because many of these positions are within the tetraloop which has been recently been determined to be quite near the signal sequence binding pocket (Bate y et al., 2000). However, we feel that these modest are changes are not of any biological relevance for two major reasons. In the first place, these enhancements were certainly less than two fold. Perhaps more importantly, the changes were seen even in the presence of the negative control dm peptide.

Probing 4.5S RNA for interactions with FtsY, GppNHp and GDP

While signal sequences did not appear to affect 4.5S RNA's footprint, we shifted our attention to FtsY, GDP, and GppNHp. At the outset of the experiments, we were confident that we would observe a footprint by FtsY on the 4.5S RNA. At the time these experiments were carried out it was thought that the interaction between Ffh and FtsY absolutely required 4.5S RNA. This simplest model therefore would have 4.5S RNA directly interacting with FtsY in order to substantially increase the affinity of Ffh/4.5S RNP for FtsY.

We were therefore very surprised to find no footprint from FtsY on 4.5S RNA from our DMS probing. As Figure 5 clearly shows, no changes in the modification pattern of 4.5S RNA appeared within in response to FtsY binding. This data, however, does not entirely rule out the possibility of contacts between 4.5S RNA and FtsY. A complete probing approach using kethoxal and hydroxy radicals would be required to come to this conclusion.

We were able to ascertain that FtsY was indeed binding to the Ffh/4.5S RNP complex. For this we took advantage of the fact that our FtsY protein was fused to GST. We were therefore able to perform affinity chromatography tests on a portion of our reaction mixtures before the modifaction step with DMS. As Figure 6 shows, specific binding was observed between our Ffh/4.5S RNP and FtsY. This binding was GppNHp dependent as had been previously observed (compare 6A and 6B).

From the control reactions in Figure 5 (lanes 8 and 10 from the left), we were able to simultaneously probe the Ffh/4.5S RNP in response to GppNHp and GDP. No specific changes were seen in the RNA's modification pattern in the presence of GppNHp or GDP. As we only looked at a DMS modification pattern, our probing was only base specific to adenines and cytidines within the RNA. This does not, therefore, rule out the possibility that subtle changes might be occurring within other portions of the RNA, such as the phosphate backbone or the other bases not targeted by DMS.

DMS probing of Ffh/4.5S RNP in the presence of ribosomes and ribosomal subunits

We therefore probed 4.5S RNA with DMS in the presence of either 70S monosomes, 30S subunits, or 50S subunits. As Figure 7 shows, no clear change in the DMS modification pattern was observed on the RNA when the Ffh/4.5S RNP was mixed with these various components. We turned our attentions to the rRNA in order to see if we could identify a discrete binding site for the Ffh/4.5S RNP on the ribosome.

Ribosomal RNA was probed with DMS in the presence and absence of the Ffh/4.5S RNP. Primer extension analysis of approximately 80% of the 23S rRNA failed to identify a potential binding site for the Ffh/4.5S RNP (data not shown). These observations taken together suggested that a high affinity interaction between Ffh/4.5S RNP and the ribosomes did not exist. Concurrently with our footprinting observations, we went on to demonstrate that the fluorescence assay was not monitoring a physiologically relevant ribosome-Ffh/4.5S RNP interaction (Appendix 1). In addition, other methods failed to detect binding between the two complexes (see Appendix 1). Therefore, we ruled that a high affinity interaction between Ffh/4.5S RNP and the ribosome was unlikely to occur in the absence of translating signal sequences.

Discussion

We have determined the minimal binding site on the 4.5S RNA for the Ffh protein using chemical probing methods directed against the RNA. Ffh protects bases within both the symmetric and asymmetric internal loops of the RNA. Many of these bases not surprisingly are phylogenetically conserved. When this work was initially carried out, we suspected that the protections by Ffh were due to direct physical contacts between the protein and these various positions. The recent crystal structure of the Ffh M-domain-4.5S RNA Domain IV complex has shown that some of these interpretations are correct and that other modification patterns are due to RNA structural reasons as well (Batey et al., 2000).

In the symmetric internal loop, the protected A47 forms a base pair interaction with C62 and is positioned in close contact with the M-domain. Amino acids Asn389 and Ser381 make specific contacts with A47 and C62 respectively. The protected G48 and G49 are found to make direct contacts with the M-domain and serve to maintain the RNA's structure within the complex. G49 interacts with Ser406 in addition to maintaining base pair interactions with A60. Meanwhile, G48 hydrogen bonds with G61, coordinates a potassium ion, and makes contacts with Ser381. Finally, G61 is seen making direct contacts with Gly405 of the M-domain, which explains its protection from kethoxal modification.

In terms of the asymmetric internal loop, A39 is the sole base which makes direct contact with the M-domain as shown in Figure 8. Upon binding Ffh, A39 makes direct contacts with Ser397 and Arg401 of the M-domain. The N1 atom (dark blue spheres in Figure 8B) of this base is buried within the protein-RNA interface and protected from modification. C40, C41, and A42 meanwhile remain highly solvent accessible as seen in Figure 8B. In accordance with this structure these bases are highly susceptible to modification both in the presence and absence of Ffh.

The hydroxyl radical protections make sense in light of this recent crystal structure. Looking closely at the structure, these regions are completely buried within the center of the complex and thus shielded from solvent.

Our results do not rule out the existence of a specific interaction between portions of the Ffh/4.5S RNP and the ribosome. As we probed the ribosome in the absence of translation using as assay which was not monitoring a relevant interaction (see Appendix 1), one can only conclude from the data presented here that we have yet to identify the appropriate conditions for ribosome binding. Since this work, functional interactions of the Ffh/4.5S RNP with ribosome-nascent chains has been observed in vitro (Powers and Walter, 1997; Valent et al., 1995; Valent et al., 1998). Perhaps the interaction requires occupancy of the M-domain with a signal sequence in order to convert the Ffh/4.5S RNP into a state which has a high affinity for ribosomes. In addition, studies have suggested that the conformational state of the ribosome may be an influencing factor upon whether an interaction with the Ffh/4.5S RNP can occur (Brown, 1987; Brown, 1989; Ogg and Walter, 1995).

Perhaps the most surprising observations from this work lies in the fact that we were unable to see additional changes in the footprint in response to FtsY. The simplest model from the GTPase work at that time strongly suggested that 4.5S RNA was likely to make direct contacts with the receptor. While we hadn't performed a complete analysis of this interaction with the kethoxal and hydroxyl radical probes, the negative result from the DMS probing suggested that a footprint was unlikely because adenine and cytidine bases comprise a majority of the conserved bases within Domain IV. Recently we have learned that others have in failed to observe a footprint from FtsY after a more extensive effort (Junutula Jagath, personal communication). It is very possible that 4.5S RNA operates indirectly through structural changes in Ffh to enhance the interaction with FtsY. From this perspective, we focused our attention to developing biochemical assays to better understand the various steps in the GTPase reaction as will be detailed in Chapters 3 and 4.

The recent crystal structure of the Ffh M-domain-4.5S RNA Domain IV complex makes it tempting to speculate that the RNA could serve as a sensor for signal sequence occupancy (Batey et al., 2000; Walter et al., 2000). While the negative footprinting results presented here would tend to argue against this notion, it is possible that the solvent accessible guanidines, G53 and G54, might be involved in signal sequence recognition. DMS probing would have failed to uncover this. Perhaps, kethoxal probing or hydrolxyl radical probing may uncover changes within or near the tetraloop that are undetectable by the DMS approach.

Lastly, our failed efforts with respect to the ribosome footprinting studies can be explained simply by the fact that we had no physical proof for the existence of an Ffh/4.5S RNP•ribosome complex in the absence of a translating nascent chain. Subsequently, we determined that the fluorescence anisotropy changes were an artifact of a non-physiologically relevant aggregation phenomenon with Ffh at very low ionic conditions.

More recently, develolpment of an *in vitro* targeting assay has demonstrated a direct interaction between Ffh/4.5S RNP and the ribosome. However, in this context, the ribosome is translating a nascent chain bearing a signal sequence. It remains entirely possible that the signal sequence is required to induce the Ffh/4.5S RNP into a high affinity state for stable interaction with the ribosome. In our studies without signal sequences, we would not have been able to obtain this putative high affinity state. Alternatively, from work in *E. coli* and *S. cerevisaiae* has suggested that the ribosome needs to be in a particular conformation in order to interact with SRP. As we made no attempts to lock our ribosomes into a specific conformation, perhaps this might explain our inability to form a complex between Ffh/4.5S RNP and the ribosome. Perhaps future efforts along these lines will be able to uncover the binding site for Ffh/4.5S RNP on the ribosome eventually.

References

Andreazzoli, M., and S.A. Gerbi. 1991. Changes in 7SL RNA conformation during the signal recognition particle cycle. *EMBO J.* 10:767-777.

Batey, R.T., R.P. Rambo, L. Lucast, B. Rha, and J.A. Doudna. 2000. Crystal structure of the ribonucleoprotein core of the signal recognition particle. *Science* 287:1232-1239.

Brown, S. 1987. Mutations in the gene for EF-G reduce the requirement for 4.5S RNA in the growth of E. coli. *Cell* 49:825-833.

Brown, S. 1989. Time of action of 4.5 S RNA in Escherichia coli translation. *J. Mol. Biol.* 209:79-90.

Chen, L., P.C. Tai, M.S. Briggs, and L.M. Gierasch. 1987. Protein translocation into Escherichia coli membrane vesicles is inhibited by functional synthetic signal peptides. *J. Biol. Chem.* 262:1427-1429.

Emr, S.D., and T.J. Silhavy. 1983. Importance of secondary structure in the signal sequence for protein secretion. *Proc. Natl. Acad. Sci. U.S.A.* 80:4599-4603.

Guerrier-Takada, C., K. Gardiner, T. Marsh, N. Pace, and S. Altman. 1983. The RNA moiety of ribonuclease P is the catalytic subunit of the enzyme. *Cell* 35:849-857.

Jovine, L., T. Hainzl, C. Oubridge, W. G. Scott, J. Li, T. K. Sixma, A. Wonacott, T. Skarzynski, K. Nagai. 2000. Crystal structure of the ffh anf EF-G binding sites in the conserved domain IV of Escherichia coli 4.5S RNA. Structure Fold. Design 8: 527-40.

Kruger, K., P.J. Grabowski, A.J. Zaug, J. Sands, D.E. Gottschling, and T.R. Cech. 1982. Self-splicing RNA: autoexcision and autocyclization of the ribosomal RNA intervening sequence of Tetrahymena. *Cell* 31:147-157.

Latham, J.A., and T.R. Cech. 1989. Defining the inside and outside of a catalytic RNA molecule. *Science* 245:276-282.

Lentzen, G., H. Moine, C. Ehresmann, B. Ehresmann, and W. Wintermeyer. 1996. Structure of 4.5S RNA in the signal recognition particle of Escherichia coli as studied by enzymatic and chemical probing. *RNA* 2:244-253.

McKnight, C.J., M.S. Briggs, and L.M. Gierasch. 1989. Functional and Nonfunctional LamB Signal Sequences Can Be Distinguished by Their Biophysical Properties. *J. Biol. Chem.* 264:17293-17297.

Miller, J.D., H.D. Bernstein, and P. Walter. 1994. Interaction of E. coli Ffh/4.5S ribonucleoprotein and FtsY mimics that of mammalian signal recognition particle and its receptor. *Nature* 367:657-659.

Miller, J.D., H. Wilhelm, L. Gierasch, R. Gilmore, and P. Walter. 1993. GTP binding and hydrolysis by the signal recognition particle during initiation of protein translocation. *Nature* 366:351-354.

Moazed, D., and H.F. Noller. 1989. Interaction of tRNA with 23S rRNA in the ribosomal A, P, and E sites. *Cell* 57:585-597.

Moazed, D., J.M. Robertson, and H.F. Noller. 1988. Interaction of elongation factors EF-G and EF-Tu with a conserved loop in 23S RNA. *Nature* 334:362-364.

Moazed, D., S. Stern, and H.F. Noller. 1986. Rapid chemical probing of conformation in 16 S ribosomal RNA and 30 S ribosomal subunits using primer extension. *J. Mol. Biol.* 187:399-416.

Noller, H.F., V. Hoffarth, and L. Zimniak. 1992. Unusual resistance of peptidyl transferase to protein extraction procedures. *Science* 256:1416-1419.

Ogg, S.C., and P. Walter. 1995. SRP Samples Nascent Chains for the Presence of Signal Sequences by Interacting with Ribosomes at a Discrete Step during Translation Elongation. *Cell* 81:1075-1084.

Poritz, M.A., K. Strub, and P. Walter. 1988. Human SRP RNA and E. coli 4.5S RNA contain a highly homologous structural domain. *Cell.* 55:4-6.

Powers, T., S. Stern, L.M. Changchien, and H.F. Noller. 1988. Probing the assembly of the 3' major domain of 16 S rRNA. Interactions involving ribosomal proteins S2, S3, S10, S13 and S14. *J. Mol. Biol.* 201:697-716.

Powers, T., and P. Walter. 1997. Co-translational protein targeting catalyzed by the Escherichia coli signal recognition particle and its receptor. *EMBO J.* 16:4880-4886.

Schmitz, U., Behrens, S., Freymann, D.M., Keenan, R.J., Lukavsky, P., Walter, P., James, T.L. 1999. Structure of the phylogenetically most conserved domain of SRP RNA. *RNA* 5:1419-1429.

Stern, S., L.M. Changchien, G.R. Craven, and H.F. Noller. 1988a. Interaction of proteins S16, S17 and S20 with 16 S ribosomal RNA. *J. Mol. Biol.* 200:291-299.

Stern, S., D. Moazed, and H.F. Noller. 1988b. Structural analysis of RNA using chemical and enzymatic probing monitored by primer extension. *Methods Enzymol.* 164:481-489.

Stern, S., T. Powers, L.M. Changchien, and H.F. Noller. 1988c. Interaction of ribosomal proteins S5, S6, S11, S12, S18 and S21 with 16 S rRNA. *J. Mol. Biol.* 201:683-695.

Valent, Q.A., D.A. Kendall, S. High, R. Kusters, B. Oudega, and J. Luirink. 1995. Early events in preprotein recognition in E. coli: interaction of SRP and trigger factor with nascent polypeptides. *EMBO J.* 14:5494-5505.

Valent, Q.A., P.A. Scotti, S. High, J.W. de Gier, G. von Heijne, G. Lentzen, W. Wintermeyer, B. Oudega, and J. Luirink. 1998. The Escherichia coli SRP and SecB targeting pathways converge at the translocon. *EMBO J.* 17:2504-2512.

Walter, P., R. Keenan, and U. Schmitz. 2000. Perspectives: structural biology. SRP--where the RNA and membrane worlds meet. *Science* 287:1212-1213.

Wood, H., J. Luirink, and D. Tollervey. 1992. Evolutionary conserved nucleotides within the E. coli 4.5S RNA are required for association with p48 in vitro and for optimal function in vivo. *Nucleic Acids Res.* 20:5919-5925.

Figure 2-1: The conserved loops of Domain IV within 4.5S RNA. The three major loop regions within Domain IV are designated by their respective colors. The asymmetric loop is pictured in red, the symmetric loop is pictured in blue, and the tetraloop is pictured in green. The evolutionarily conserved bases within each loop are designated by the appropriate colors.

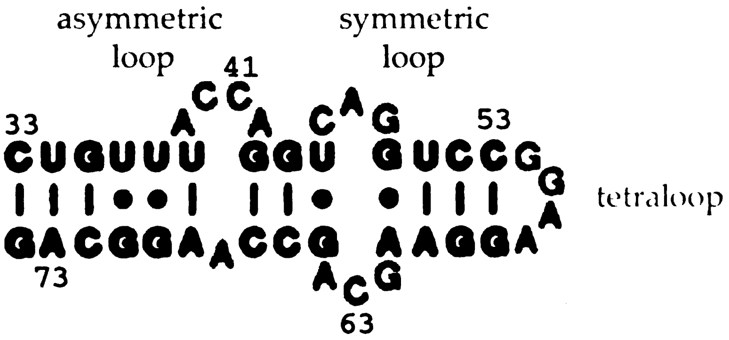
asymmetric loop
symmetric loop
41
33
53
CUGUUU GGU GUCCG
GACGGAACCG AAGGA
73
63
tetraloop

Figure 2-2: **Footprint of Ffh on 4.5S RNA using base specific and hydroxyl radical probing.** The conditions for each reaction reaction are noted above each lane appropriately. The designation "4.5S RNA" is meant to represent the 4.5S RNA$^{3'5'del}$ variant described in the Materials and Methods. Regions protected by Ffh from hydroxy radical cleavage are desgnated by the brackets. Base-specific protections or enhancements are designated by the arrows. The asterix denotes the atypical modification of position A60 by kethoxal which would seem unlikely given kethoxal's selectivity for guanidine.

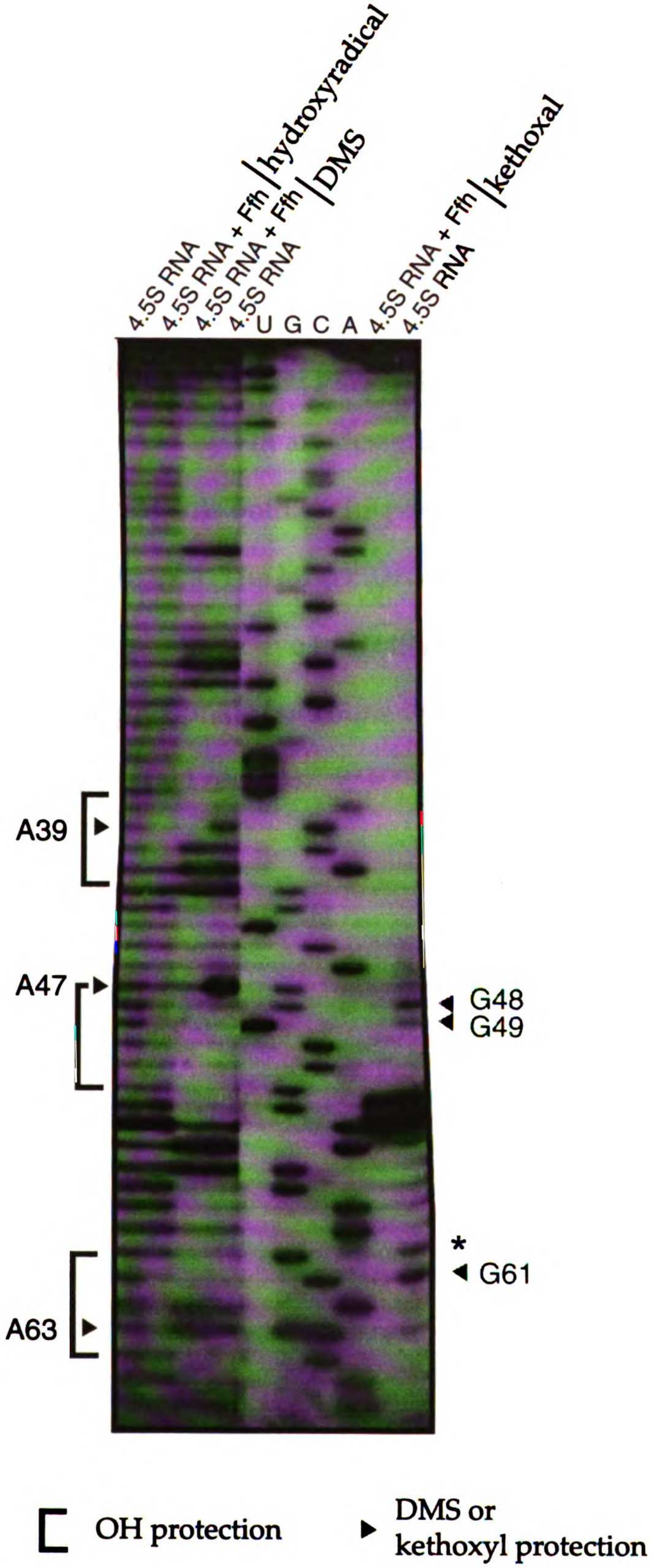
4.5S RNA
4.5S RNA + Ffh
hydroxyradical
4.5S RNA + Ffh
4.5S RNA
DMS
U
G
C
A
4.5S RNA + Ffh
4.5S RNA
kethoxal
A39
A47
A63
G48
G49
*
G61
OH protection
DMS or
kethoxyl protection

Figure 2-3: Composite of RNA chemical probing studies in the presence and absence of Ffh. Bases protected by Ffh are designated in red. Bases which are accessible to modification reagents both in the presence and absence of Ffh are designated by the smaller arrows. The larger arrow at position A63 denotes the fact that this base becomes more reactive to DMS modification in the presence of Ffh. Finally, regions of the phosphate backbone which are protected by Ffh are designated with the grey shaded regions.

4.5S RNA

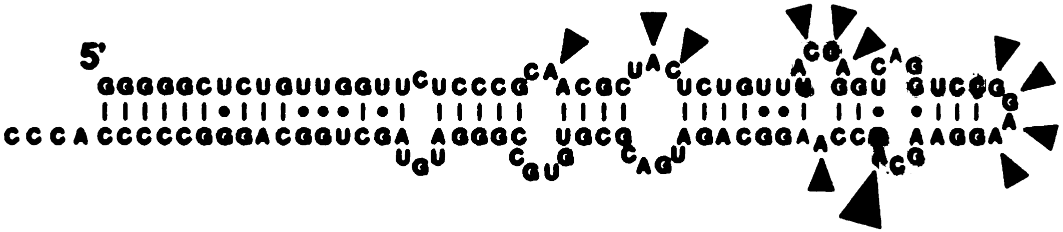
5'
GGGGGCUCUGUUGGUUCUCCCGCAACGCUACUCUGUUA CG ACGU CAG GUCGG
CCCACCCCCGGGACGGUCGAAGGGCUGCGAGACGGAACCAAGGA

▶ = **DMS or kethoxyl reactive bases in presence of Ffh**

● = bases protected by Ffh

= hydroxyradical backbone protections by Ffh

Figure 2-4:

Reaction co

designation

Materials an

designated b

designated b

Figure 2-4: RNA footprinting results with the signal sequence peptides. Reaction conditions are designated at the top of each lane accordingly. The designation "4.5S RNA" actually refers to the 4.5S$^{3'5'del}$ form as discussed in the Materials and Methods section. *Bona fide* protections or enhancements are designated by the arrows with the appropriate base position. Changes are designated by the asterix. See Results Section for more on these positions.

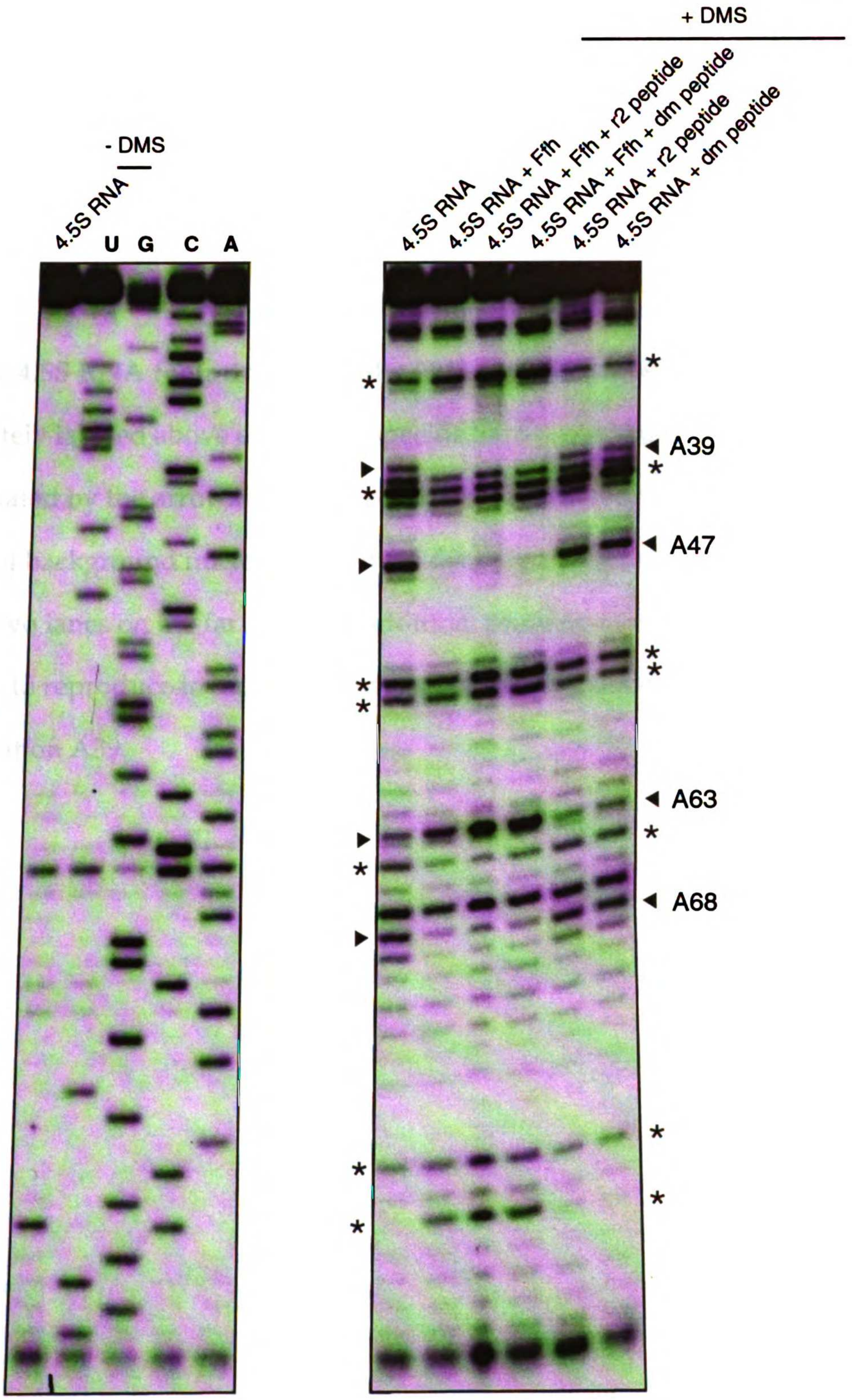
- DMS
4.5S RNA
U
G
C
A
+ DMS
4.5S RNA
4.5S RNA + Ffh
4.5S RNA + Ffh + r2 peptide
4.5S RNA + Ffh + dm peptide
4.5S RNA + r2 peptide
4.5S RNA + dm peptide
A39
A47
A63
A68

Figure 2-5: 4.5S RNA footprinting results with FtsY. Reaction conditions are appropriately labeled above each lane. Specific base protections or enhancements are designated by the arrows and the appropriate position designation. The presence of background nuclease activity is denoted by the asterix above position A39 (see two lanes on the far right). In addition, protections or enhancements that failed to reproduce in multiple assays are also designated by the asterix below position A39.

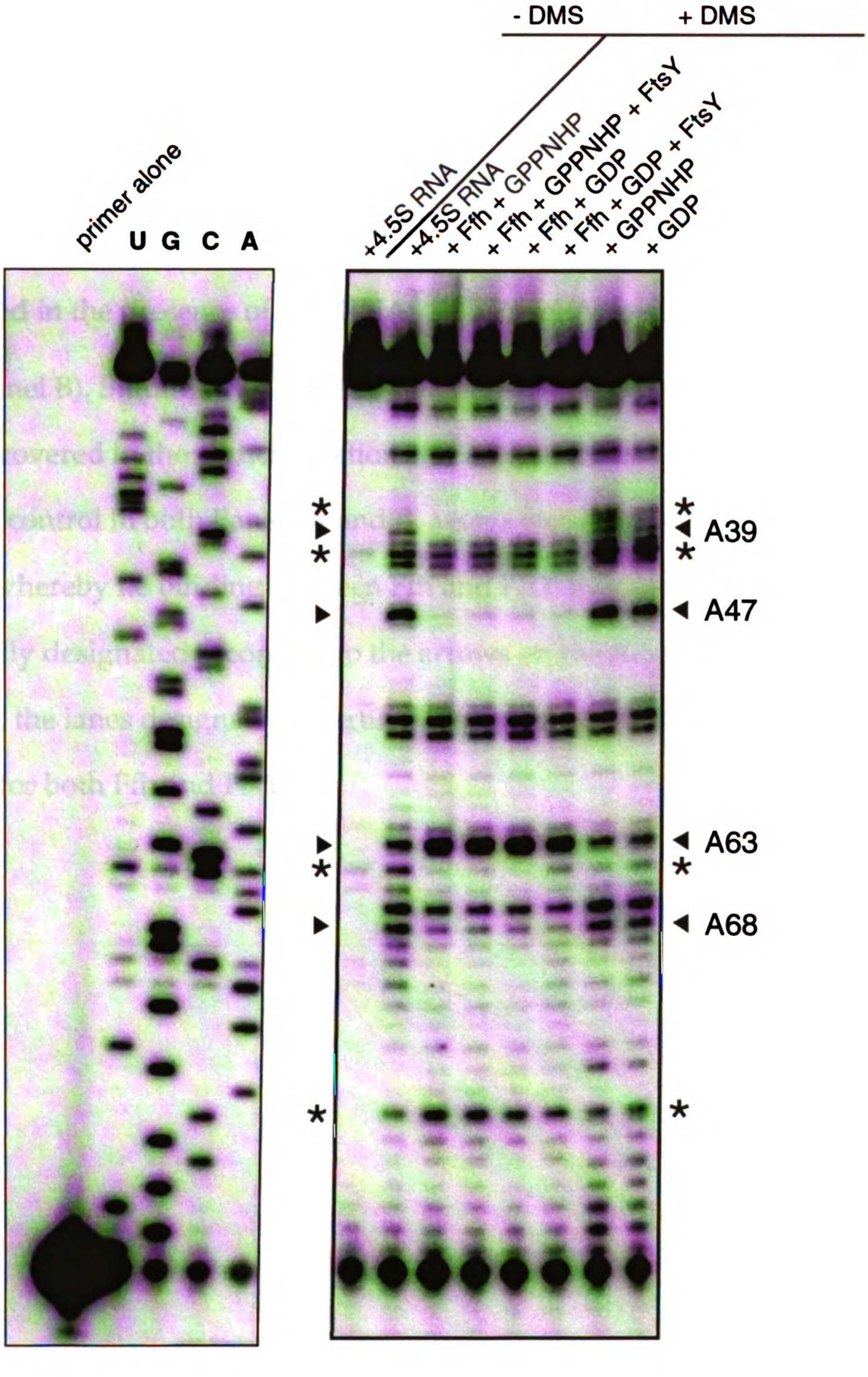
- DMS
+ DMS
primer alone
U
G
C
A
+4.5S RNA
+4.5S RNA
+ Ffh + GPPNHP
+ Ffh + GPPNHP + FtsY
+ Ffh + GDP
+ Ffh + GDP + FtsY
+ GPPNHP
+ GDP
A39
A47
A63
A68

Figure 2-6: Binding assay of Ffh/4.5S RNA$^{3'5'del}$ RNP with FtsY. Assays were performed in the presence of 4.5S RNA$^{3'5'del}$ (Panel A) versus the absence of the RNA (Panel B). Binding was assessed qualitatively based on the relative amounts of Ffh recovered in the elution fractions for each of the conditions tested. As a negative control in both Panels A and B, assays were carried out in the presence of GDP whereby no binding between Ffh and FtsY was expected. The bands are specifically designated according to the arrows on the sides of each gel. In addition, the lanes designated "starting" represented the total amount of protein assayed for both Ffh and FtsY.

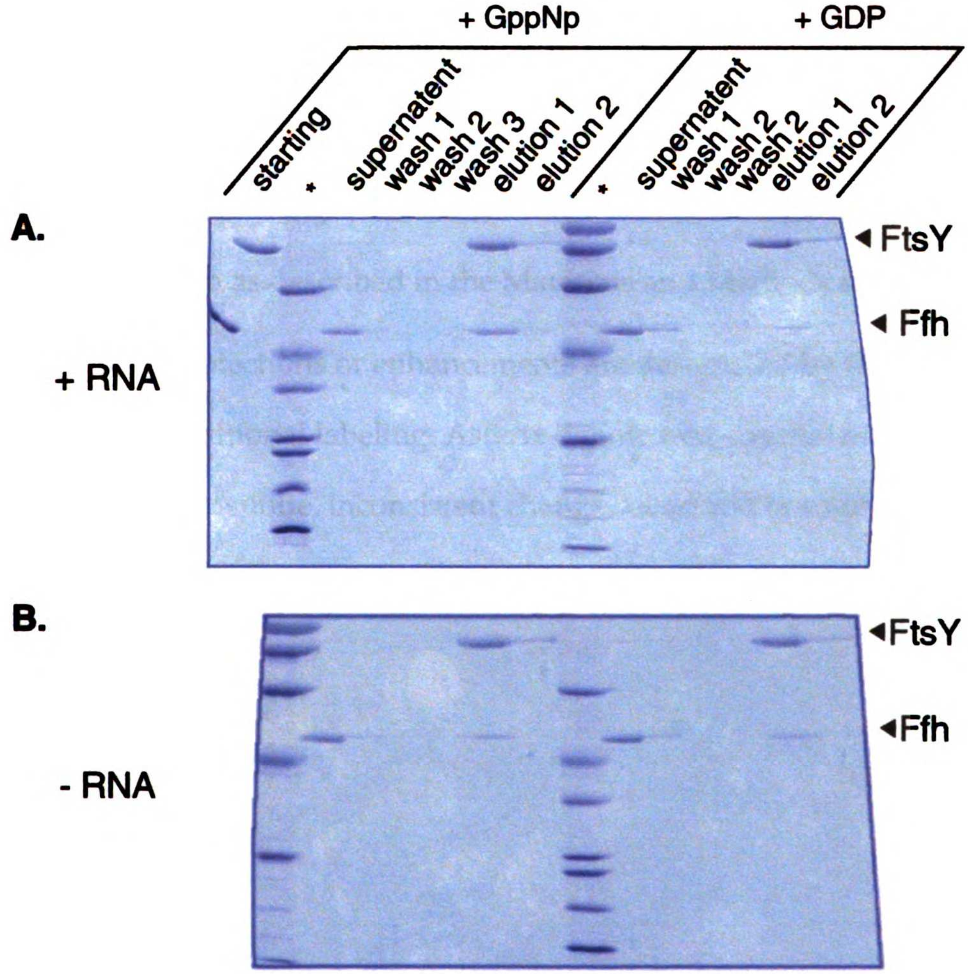
+ GppNp
+ GDP
starting
*
supernatent
wash 1
wash 2
wash 3
elution 1
elution 2
*
supernatent
wash 1
wash 2
wash 2
elution 1
elution 2
A.
+ RNA
FtsY
Ffh
B.
- RNA
FtsY
Ffh

Figure 2-7: Footprinting results with 70S ribosomes and ribosomal subunits. The various reaction conditions are appropriately labeled above each of the respective lanes accordingly. The designation "4.5S RNA" specifically means the 4.5S RNA$^{3'5'del}$ form as described in the Materials and Methods section.

Significant base protections or enhancements are designated by the arrows with the appropriate positional labeling. Asterix denote non-specific nuclease cleavages and other subtle, inconsistent changes observed but not considered to be significant.

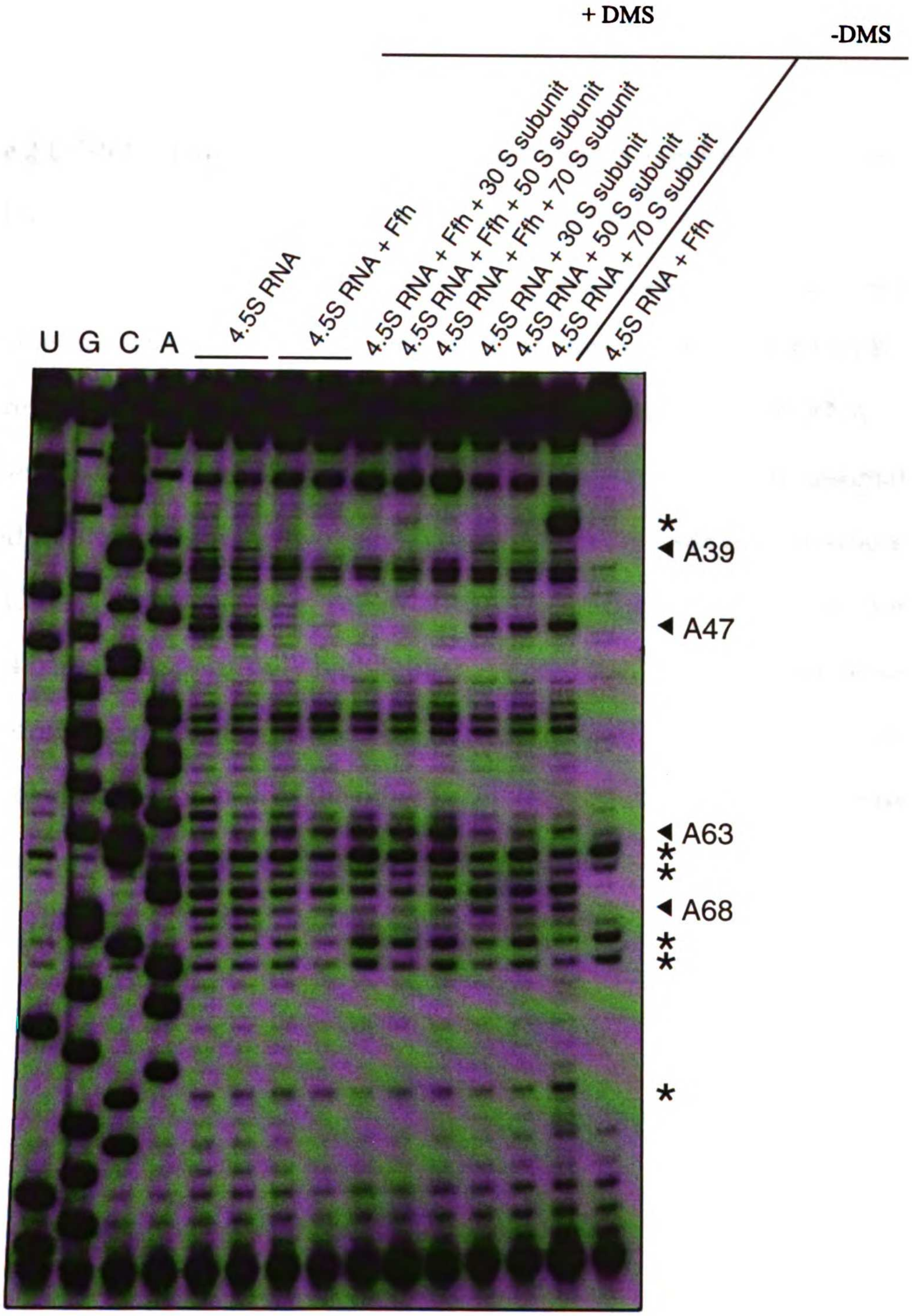
+ DMS
-DMS
U G C A
4.5S RNA
4.5S RNA + Ffh
4.5S RNA + Ffh + 30 S subunit
4.5S RNA + Ffh + 50 S subunit
4.5S RNA + Ffh + 70 S subunit
4.5S RNA + 30 S subunit
4.5S RNA + 50 S subunit
4.5S RNA + 70 S subunit
4.5S RNA + Ffh
*
A39
A47
A63
*
*
A68
*
*
*

Figure 2-8: Molecular basis for the protection of base A39 by Ffh. In Panel A, a model of the free 4.5S RNA is depicted as adapted from (Jovine, L, T., et al., 2000). Bases A39-A42 from the asymmetric loop are all seen to be highly solvent accessible as evidenced by their strong reactivity toward DMS. In Panel B, the same region is shown in a space-filled model of the M-domain-4.5S RNA complex as adapted from (Batey, R. T., et al., 2000). The same color designations are ued for the bases in the two panels: bases A39 is depicted in cyan whereas bases C40-A42 are depicted in yellow. The DMS-reactive nitrogen atoms for each of the 4 bases are specifically highlighted in dark blue. As can be clearly seen, the M-domain completely protects the nitrogen of base A39. Meanwhile, the reactive nitrogens for each of the other bases within the asymmetric loop remain highly solvent accessible, even in the presence of Ffh.

A.

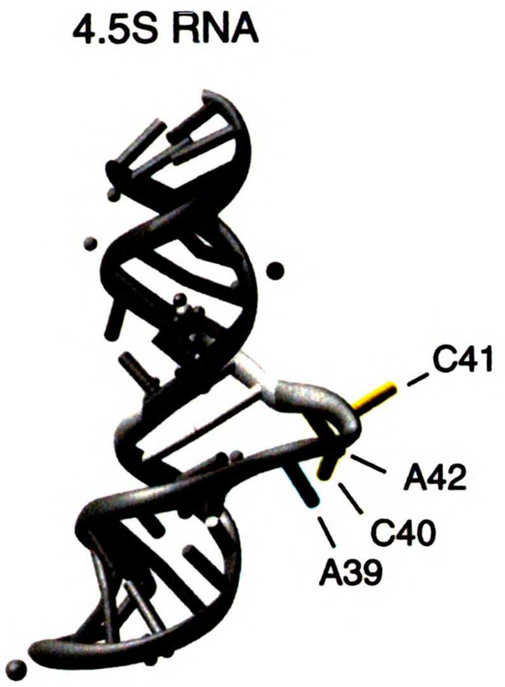
4.5S RNA
C41
A42
C40
A39

B.

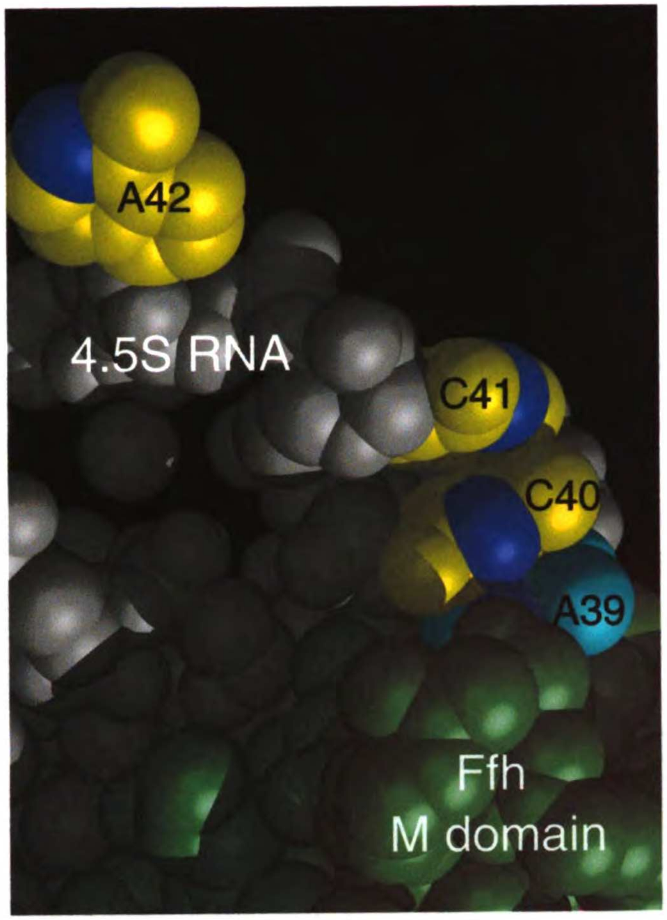
A42
4.5S RNA
C41
C40
A39
Ffh
M domain

Chapter 3. Catalytic Role of 4.5S RNA in Assembly of the Bacterial Signal Recognition Particle with Its Receptor

(published in *Science* 288:1640-1643)

Role of 4.5 S RNA in Assembly of the Bacterial Signal Recognition Particle with Its Receptor

Paul Peluso, Daniel Herschlag[1], Silke Nock, Douglas M. Freymann[3],
Arthur E. Johnson[2], and Peter Walter

Howard Hughes Medical Institute and
Department of Biochemistry and Biophysics
University of California at San Francisco
San Francisco, CA 94143-0448, USA

Tel.: 415-476-5017
Fax: 415-476-5233
walter@cgl.ucsf.edu

1 Department of Biochemistry, Stanford University, Stanford, CA 94305

2 Texas A&M University, System Health Science Center, College Station, TX 77843

3 present address: Department of Molecular Pharmacology and Biological Chemistry, Northwestern University Medical School, 303E Chicago Avenue, Chicago, IL 60611

The mechanism of signal recognition particle (SRP) and SRP receptor-mediated protein targeting to the endoplasmic reticulum or to the bacterial plasma membrane is evolutionarily conserved. In E. coli, this reaction is mediated by the Ffh/4.5S RNA ribonucleoprotein complex (Ffh/4.5S RNP; the SRP), and the FtsY protein (the SRP receptor). We have quantified the effects of 4.5S RNA on Ffh•FtsY complex formation by monitoring changes in tryptophan fluorescence. Surprisingly, 4.5S RNA facilitates both assembly and disassembly of the Ffh•FtsY complex to a similar extent. These results provide the first example of an RNA molecule facilitating protein•protein interactions in a catalytic fashion.

Ffh and FtsY are both GTPases (1-5) that interact with each other in a GTP-dependent manner and reciprocally stimulate each other's GTPase activity (6, 7). The GTPase domains of Ffh and FtsY define them as members of a GTPase subfamily with unique properties (8, 9, 10, 11). 4.5S RNA enhances association of Ffh and FtsY, which suggested a role for the RNA in stabilizing the complex (6). To analyze the role of 4.5S RNA in this reaction in more detail, we took advantage of the fact that FtsY contains tryptophan residues whereas Ffh contains none. This allowed us to monitor the interaction of Ffh and FtsY spectroscopically (Fig. 1). Recently, a similar assay was independently developed by Jagath and coworkers (12). In our studies we used an amino-terminally truncated version of FtsY (residues 48-494) that was previously shown to interact with Ffh in a manner indistinguishable from that of full-length FtsY (5).

Incubation of FtsY with Ffh/4.5S RNP in the presence of the non-hydrolyzable GTP analogue, GppNHp (5′-guanylylimidodiphosphate), shifted the tryptophan fluorescence emission maximum ~10 nm and increased the fluorescence intensity two-fold (Fig. 1A). This is consistent with burial of one or both of the tryptophans in a more hydrophobic environment upon formation of a Ffh•FtsY complex. These fluorescence changes occurred only in the presence of GppNHp and not in the presence of GDP (Fig. 1B), consistent with the GppNHp-dependence for complex formation determined by affinity chromatography (6).

Complex formation and stimulation of GTPase activity were previously shown to be dependent on the presence of 4.5S RNA. We were therefore surprised to observe that in the absence of 4.5S RNA, addition of GppNHp resulted in an increase and shift in fluorescence that was indistinguishable from that observed with the Ffh/4.5S RNP (Fig. 1C and 1D). To understand the origin of this paradox and the role of 4.5S RNA in complex formation, we carried out a kinetic and thermodynamic analysis of the reaction.

We compared the kinetics of association between Ffh and FtsY in the absence and presence of 4.5S RNA (Fig. 2A and B). The association with FtsY, monitored by fluorescence, was >100 fold faster for Ffh/4.5S RNP than for the same concentration of Ffh. Analogous determinations at a series of Ffh and Ffh/4.5S RNP concentrations gave second-order rate constants for association of k_{on} of 5.6×10^2 $M^{-1}s^{-1}$ and 9.2×10^4 $M^{-1}s^{-1}$, respectively (Fig. 2A and B, insets). These observed association rate constants are much smaller than those typically observed for protein-protein association of 10^6 - 10^8 $M^{-1}s^{-1}$ (13), suggesting that the association of SRP and its receptor requires conformational rearrangements.

The difference in association rate constants explains the apparent requirement for 4.5S RNA in previous GTP hydrolysis and binding studies. The Ffh•FtsY complex would not be expected to have formed over the time course and at the concentrations used in published assays (5 – 150 nM; 20 minutes). When Ffh•FtsY complex formation is driven by high concentrations of the interacting components, however, GTP hydrolysis is stimulated (Peluso and Walter, unpublished; ref 14).

The enhanced rate of complex formation might be readily explained if 4.5S RNA increases the affinity of FtsY for Ffh. This could arise, for example, if 4.5S RNA binding to Ffh preorders the protein for interaction with FtsY (15) or if 4.5S RNA interacts directly with FtsY. To test this prediction, we followed the dissociation of the Ffh/4.5S•FtsY and Ffh•FtsY complexes. Ffh•FtsY and Ffh/4.5S•FtsY complexes were preformed in the presence of GppNHp and the change in tryptophan fluorescence was monitored as a function of time following addition of an excess of GDP (Fig. 2C and D). After dissociation, Ffh and FtsY rapidly exchange GppNHp for GDP (data not shown; (16, 17)) and hence are trapped in the dissociated state.

To our surprise, the Ffh/4.5S•FtsY complex dissociated much faster than the Ffh•FtsY complex (Fig. 2C and D). The rate constant determined for the dissociation of the Ffh/4.5S•FtsY complex of $k_{off} = 3.3 \times 10^{-3}\ s^{-1}$ was 200-fold greater than the value for the Ffh•FtsY complex of $k_{off} = 1.2 \times 10^{-5}\ s^{-1}$. To confirm that the change in fluorescence observed upon addition of GDP indeed measured complex dissociation, we used two additional approaches: i) dilution, and ii) addition of an excess of an non-fluorescent mutant FtsY(W128F,W343F). Both approaches gave dissociation rate constants indistinguishable from those described above ($k_{off} = 5.1 \times 10^{-3}\ s^{-1}$ and $6.3 \times 10^{-3}\ s^{-1}$ for the Ffh/4.5S•FtsY complex via approach i and ii, respectively; data not shown). These rates are much slower than those measured for GppNHp release from the individual components; GppNHp release is therefore significantly slowed in Ffh•FtsY complexes, akin to "classical" GTPases that hold on tightly to bound nucleotides (18, 19). The decreased rate of nucleotide release from the complexes could be due to conformational changes in the nucleotide binding sites or to steric occlusion of the nucleotide exit routes.

The above results show that 4.5S RNA enhances dissociation of the complex between the Ffh and FtsY. A prediction arising from these observations is that addition of 4.5S RNA to preformed Ffh•FtsY complex would facilitate its dissociation. Addition of 4.5S RNA does indeed increase the dissociation rate (Fig. 2D inset). The observed 200-fold increase is the same, within error, as that described above, indicating that the Ffh•FtsY complex is rapidly and completely converted to the faster dissociating Ffh/4.5S•FtsY complex. This effect was specific for 4.5S RNA as addition of an equivalent amount of tRNA did not result in enhanced dissociation. These experiments show that the Ffh•FtsY complex is not irreversibly trapped in a slowly dissociating state.

The equilibrium dissociation constants calculated from the observed association and dissociation rate constants give similar values of $k_d = (k_{off}/k_{on}) = 0.024$ and $0.036\ \mu M$ for the Ffh•FtsY and Ffh/4.5S•FtsY complexes, respectively. Equilibrium binding assays, carried out with Ffh and FtsY or with Ffh/4.5S RNP and FtsY revealed strong binding in both cases (Fig. 3). Because of the strong binding, only upper limits could be obtained for the dissociation constants, with values of $\leq 0.09\ \mu M$ and $\leq 0.017\ \mu M$ for the Ffh•FtsY and Ffh/4.5S•FtsY, respectively. These limits are consistent within error with the dissociation constants calculated from the kinetic data.

Taken together, the above data show that 4.5S RNA not only speeds formation of the Ffh•FtsY complex by ~200-fold but also accelerates its dissociation to a similar extent. In analogy to an enzymatic reaction, the RNA therefore stabilizes a transition state for the binding reaction, lowering the energetic barrier separating free and complexed components by ~3 kcal mol^{-1} (Fig. 4A). 4.5S RNA therefore carries out a "catalytic" function in the assembly reaction. In contrast to conventional catalysts that facilitate multiple reactions when present in substoichiometric amounts, 4.5S RNA remains tightly bound to Ffh in a stoichiometric complex.

How could the 4.5S RNA stabilize the transition state for association and dissociation without substantially altering the equilibrium for protein•protein association (Fig. 4A), and what might the significance of these observations for SRP function? A plausible model to account for the catalytic behavior is that 4.5S RNA can serve as a transient tether, linking the two interacting proteins temporarily. Transient tethering would lengthen the time window subsequent to the initial collisional encounter of the components in which they can convert to the stably bound complex (Fig. 4B). Within a transiently formed complex, the two proteins might be able to find the rare conformations within or between the proteins that are competent for stable binding. As noted above, the observation that the association rate constant, even in the presence of RNA, is much lower than typically observed for protein-protein interactions suggests a requirement for such rearrangements prior to formation of the stable complex.

The simplest molecular model posits a direct role of the 4.5S RNA in providing the transient tether. Alternatively, the RNA could form the tether together with part of the Ffh protein or induce conformational changes in Ffh in a region, such as the M domain of Ffh to which 4.5S RNA binds (15, 20, 21), that then serves as the tether. In either case, the stable complex might result from direct interaction of structurally related GTPase domains (NG domains) of Ffh and FtsY, as is suggested from the reciprocal stimulation of GTP hydrolysis (7). Furthermore, mutagenesis studies show that the tryptophan responsible for observed fluorescence changes resides in the NG domain of FtsY (see legend to Figure 1 and ref 12). It is critical to emphasize that, according to the transient tether model, the region used as the tether would not be involved in stabilizing contacts in the final complex. Consistent with this notion, no changes in the footprint of Ffh on 4.5S RNA were observed upon binding to FtsY (data not shown).

Although we have characterized here the consequences of the presence or absence of 4.5S RNA on Ffh•FtsY complex formation, an extension of these results suggests that the catalytic activity of 4.5S RNA could serve as a built in regulator for the SRP targeting cycle. As the M domain also contains the signal sequence binding site of Ffh (20), signal sequence binding could induce minor changes in RNA conformation (on the order of 3 kcal mol $^{-1}$, i.e., breaking or forming only a few hydrogen bonds) which in turn could effect dramatic changes in kinetics controlling Ffh•FtsY complex formation. Indeed, the structure of SRP RNA bound to the Ffh M domain shows that SRP RNA is closely juxtaposed to the signal sequence binding pocket, emphasizing the feasibility of direct cross talk between bound signal sequences and the RNA (22, 23). It is therefore an appealing hypothesis that protein targeting by SRP and SRP receptor could be controlled through conformational changes in the RNA in addition to nucleotide occupancy of the GTPase domains. According to this view, SRP RNA would play a much more active role than previously presumed to regulate the interaction between the two GTPases.

The catalytic properties shown here for 4.5S RNA may not be unique to this system but may be a paradigm for other ribonucleoprotein assemblies, such as spliceosomes and ribosomes, that go through dynamic cycle (24, 25). Like SRP-mediated protein targeting, these biological processes depend on the coordinated formation and dissociation of complex ribonucleoprotein assemblies. Perhaps the RNA components in these complexes affect conformational changes in a manner analogous to 4.5S RNA and thus provide new means for regulation by modulating the kinetic parameters that govern complex formation and disassembly.

Figure 3-1: Changes in tryptophan fluorescence allow monitoring of Ffh•FtsY complex formation. Fluorescence emission spectra of FtsY (1 μM) in the presence (●) or absence (○) of 8 μM Ffh/4.5S RNP (panels A and B) or 6 μM free Ffh (panels C and D). Spectra in panels A and C were obtained under standard assay conditions (27) with 1 mM GppNHp•Mg^{2+}, and those in panels B and D with 0.5 mM GDP•Mg^{2+}. Analysis of a mutant form of FtsY, FtsY(W128F), but not of FtsY(W343F) showed similar fluorescence changes upon complex formation with Ffh (data not shown and (12)), indicating that this assay exclusively measures the environment of tryptophan 343, which is positioned near the nucleotide binding site. Spectra were acquired using a photon-counting SLM 8100 spectrofluorometer. The samples were excited with 290 nm. To control for inner filter effects, 4.5S RNA was added to the '-Ffh/4.5S RNP' samples in panels A and B.

Figure 3-2: Association and dissociation kinetics for the Ffh•FtsY and Ffh/4.5S RNP•FtsY complexes. FtsY (0.35 μM) fluorescence was monitored over time in the presence of 500 μM GppNHp•Mg^{2+} and 7.3 μM Ffh (panel A) and

7.7 μM Ffh•4.5S (panel B). The data were fit to a single exponential, yielding k_{obs} = 0.70 s^{-1} and 0.0061 s^{-1} respectively. Values of k_{obs} from experiments as in panels A and B were plotted against [Ffh] and [Ffh/4.5S RNP] (panels A and B, insets; open symbols with different symbols representing independent experiments in panel A inset). The closed symbols are the experimentally determined k_{off} values from panels C and D. A fit of the data to the equation: $k_{obs} = k_{on}[\text{protein}] + k_{off}$, gave values of $k_{on} = (5.6 \pm 0.6) \times 10^{2}\ M^{-1}s^{-1}$ and $(9.2 \pm 0.7) \times 10^{4}\ M^{-1}s^{-1}$ for the binding of Ffh and the Ffh/4.5S RNP, respectively, to FtsY. (The latter value is in reasonable agreement with that measured by Jagath et al. ($1.8 \times 10^{5}\ M^{-1}s^{-1}$, (12)) using a similar assay and employing GTP in place of the non-hydrolyzable GTP analog used here.) Ffh, Ffh/4.5S RNP, FtsY were preincubated individually with 500 μM GppNHp•Mg^{2+} for 20 min prior to each initiation of the reactions. For binding reactions of Ffh/4.5S RNP to FtsY, measurements were made using a KinTek Stopped-Flow apparatus.

In panels C and D, dissociation rates of Ffh•FtsY and Ffh/4.5S RNP•FtsY complexes were measured. Fluorescence intensity was monitored at 340 nm after mixing 1.5 μM Ffh•FtsY complex (panel C) and 2 μM Ffh/4.5S RNP•FtsY complex (panel D) with 5 mM GDP•Mg^{2+} to trap dissociated components. Fits of the data to single exponentials gave values of $k_{off} = (3.30 \pm 0.02) \times 10^{-3}\ s^{-1}$ and $(1.20 \pm 0.04) \times 10^{-5}\ s^{-1}$ for dissociation of the Ffh/4.5S RNP•FtsY and Ffh•FtsY complexes, respectively. Reactions were carried out in triplicate. Complexes were preformed at 2x concentration in the presence of 100 μM GppNHp•Mg^{2+}. To initiate reactions, samples were diluted 1:1 in buffer containing 10 mM GDP•Mg^{2+}. Dissociation of Ffh•FtsY complex was accelerated upon addition of 4.5S RNA (panel D inset). Fluorescence changes were monitored after mixing 2.5 μM Ffh•FtsY complex with 5 mM GDP•Mg^{2+}. At the time indicated (arrow) either 5.5 μM 4.5S RNA (lower trace) or 12 μM yeast tRNA (upper trace) was added to the sample. Fluorescence intensity changes were corrected for photobleaching (<5% of total fluorescence). The data obtained after 4.5S RNA addition were fit to a single exponential, yielding a rate constant of (2.7 ± 0.2) x 10^{-3} s^{-1}. We also analyzed the hydrodynamic properties of the Ffh•FtsY complex by gel filtration and velocity centrifugation (data not shown). In both cases, the Ffh•FtsY complex behaved as a uniform species fractionating in the size range of 100 - 150 kDa, consistent with a composition of one molecule each of Ffh and FtsY.

__Figure 3-3:__ **Equilibrium binding of Ffh and Ffh/4.5S RNP to FtsY.** Binding reactions were carried out for 40 hr with Ffh (A) and for 20 min with Ffh/4.5S RNP (B) in the presence of 0.1 μM FtsY and 500 μM GppNHp•Mg^{2+} . Because the maximal fluorescence change is observed at concentrations of Ffh and Ffh/4.5S near the FtsY concentration, the data were fit using a quadratic equation (see ref 23; solid lines). The dissociation constants obtained of (0.092 ± 0.038) and (0.016 ± 0.010) μM for Ffh and Ffh/4.5S RNP, respectively, should be considered as upper limits for the true K_d values (26). The dashed lines show the binding curves calculated from the K_d values obtained from the k_{on} and k_{off}

measurements in Figures 2 and 3. Deviations in panel A are likely due to incomplete equilibration at the lower protein concentrations. Background intensities for each Ffh concentration were simultaneously measured and subtracted from each corresponding reaction prior to calculating (F-Fo)/Fo values. For the binding reactions in panel B, 4.5S RNA was maintained at a constant concentration of 3.0 μM in each sample to control for inner filter effects.

Figure 3-4: **Effect of 4.5S RNA on the Ffh•FtsY binding reaction.** (A) Free energy-reaction profile for Ffh•FtsY association in the absence (solid line) and presence (dashed line) of bound 4.5S RNA. The relative energy levels are shown for a standard state of 1 M and were calculated from the observed association and dissociation rate constants using the equation: $\Delta G = -RT \ln(k\, h/k_B\, T)$(13), in which $R = 1.987$ kcal mol^{-1} K^{-1}, $k_B = 3.3 \times 10^{-27}$ kcal K^{-1}, $h = 1.58 \times 10^{-37}$ s^{-1}, $T = 298$ K.

(B) Schematic diagram depicting a model for how 4.5S RNA may act catalytically in Ffh•FtsY complex formation. In this model, 4.5S RNA helps form a transient tether between Ffh and FtsY, which allows a complex to form long enough for Ffh, FtsY, or both (as depicted) to obtain the correct conformation to become more stabily locked. The presence of the RNA lowers the energy barrier to this "transition state(s)" within the brackets by approximately 3 kcal mol^{-1} as indicated by the arrows in (A). The tether would be transient, however, as the complex is not measurably stabilized in the presence of the RNA.

1. P. Walter and A. E. Johnson, *Annu. Rev. Cell Biol.* **10,** 87 (1994).
2. J. Luirink, et al., *EMBO J.* **13,** 2289 (1994).
3. G. J. Phillips, and T. J. Silhavy, *Nature* **359,** 744 (1992).
4. V. Ribes, K. Römisch, A. Giner, B. Dobberstein, and D. Tollervey, *Cell* **63,** 591 (1990).
5. T. Powers, and P. Walter, *EMBO J.* **16,** 4880 (1997).
6. J. D. Miller, H. D. Bernstein, and P. Walter, *Nature* **367,** 657 (1994).
7. T. Powers, and P. Walter, *Science* **269,** 1422 (1995).
8. K. Römisch, et al., *Nature* **340,** 478 (1989).
9. D. M. Freymann, R. J. Keenan, R. M. Stroud, and P. Walter, *Nature* **385,** 361 (1997).
10. G. Montoya, C. Svensson, J. Luirink, and I. Sinning, *Nature* **385,** 365 (1997).
11. H. D. Bernstein, et al., *Nature* **340,** 482 (1989).
12. J. R. Jagath, M. V. Rodnina, and W. Wintermeyer, *J Mol Biol* **295,** 745 (2000).
13. A. Fersht, *Enzyme Structure and Mechanism* (W. H. Freeman and Co., New York, ed. Second, 1985).
14. B. Macao, J. Luirink, and T. Samuelsson, *Mol. Microbiol.* **24,** 523 (1997).
15. N. Zheng, and L. M. Gierasch, *Mol. Cell* **1,** 79 (1997).
16. C. Moser, O. Mol, R. S. Goody, and I. Sinning, *Proc. Natl. Acad. Sci. U S A* **94,** 11339 (1997).
17. J. R. Jagath, M. V. Rodnina, G. Lentzen, and W. Wintermeyer, *Biochemistry* **37,** 15408 (1998).

18. C. Klebe, H. Prinz, A. Wittinghofer, and R. S. Goody, *Biochemistry* **34**, 12543 (1995).

19. J. John, et al., *Biochemistry* **29**, 6058 (1990).

20. D. Zopf, H. D. Bernstein, A. E. Johnson, and P. Walter, *EMBO J.* **9**, 4511 (1990).

21. K. Römisch, J. Webb, K. Lingelbach, H. Gausepohl, and B. Dobberstein, *J. Cell Biol.* **111**, 1793 (1990).

22. R. T. Bately, R. P. Rambo, L. Lucast, B. Rha, and J. A. Doudna, *Science,* **287**, 1232 (2000).

23. P. Walter, R. Keenan, and U. Schmitz, *Science,* **287**, 1212 (2000).

24. K. S. Wilson, and H. F. Noller, *Cell* **92**, 337 (1998).

25. J. P. Staley, and C. Guthrie, *Cell* **92**, 315 (1998).

26. R. S. Goody, M. Frech, and A. Wittinghofer, *Trends Biochem Sci* **16**, 327 (1991).

27 . Fluorescence spectra were obtained and reactions carried out in 50 mM Hepes, pH 7.5, 150 mM KOAc, 1.5 mM $Mg(OAc)_2$, 0.01% (v/v) Nikkol detergent, 2 mM DTT) at 25 °C. *E. coli* Ffh, 4.5S RNA, and FtsY were prepared as previously described (5). Ffh/4.5S RNP was assembled using a 2-fold molar excess of RNA over Ffh and used without further purification (6).

28. We would like to thank Coleen Murphy for help with setting up the stopped flow experiments. We also thank Alan Frankel, Dave Agard, Dyche Mullins, Ted Powers, Jim Hartman, Shu-ou Shan, Alan Derman, Ursula Rüegsegger, Christine Guthrie, Carol Gross, Joe Derisi, and Roger

Altman for helpful discussions and/or comments on the manuscript. This work was supported by grants from the NIH to PW, DH and AEJ. PW is an Investigator of the Howard Hughes Medical Institute.

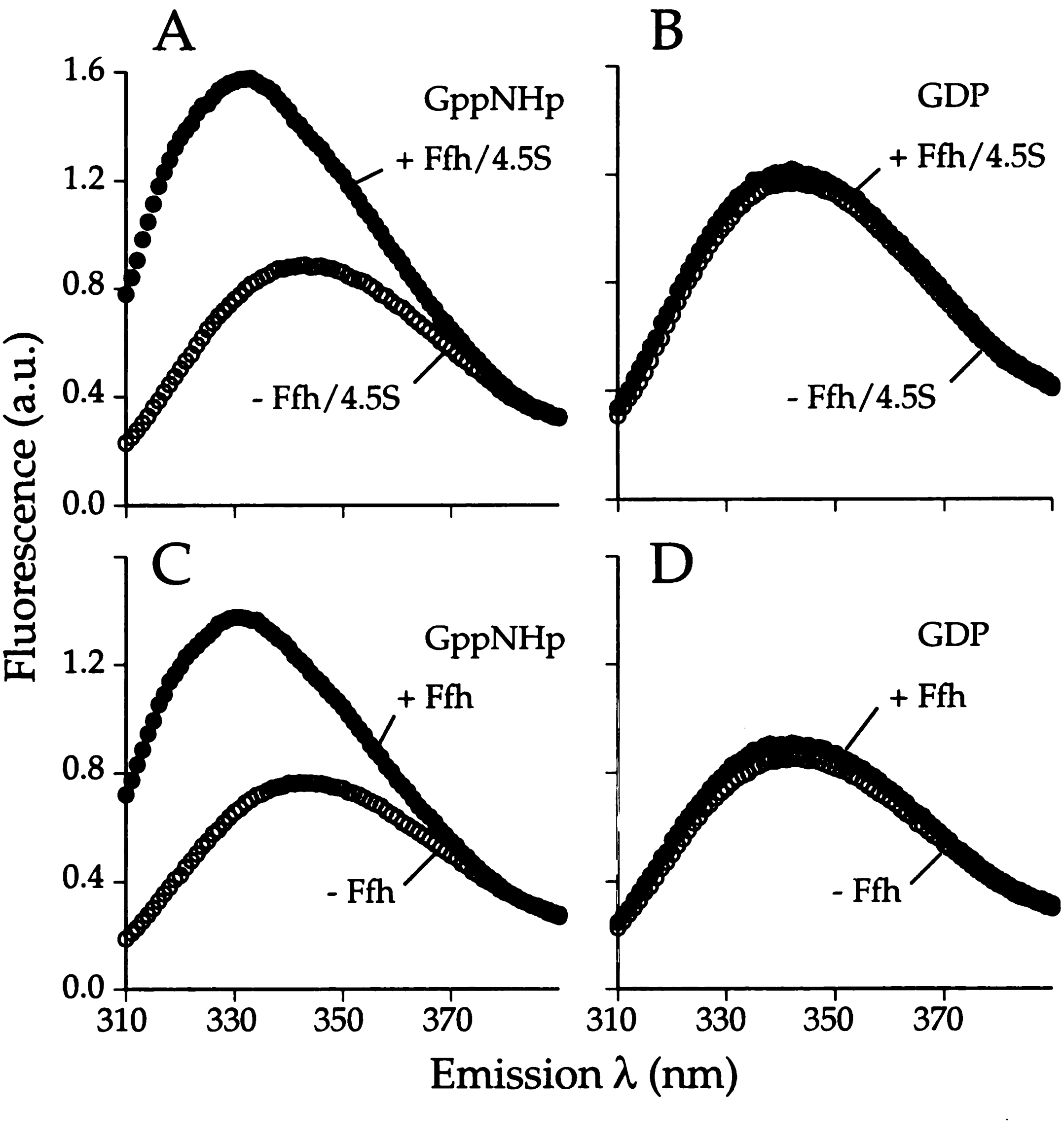
A
B
C
D
GppNHp
GDP
+ Ffh/4.5S
- Ffh/4.5S
+ Ffh
- Ffh
Fluorescence (a.u.)
Emission λ (nm)
0.0
0.4
0.8
1.2
1.6
310
330
350
370

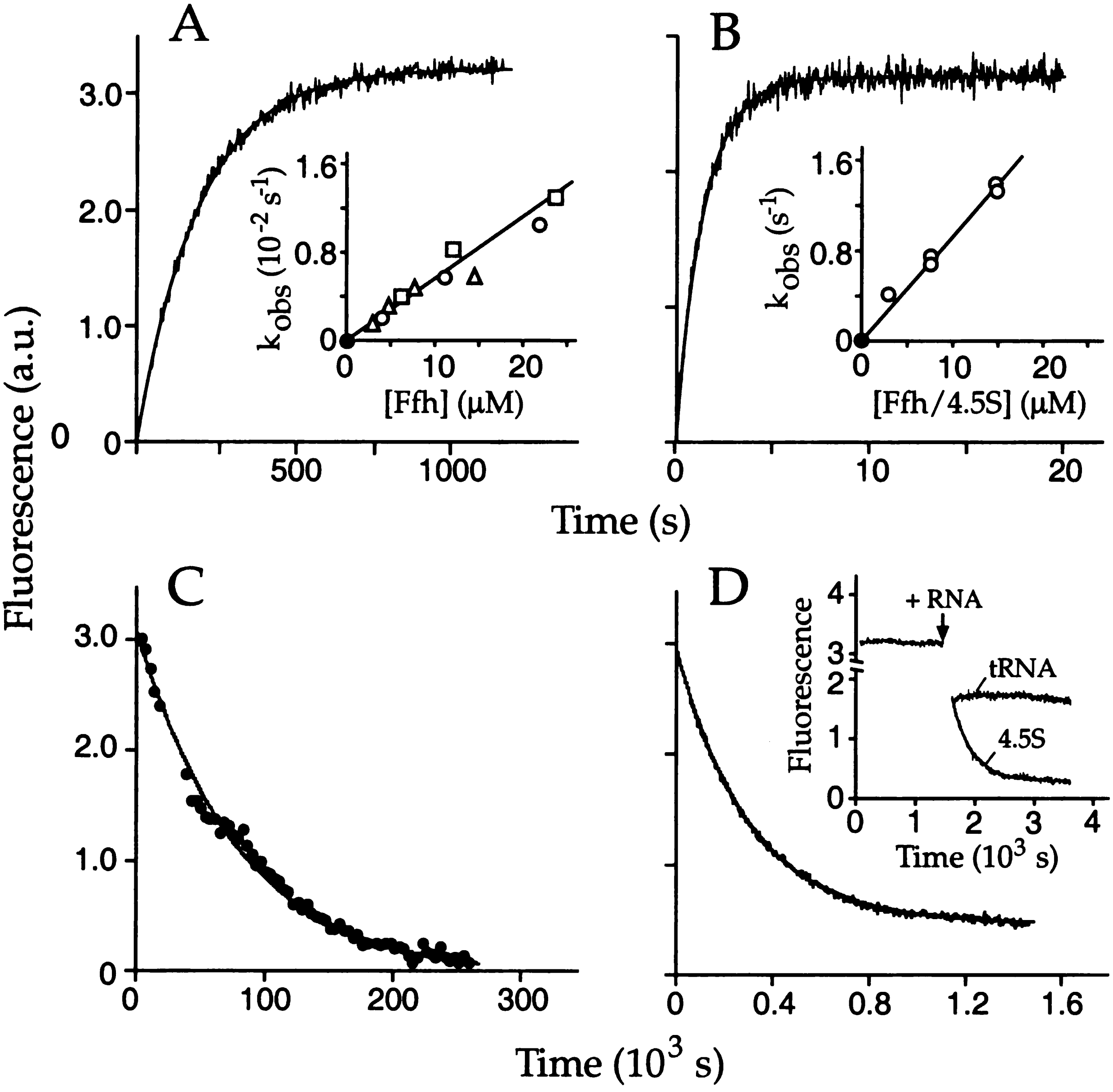
A
B
C
D
Fluorescence (a.u.)
3.0
2.0
1.0
0
500
1000
10
20
Time (s)
k_{obs} (10^{-2} s^{-1})
1.6
0.8
[Ffh] (μM)
k_{obs} (s^{-1})
[Ffh/4.5S] (μM)
100
200
300
0.4
0.8
1.2
1.6
Time (10^3 s)
Fluorescence
+ RNA
tRNA
4.5S
Time (10^3 s)

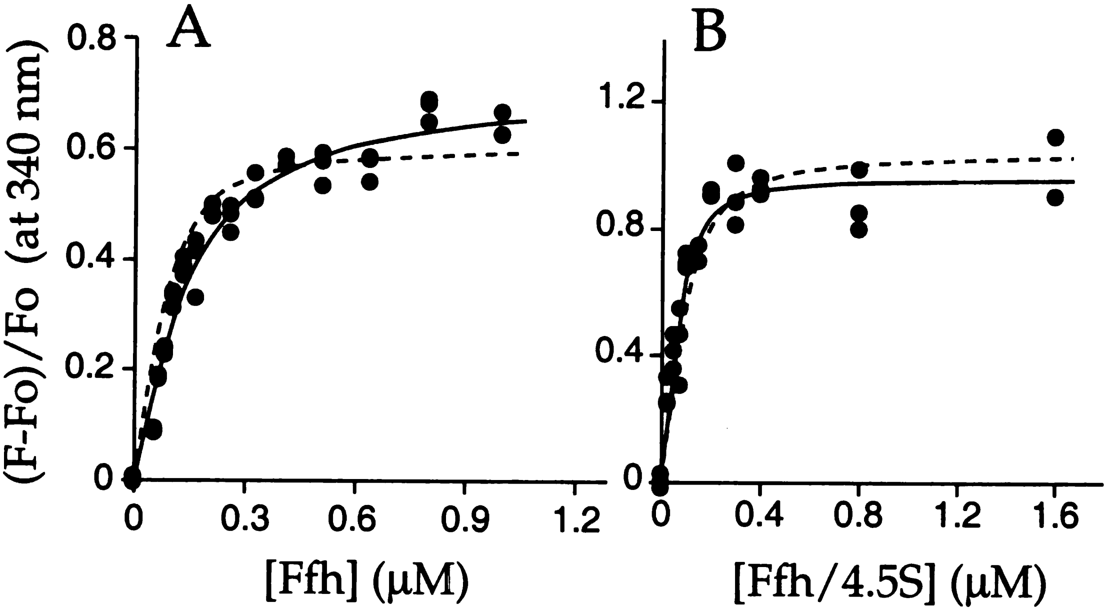
A
B
(F-Fo)/Fo (at 340 nm)
0.8
0.6
0.4
0.2
0
1.2
0.8
0.4
0
0
0.3
0.6
0.9
1.2
0
0.4
0.8
1.2
1.6
[Ffh] (μM)
[Ffh/4.5S] (μM)

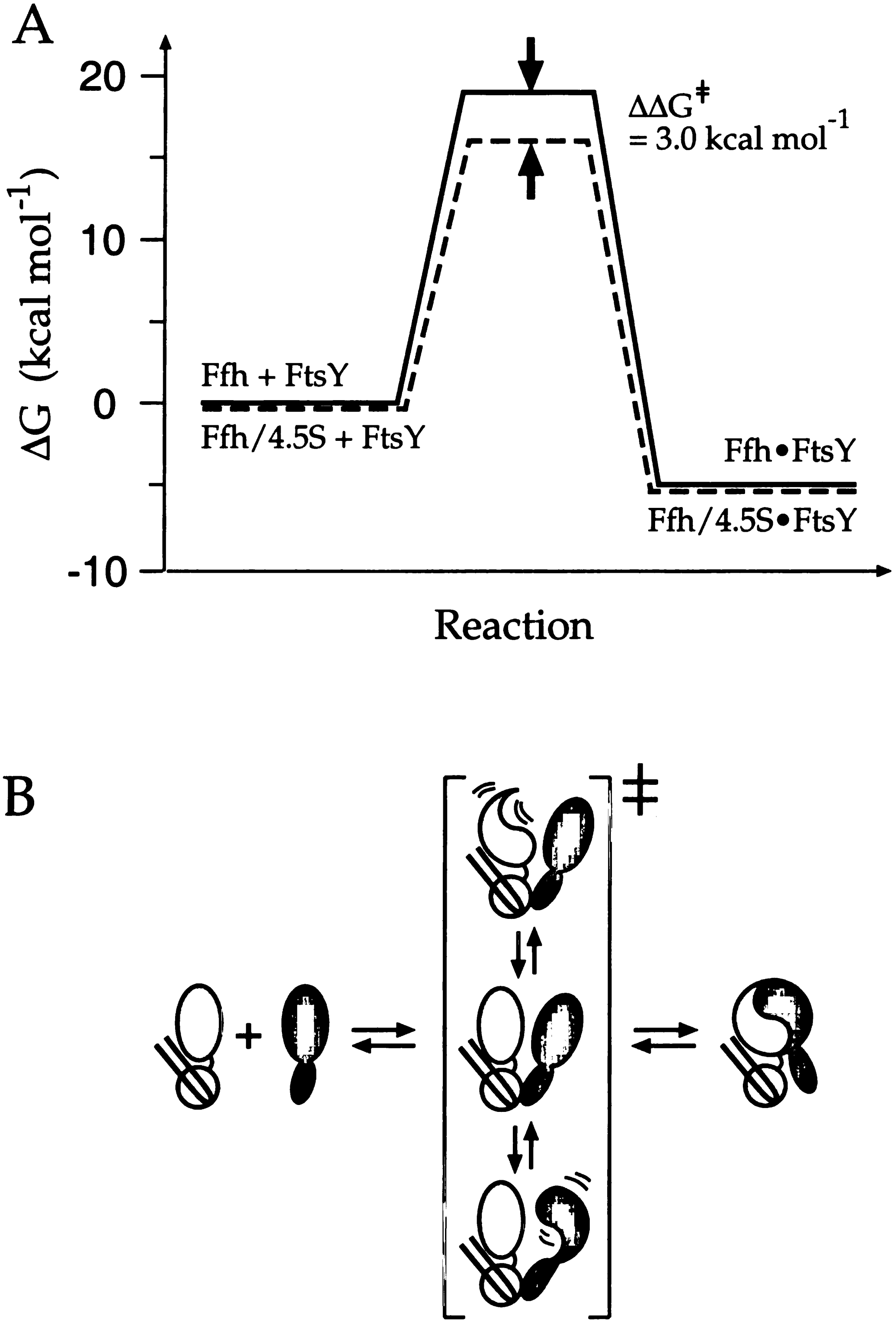
A
20
10
0
-10
ΔG (kcal mol-1)
Reaction
Ffh + FtsY
Ffh/4.5S + FtsY
ΔΔG‡
= 3.0 kcal mol-1
Ffh•FtsY
Ffh/4.5S•FtsY
B
‡
+

Chapter 4: Kinetics of the Ffh/4.5S RNP•FtsY GTPase Complex: the Role of 4.5S RNA

Abstract: Ffh/4.5S RNP and FtsY, the bacterial homologues of the Signal Recognition Particle (SRP) and the SRP Receptor form a unique GTPase complex in which both proteins hydrolyze GTP and act as GTPase activating proteins (GAPs) for each other (Powers and Walter, 1995; Walter, 1996). It has been previously shown that the 4.5S RNA associated with Ffh greatly enhances the GTPase activity of this complex (Macao et al., 1997; Miller et al., 1994). We present kinetic data explaining how 4.5S RNA enhances the activity of the Ffh/4.5S RNP•FtsY complex. In agreement with our previous findings, we demonstrate that 4.5S RNA dramatically enhances the rate of association between the two proteins (Peluso et al., 2000). Because Ffh-FtsY association is rate determining for the observed GTPase reaction, facilitation of complex formation leads to stimulation of apparent GTPase activity. In addition, we find that 4.5S RNA increases the rate of GTP hydrolysis once the complex is formed. This suggests that the RNA favors a conformation within the Ffh-FtsY complex which is conducive to GTP hydrolysis.

Introduction

The signal recognition particle (SRP) is a cytosolic ribonucleoprotein complex, consisting of 6 polypeptides and an RNA molecule, that mediates co-translational targeting of proteins to the endoplasmic recticulum (ER) (Walter, 1996; Walter and Johnson, 1994). SRP identifies the correct ribosome-nascent chain complexes that bear N-terminal signal sequences (Walter et al., 1981). Upon forming a tight complex with the ribosome-nascent chain, SRP causes an arrest in translation which provides a larger time window during which SRP targets the ribosome-nascent chain complex to the ER membrane (Walter and Blobel, 1981). Targeting is accomplished by interaction of SRP with its receptor (Gilmore et al., 1982a; Gilmore et al., 1982b). At the ER membrane, SRP dissociates from the ribosome-nascent chain complex resulting in release of the translation arrest and subsequent co-translational translocation of the nascent chain across the ER membrane (Walter and Blobel, 1981).

Targeting of secretory and membrane proteins to the ER or bacterial plasma membrane by the SRP pathway is evolutionarily conserved (Walter, 1996; Walter and Johnson, 1994). In *E. coli*, the Ffh/4.5S RNA complex (Ffh/4.5S RNP) and FtsY function as the bacterial SRP and SRP receptor, respectively (Luirink et al., 1994; Phillips and Silhavy, 1992; Poritz et al., 1990; Ribes et al., 1990). This minimal system maintains the central functional elements of the pathway. Ffh, the homologue to SRP54, interacts with signal sequences and the SRP receptor.

FtsY, meanwhile, provides the component of the SRP receptor that interacts specifically with Ffh at the membrane.

Both Ffh and FtsY, and their mammalian counterparts SRP54 and SRα, contain GTPase domains which interact with each other in a GTP-dependent fashion (Miller et al., 1994; Miller et al., 1993). These GTPase domains play a critical role in the SRP-dependent targeting process as GTP is known to be an essential co-factor for the targeting reaction (Gilmore, 1988). Moreover, SRP54 lacking its GTPase domain can specifically interact with ribosome-nascent chains but is unable to target these ribosome nascent chains to the membrane (Zopf et al., 1993). In addition, hydrolysis of the GTP is crucial for the recycling of the SRP components (Connolly and Gilmore, 1993). This model follows from *in vitro* studies in which the non-hydrolyzable GTP analogue 5′guanylylimidodiphosphate (GppNHp) is substituted as a co-factor. In such experiments, only a single round of targeting is observed with SRP remaining stuck at the membrane (Connolly and Gilmore, 1993).

The GTPase domains of Ffh and FtsY define them as members of a unique subfamily of GTPases with interesting properties (Walter, 1996). Biochemical and x-ray crystallographic studies have demonstrated a high degree of symmetry to the Ffh/4.5S $\mathrm{RNP}^{\mathrm{GTP}}\bullet\mathrm{FtsY}^{\mathrm{GTP}}$ complex. Both Ffh and FtsY were found to contain structurally identical 4-helix-bundle and GTPase domains, called collectively NG-domains (Freymann et al., 1997; Montoya et al., 1997) Moreover, from their crystal structures, the NG-domains were also shown to share a common amino acid structural element which has been termed the Insertion Box Domain, or IBD (Freymann et al., 1997; Montoya et al., 1997). Amino acids within this unique IBD provide salt bridges which help stabilize the nucleotide-free state of these GTPases (Freymann et al., 1999). This could account for the fact that these GTPases release nucleotides much faster than the classical Ras-like GTPases (John et al., 1990).

Perhaps the most striking feature of Ffh and FtsY is their ability to act dually as GTPases and GTPase activating proteins, or GAPs. Using an engineered FtsY mutant with specificity for xanthosine triphosphate (XTP), both Ffh and FtsY were found to hydrolyze their respective substrates upon binding to each other (Powers and Walter, 1995). Moreover, both Ffh and FtsY reciprocally act as GAPs for each other in the nucleotide triphosphate bound state which further emphasizes the symmetry inherent in the Ffh•FtsY complex.

While Ffh and FtsY share a common NG-common, both possess specialized domains that enable them to mediate protein targeting. FtsY has an N-terminal acidic domain, or A-domain, which enables FtsY to interact with the membrane (Zelazny et al., 1997). Potentially, membrane interactions via this A-domain may regulate FtsY's GTPase activity (de Leeuw et al., 2000). Ffh, in turn, possesses a unique C-terminal M-domain which is so named because it has an atypical abundance of methionine residues (Bernstein et al., 1989). Biochemical studies have demonstrated that the M-domain mediates interactions with both the signal sequence (Lütcke et al., 1992; Zopf et al., 1990) and the 4.5S RNA (Römisch et al., 1990). In addition, crystallographic studies have also shown this domain to contain a hydrophobic cleft ideally suited for signal sequence recognition and a positively charged helix-turn-helix motif which would facilitate 4.5S RNA binding (Keenan et al., 1998). Moreover, a recent crystal structure of the M-domain bound to 4.5S RNA has provided molecular insights into the M-domain-4.5S RNA interaction (Batey et al., 2000; Walter et al., 2000). Through this domain architecture, Ffh and FtsY have evolved as "molecular matchmakers" (Walter, 1996). Ffh and FtsY interact with each other and by doing so are able to bring the ribosome-nascent chain together with the protein translocation machinery at the membrane.

While early biochemical studies identified specific functional roles for the different protein subunits (Siegel and Walter, 1988), SRP RNA appeared to be nothing more than a scaffold which held these proteins together in a complex (Walter and Blobel, 1982). The identification of a smaller SRP RNA in *E. coli*, 4.5S RNA, was intriguing. This smaller RNA contained the most phyllogenetically conserved region of the SRP RNA, Domain IV, which was likely to have been maintained for functional purpose. Moreover, from chemical probing studies, many of these conserved bases were found to be highly solvent accessible even in the presence of Ffh suggesting that they might facilitate some interaction with another component of the SRP pathway (Lentzen et al., 1996).

A specific role for 4.5S RNA was identified through biochemical studies focusing on the GTPase activity of Ffh/4.5S RNP^{GTP}•FtsY^{GTP} complex. Initially, 4.5S RNA was thought to be required for the formation of the Ffh/4.5S

$RNP^{GTP} \bullet FtsY^{GTP}$ complex (Miller et al., 1994). However studies of the *Mycoplasma Mycoides* SRP components demonstrated that the SRP RNA was not essential for the formation of the $Ffh^{GTP} \bullet FtsY^{GTP}$ complex and subsequent stimulated hydrolysis (Macao et al., 1997). In fact, Ffh's NG-domain was found to independently interact with FtsY and exhibit stimulated GTP hydrolysis. However, GTPase activity was found to be optimal in the presence of the RNA (Macao et al., 1997) which suggested that the RNA was enhancing some step in the reaction pathway.

In order to quantitatively study the Ffh-FtsY interaction, we and others have recently developed a fluorescence assay which directly monitors the interaction between Ffh and FtsY (Jagath et al., 2000; Peluso et al., 2000). With this assay, we have recently demonstrated a novel catalytic role for the 4.5S RNA in the formation of the Ffh/4.5S $RNP^{GTP} \bullet FtsY^{GTP}$ complex (Peluso et al., 2000). Rather than enhancing the affinity between Ffh and FtsY, 4.5S RNA accelerates both their association and dissociation. These observations suggest that the Ffh/4.5S $RNP^{GTP} \bullet FtsY^{GTP}$ complex undergoes intricate conformational rearrangements during its formation and subsequent GTP hydrolysis.

We were interested in determining whether 4.5S RNA affects additional steps in the $Ffh^{GTP} \bullet FtsY^{GTP}$ complex's enzymatic cycle. Through a characterization of the reaction pathway, we set out to determine whether 4.5S RNA increases the catalytic activity of the $Ffh^{GTP} \bullet FtsY^{GTP}$ complex. We demonstrate here that 4.5S RNA enhances the rate of $Ffh^{GTP} \bullet FtsY^{GTP}$ complex formation in a manner similar to what we have previously observed in the presence of GppNHp. In addition, the association between Ffh and FtsY is sensitive to single atomic modification of the GTP substrate. The binding of Ffh to FtsY in the presence of GTP is 10-fold faster than association rates previously measured in the presence of GppNHp (Peluso et al., 2000). Moreover, we find that 4.5S RNA enhances an additional step within the reaction cycle which precedes GTP hydrolysis. Taken together, we offer evidence to suggest that 4.5S RNA modulates the conformation of the $Ffh^{GTP} \bullet FtsY^{GTP}$ complex and may, in turn, regulate its GTPase activity during the SRP functional cycle.

Materials and methods

Buffers

Buffer A (20 mM Hepes, pH 8.0, 2 mM EDTA, 2 mM DTT), Buffer B (50 mM Tris-HCl, pH 7.5, 1 mM EDTA, and 2 mM DTT), Buffer C (20 mM KOAc, pH 4.7), Buffer D (20 mM PIPES, pH 6.8, 500 mM KOAc, 1 mM $Mg(OAc)_2$), Buffer E (50 mM Hepes, pH 7.5, 150 mM KOAc, 1.5 mM $Mg(OAc)_2$, 0.01% Nikkol, 2 mM DTT)

Ffh expression and purification

Ffh was overexpressed from the pDMF6 plasmid (D. Freymann and P Walter unpublished) in BL21(DE3) (Stratagene) cells which also contained the pLysE plasmid (Novagen). Cells were grown to an A_{600} of 0.5 – 0.7 at which time IPTG was added to the media to a final concentration of 1 mM. Cells expressing Ffh were harvested by centrifugation and resuspended in Buffer A containing 250 mM NaCl and 200 μM PMSF. The cells were sonicated on ice, and the lysate was centrifuged at 31,000g for 30 minutes. The supernatant was loaded onto an SP-sepharose Fast Flow column. The column was washed with 10 column volumes of Buffer A containing 250 mM NaCl. The Ffh was eluted from the column with a 250 mM – 750 mM NaCl gradient. The Ffh was then precipitated in 80% ammonium sulfate and dialyzed against Buffer A containing 250 mM NaCl. Following a high speed ultracentrifuagation step to remove insoluble matter, the Ffh was further purified over a Superose-12 column. The Ffh-containing fractions were pooled and concentrated. The purified Ffh was stored at –20 °C in Buffer A containing 250 mM NaCl and 50% glycerol. The concentration of Ffh was determined by Bradford assay using an extinction coefficient of 0.10 A_{595} units/μg of Ffh. This extinction coefficient was derived from amino acid analysis measurements and Bradford readings of pure Ffh samples.

FtsY expression and purification

FtsY used in this study is the FtsY(47-497) whose cloning, expression, and purification has previously been described (Powers and Walter, 1997). One additional purification step was added for the present study. As a final step in the purification , FtsY was chromatographed on a MonoQ column using a Buffer B containing 150 mM to Buffer B containing 450 mM NaCl gradient. The purified FtsY was stored at –80°C in Buffer B containing 250 mM NaCl and 20% glycerol. The concentration of FtsY was determined from Bradford assay measurements using an extinction coefficient of 0.063 A_{595} units/μg of FtsY. This extinction coefficient was determined in a similar fashion as the one for Ffh.

4.5S RNA expression and purification

DH5α cells containing the pSN1 plasmid (Brown et al., 1984) were grown in LB containing ampicillin (100 μg/ml) and IPTG (1 mM). After growing the cells to saturation, the cells were harvested via centrifugation in an RC3B centrifuge at 4000 rpm. The cells were resuspended in 20 ml of Buffer C per liter grown. The cell suspension was lysed in an equal volume of acid phenol:chloroform (Ambion). The aqueous phase was separated from the organic phase by centrifugation in an SS-34 rotor at 4000 rpm. The lysate was extracted 3 times in total with the acid phenol:chloroform mix. After adding sodium acetate, pH 5.0, to a final concentration of 0.3 M, 0.6 - 1.0 volumes of isopropanol were added to the aqueous mixture to precipitate the nucleic acid. The precipitation step was typically carried out overnight at –20 °C. The precipitated RNA was harvested by centrifugation at 4000 rpm in an RC3B centrifuge. The pellet was resuspended in H_2O. At this stage the only other major nucleic acid contaminant was tRNA from the cells roughly at equal amount to that of 4.5S RNA coming out of the cells. 4.5S RNA was separated from the tRNA by running the sample over a TSK3000SW gel filtration column in Buffer D. The 4.5S RNA fraction was extracted twice with an equal volume of phenol followed by 2 chloroform extractions. After raising the concentration of NaOAc to 0.3 M, the 4.5S RNA was precipitated in ethanol and stored as 1 mg precipitates in ethanol at –20 °C. The concentration of 4.5S RNA was determined by measuring the A_{260} and assuming an extinction coefficient of 1.0 $A_{260} = 40\ \mu g/ml$ (Sambrook, et al., 1989). The RNA was analyzed on native 10% acrylamide and denaturing acid-urea 10% acrylamide gels in order to verify that it was in tact after purification.

Buffer exchanging Ffh and FtsY

Prior to any functional assays, Ffh and FtsY were buffer-exchanged into Buffer E using Bio-Gel P-6 DG (Biorad) spin columns. After buffer exchange Ffh and FtsY were typically centrifuged at 300,000 g in a TLA100 rotor for 1 hour. After centrifugation, the protein concentrations were verified using the Bradford assay as described above. There would typically be a 10% loss of the proteins during this procedure. All the functional assays detailed below were carried out in Buffer E unless otherwise specified.

GTP hydrolysis assays

All GTPase reactions were performed using α-^{32}P-labelled GTP in the following final conditions 50 mM Hepes pH 7.5, 150 mM KOAc, 1.5 mM $Mg(OAc)_2$, 0.01% Nikkol, and 2 mM DTT at 25°C. Reactions were initiated by addition of GTP with a stoichiometric amount of $Mg(OAc)_2$. At the desired times the reactions were quenched in 0.75 M potassium phosphate, pH 3.5. The GDP produced in the reaction was separated from the unhydrolyzed GTP by thin layer chromatography using PEI Cellulose F in 0.75 M potassium phosphate, pH 3.5. The plates were imaged and the amount of GTP hydrolyzed was quantified using either a Molecular Imager System GS-363 (Biorad) or a Molecular Dynamics Storm 840.

Kinetic measurements of Ffh-FtsY association

Ffh-FtsY association was monitored using a fluorescence assay as previously described (Jagath et al., 2000; Peluso et al., 2000). All experiments were performed in a Kintec Stopped Flow apparatus at 25° C. FtsY at 0.5 μM was assayed against varying concentrations of either Ffh or Ffh/4.5S RNP. Reactions were initiated by rapidly mixing the proteins with 1 mM $GTP \bullet Mg^{2+}$. This level of GTP was predetermined to give the maximal rate of protein association (data not shown). In addition it approximated the cellular level of GTP present in *E. coli* (Neidhardt, 1987).

For both binary complex and ternary complex kinetics, the changes in fluorescence were fit with single exponential curves. The exponential rate constants were plotted vs. their respective concentrations of either Ffh or Ffh-4.5S RNP. Applying pseudo-first order analysis to these plots, the data was fit with the equation $k_{obs} = k_{on}[Ffh\pm4.5S\ RNA] + k_{off} + k_{chem}$ in order to derive the rate constants for the binding reactions. The fits were very good possessing R^2 values of greater than 0.98. The rate of Ffh-FtsY complex dissociation was independently determined as outlined below.

Kinetic measurements of Ffh-FtsY dissociation

Double mixing experiments were performed to monitor the decay of the Ffh•FtsY complex in the presence and absence of 4.5S RNA. All reactions were perfromed in a Kintek Stopped Flow apparatus at 25° C. First, FtsY was mixed with Ffh or Ffh/4.5S RNA in the presence of GTP at approximately 60 μM. After the appropriate delay time enabling the complex formation to reach steady-state as assessed by tryptophan fluorescence, the samples were mixed with a 50-fold excess of $GDP \bullet Mg^{2+}$ over GTP. The data was fit with a single exponential functions which yielded first order rate constants as has previously been seen (Peluso et al., 2000).

Results

4.5S RNA enhances the observed rate of GTP hydrolysis by the Ffh^{GTP}•FtsY^{GTP} complex

While we have previously shown that Ffh can bind to FtsY in the absence of 4.5S RNA, a remaining question is whether 4.5S RNA has additional effect on the intrinsic GTPase activity of the complex. Previous work in *M. mycoides* has demonstrated that the Ffh^{GTP}•FtsY^{GTP} complex is enzymaticly active, but shows reduced activity levels compared to the complex in the presence of the RNA (Macao et al., 1997). Similarly, the data in Figure 2 shows that 4.5S RNA enhances the GTPase activity of the Ffh^{GTP}•FtsY^{GTP} complex. Ffh and FtsY can exhibit stimulated GTPase activity in the absence of 4.5S RNA as a mixture of Ffh and FtsY (closed squares) exhibits a significantly enhanced GTPase activity relative to what has been seen for each protein alone (Miller et al., 1994; Powers and Walter, 1995). Interestingly, in the presence of 4.5S RNA, the mixture exhibits a still 5 to 10-fold higher GTPase activity (closed circles). Perhaps this observation is not all that surprising, as we have recently shown that 4.5S RNA greatly enhances the association rate between Ffh and FtsY by some 100-fold (Peluso et al., 2000) which could potentially account for the differences observed in Figure

2. However, we were interested in ascertaining whether 4.5S RNA was affecting additional steps in the $Ffh^{GTP}\bullet FtsY^{GTP}$ reaction pathway .

The reaction mechanism in Figure 1 depicting the stimulated GTPase reaction of the $Ffh^{GTP}\bullet FtsY^{GTP}$ complex involves a number of steps in addition to the binding of Ffh to FtsY (Step 3). Any of these steps could, in principle, be rate limiting for the GTPase reaction. For instance, the intrinsic GTPase activity of the complex (Step 4) or even of Ffh (Step 1) . Finally, as we are looking at multiple rounds of GTP hydrolysis per protein complex, it is also possible that 4.5S RNA could be functioning after the GTP hydrolysis step, for instance, the dissociation of Ffh and FtsY after substrate turnover (Step 5). We wished to determine exactly how 4.5S RNA was, in fact, modulating the GTPase activity of the $Ffh^{GTP}\bullet FtsY^{GTP}$ complex by studying each step of the reaction mechanism detailed in Figure 1.

4.5S RNA does not affect the basal GTPase activity of Ffh.

To determine the Ffh's affinity for substrate as well as its basal GTPase rate in the absence or presence of 4.5S RNA, we monitored single turnover events per Ffh molecule as shown in Figure 3A and 3B. This was achieved by assaying low GTP (5 nM) concentration relative to much higher concentrations of Ffh or Ffh/4.5S RNP (100 nM – 8 μM). At various enzyme concentrations, GTP hydrolysis was followed to completion as a function of time, and apparent rates were determined from single exponential fits to the data. The observed rate constants for each time course were plotted as a function of the respective enzyme concentration for Ffh (Figure 3A) and Ffh/4.5S RNP (Figure 3B). From the saturation points of the respective curves we derived $k_{chem\ app}$ values for Ffh and Ffh/4.5S RNP of 1.6 (± 0.02) x 10^{-3} s^{-1} to 2.4 (± 0.3) x 10^{-3} s^{-1}, respectively, demonstrating that the RNA does not significantly enhance Ffh's intrinsic rate of GTP hydrolysis. While there is a slight increase between the $k_{chem\ app}$ for the Ffh/4.5S RNP over that of Ffh in Figure 3, we feel this difference is not significant as subsequent single turnover assays for Ffh/4.5S RNP, which were carried farther to completion, have shown the k_{chem} value to be 1.5 x 10^{-3} s^{-1} (P. Peluso, S. Shan et al., unpublished observations).

From the same plots we determined the $K_{1/2}$ values to be approximately 0.30 (± 0.02) μM and 1.9 (± 0.4) μM for Ffh and Ffh/4.5S RNP. These $K_{1/2}$ values are within a factor of 4 of the recently published K_d values 1.2 μM and 1.6 μM determined for Ffh and Ffh/4.5S RNP from a spectroscopic assay employing fluorescently-labelled nucleotides (Jagath et al., 1998). Performing a similar analysis for FtsY, we measured a basal $k_{chem\ app}$ of 4.0 (± 0.3) x 10^{-4} sec^{-1} and a $K_{1/2}$ of 30 (± 6) μM. This $K_{1/2}$ value is within a factor of 3 of the previously published K_d value of 10.2 μM which was determined from a fluorometric-based assay (Moser et al., 1997).

Both 4.5S RNA and GTP enhance the association rate between Ffh and FtsY.

In previous work we have demonstrated that 4.5S RNA increases the association rate of Ffh to FtsY (Peluso et al., 2000). In this earlier work, we trapped the Ffh•FtsY and Ffh/4.5S •FtsY complexes by carrying out all binding reactions in the presence of the non-hydrolyzable GppNHp. Binding was monitored using a novel fluorescence assay developed independently by us and others (Peluso et al., 2000; Jagath et al., 2000).We wished to verify whether the same rate enhancement occurred in the presence of GTP. Using the tryptophan fluorescence assay, we found that 4.5S RNA increased the k_{on} by some 400-fold from 5.6 (± 0.3) x $10^3 M^{-1}s^{-1}$ to 1.8 (± 0.06) x $10^6 M^{-1}s^{-1}$ for the binding of Ffh to FtsY (Figure 4).

Interestingly, the rate constants were approximately 10-fold faster in the presence of GTP as compared to our results previously obtained using GppNHp where the k_{on} were measured to be 5.6 x 10^2 M^{-1} s^{-1} and 9.2 x 10^4 M^{-1} s^{-1} for the Ffh^{GppNHp}•$FtsY^{GppNHp}$ and Ffh/4.5S RNP^{GppNHp}•$FtsY^{GppNHp}$ complexes respectively (Peluso et al., 2000). Considering Ffh and FtsY function both as GTPases and GTPase activating proteins, one might expect the formation of a complex between these two proteins to be sensitive to chemical nature of the β-γ backbone of the GTP substrate.

Similarly to what we have found previously using GppNHp, 4.5S RNA enhances the kinetics of association by two orders of magnitude. Despite the rate enhancements from the combined effect of the GTP and the presence of 4.5S RNA, the rate is still an order of magnitude slower than expected for a diffusion limited protein-protein association (Fersht, 1985). This would suggest that the $Ffh^{GTP} \bullet FtsY^{GTP}$ complex requires conformational rearrangements during its formation. Other effector molecules, like the 4.5S RNA in this case, could influence the kinetics of the complex's formation.

Dissassembly of $Ffh^{GTP} \bullet FtsY^{GTP}$ complex is faster in the presence of 4.5S RNA

In order to determine the k_{off} for $Ffh^{GTP} \bullet FtsY^{GTP}$ and Ffh/4.5S $RNP^{GTP} \bullet FtsY^{GTP}$ complexes, we employed a "GDP trap" assay and measured the dissociation rates by monitoring FtsY's tryptophan fluorescence. This was achieved by performing double mixing experiments in which Ffh and FtsY were first incubated with GTP for a sufficient time period to enable $Ffh^{GTP} \bullet FtsY^{GTP}$ and Ffh/4.5S $RNP^{GTP} \bullet FtsY^{GTP}$ complex formation to reach steady state followed by the subsequent addition of excess GDP. After the addition of GDP, the change in FtsY's tryptophan fluorescence was monitored in order to measure the rate of dissociation. From this experiment we could ask whether 4.5S RNA enhanced the dissociation rate as we have previously seen with GppNHp (Peluso et al., 2000).

As shown in Figure 5, we find that the disassembly reactions show apparent first order kinetics with rate constants of 1.5×10^{-1} s^{-1} and 7.2×10^{-1} s^{-1}

for the $Ffh^{GTP} \bullet FtsY^{GTP}$ and $Ffh/4.5S\ RNP^{GTP} \bullet FtsY^{GTP}$ complexes, respectively. 4.5S RNA only enhanced the dissociation rate 5-fold, which is in contrast to our previous findings (Peluso et al., 2000), whereby 4.5S RNA increased the dissociation of the $Ffh^{GppNHp} \bullet FtsY^{GppNHp}$ complex by 2 orders of magnitude (Peluso et al., 2000). The reaction using GTP is more complicated than that previously performed using GppNHp, as there are three reaction steps which, in principle, could lead to apparent $Ffh^{GTP} \bullet FtsY^{GTP}$ dissociation as shown in Figure 1. These steps are $Ffh^{GTP} \bullet FtsY^{GTP}$ dissociation (Step 3) and GTP hydrolysis followed by $Ffh^{GDP \bullet P} \bullet FtsY^{GDP \bullet P}$ dissociation (Steps 4 and 5). We, therefore, needed to determine the maximal rate of GTP hydrolysis for the $Ffh^{GTP} \bullet FtsY^{GTP}$ and the $Ffh/4.5S\ RNP^{GTP} \bullet FtsY^{GTP}$ complexes in order to determine which step was governing the dissassembly of the complex.

GTP hydrolysis by the $Ffh^{GTP} \bullet FtsY^{GTP}$ and $Ffh/4.5S\ RNP^{GTP} \bullet FtsY^{GTP}$ complexes is the primary reaction patheway by which the complexes dissassemble

We next set out to determine the maximal rates of GTP hydrolysis by the two complexes. The lower basal activity of FtsY enabled us, in the presence of fixed low concentrations of Ffh and Ffh/4.5S RNP, to vary the concentration of FtsY over a broad range. As seen in Figure 6, the GTPase rates of the Ffh•FtsY and Ffh/4.5S •FtsY complexes follow standard Michaelis-Menten kinetics and plateau at high concentrations of FtsY. The plateaus, defining the apparent maximal rates for the Ffh•FtsY and Ffh/4.5S•FtsY complexes respectively, differ by about five-fold ($V_{max} = 1.2 \times 10^{-1}$ GTP s^{-1} for Ffh•FtsY and 7.1×10^{-1} GTP s^{-1} for Ffh/4.5S•FtsY). Thus 4.5S RNA affects the maximal rate of GTP hydrolysis in addition to the kinetic parameters that govern the association of the two proteins with each other.

In both cases (± 4.5S RNA), the maximal rate of GTP hydrolysis was similar to the first order dissociation rate determined in Figure 5. The simplest interpretation is that the dissociation of Ffh^{GTP}•$FtsY^{GTP}$ or Ffh/4.5S RNP^{GTP}•$FtsY^{GTP}$ in Step 3 is slower than the subsequent steps in the pathway (Steps 4, 5, and 6). Moreover, 4.5S RNA appears to enhance the kinetics of this step. Therefore, in addition to promoting the bimolecular association of Ffh with FtsY, the RNA promotes the GTPase activity of the complex.

Because the reactions in Figure 6 were monitored multiple turnover events per enzyme molecule, there are several steps in the reaction mechanism of Figure 1 where the RNA could function to enhance the overall GTPase activity. For instance, the additional first order step affected by 4.5S RNA could be a conformational change directly preceding hydrolysis (which would subdivide Step 4 into Step 4A and Step 4B). Alternatively, dissociation of the Ffh•FtsY complex after the hydrolysis GTP (Step 5) or release of the GDP and or P_i (Step 6)

from the enzymes could be the rate determining step. We therefore wished to distinguish which of these possibilities was in fact the case.

4.5S RNA either affects the intrinsic catalyis by the Ffh•FtsY complex or a conformational change in the complex directly preceding GTP hydrolysis

Because the reactions in Figure 6 were monitored multiple turnover events per enzyme molecule, there are several steps in the reaction mechanism of Figure 1 where the RNA could function to enhance the overall GTPase activity. For instance, the additional first order step affected by 4.5S RNA could be a conformational change directly preceding hydrolysis (which would subdivide Step 4 into Step 4A and Step 4B). Alternatively, dissociation of the Ffh•FtsY complex after the hydrolysis GTP (Step 5) or release of the GDP and or P_i (Step 6) from the enzymes could be the rate determining step. We therefore wished to distinguish which of these possibilities was in fact the case.

This could be tested by simply performing GTPase reactions at sufficiently high enzyme concentrations which would facilitate the detection of biphasic kinetics. In multiple turnover reactions with saturating GTP, a burst of product formation followed by a slower reaction would suggest that a step following GTP hydrolysis was rate limiting. At the lower enzyme concentrations (0.1 - 0.5 μM) used in the assays shown in Figure 6 the detection of a potential burst phase in the presence of 1mM GTP was unlikely. We therefore carried out GTPase reactions at sufficiently high enzyme concentrations (20 mM Ffh and 79 mM FtsY) whereby a burst would be readily observable if in fact one existed.

As seen in Figure 7, the GTPase velocities of the Ffh•FtsY complex is monophasic before reaching a plateau whereby greater than 80% of the substrate has been turned over. From a linear fit to the initial velocity of the reaction, a GTPase rate of 3.5 (± 0.05) x 10^{-2} GTP complex^{-1} s^{-1} was calculated which is within a factor of 3 of the maximal GTPase rate of 1.2 x 10^{-1} complex^{-1} s^{-1} as determined by the experiments in Figure 6. Since we do not observe a burst phase in Figure 7, we can conclude that Step 4 is rate limiting for GTP hydrolysis by the Ffh^{GTP}•FtsY^{GTP} complex under the conditions assayed. In order for 4.5S RNA to enhance the maximal rate of GTP hydrolysis, it would have to increase the rate of the slowest step in the reaction pathway. It follows, therefore, that 4.5S RNA must be affecting Step 4 of the reaction pathway.

Previous studies looking at release of GDP from Ffh have shown the k_{off} to be very fast, approximately 13 s^{-1} (Jagath et al., 1998). This would argue against GDP release being a rate limiting step in the reaction pathway which is also consistent with what we observe in Figure 7. From this one would predict that the inhibition constant , or K_i, of GDP for Ffh's basal GTPase activity would also not be affected by 4.5S RNA. In order to verify this, we quantified GDP inhibition of Ffh's basal GTPase activity in the presence and absence of 4.5S RNA (Figure 8). We observed similar K_i values for GDP of 322 (± 100) nM and 203 (±

78) nM for Ffh and Ffh/4.5S RNP, respectively. Moreover, at half maximal inhibition levels of GDP, millimolar concentrations of inorganic phosphate were required to see enhanced inhibition due to the presence of the added phosphate (data not shown). This would argue against the formation of a very stable Ffh•GDP or Ffh•GDP•P_i complex after hydrolysis. Moreover, the data is consistent with the notion that 4.5S RNA is enhancing the GTPase reaction pathway at step prior to hydrolysis, namely Step4.

DISCUSSION

We describe here the characterization of the GTPase mechanism for the Ffh^{GTP}•$FtsY^{GTP}$ complex. From this work , we have described a series of rate constants which serve as the basis for our understanding of the various steps involved in the hydrolysis of GTP by the Ffh/4.5S RNP•FtsY complex. Also in the process, we have gained a better perspective of how 4.5S RNA specifically enhances the GTPase activity of the complex. Moreover, our findings provide insights concerning how the RNA may function in regulating the GTPase complex during the SRP-dependent protein targeting cycle.

As 4.5S RNA exhibited no dramatic influence on the basal GTPase and nucleotide binding properties of Ffh, its major role would seem to be directed towards the communication between SRP and the receptor, specifically the GAP activity(ies) of this complex. Based on our discovery of 4.5S RNA's catalytic role in the formation of the Ffh•FtsY complex, we were not surprised to find that 4.5S RNA dramatically stimulated the association of the two proteins for one another in the presence of GTP (Peluso et al., 2000). This increased association rate by over 2 orders of magnitude would easily explain the earlier observations that concluded that 4.5S RNA was absolutely essential to the interaction between Ffh and FtsY. At the concentrations assayed in the previous studies (typically 5 nM and 50 nM for Ffh and FtsY, respectively) (Miller et al., 1994), Ffh's basal GTPase rate would have been faster than the association of the two proteins. Stimulated GTPase activity could not have been observed in this case.

We were surprised to observe that the association rates in the presence of GTP were a whole order of magnitude faster than those measured previously in the presence of GppNHp. Perhaps this finding is best explained by the fact that both proteins in the $\mathrm{Ffh}^{\mathrm{GTP}}\bullet\mathrm{FtsY}^{\mathrm{GTP}}$ complex as GTPases and as GAP proteins. A unique enzyme complex, like this, is very sensitive to the chemical nature of the substrate, specifically at the β-γ-phosphate bridge of the GTP molecule.

We have also provided here through this work a better estimate for the magnitude of the stimulated GTPase activity seen for the $\mathrm{Ffh/4.5S\ RNP}^{\mathrm{GTP}}\bullet\mathrm{FtsY}^{\mathrm{GTP}}$ complex. Previously, studies have demonstrated ~ 4-8 fold stimulation in the turnover of GTP relative to Ffh's basal GTPase activity (Macao et al., 1997; Miller et al., 1994). This observed stimulation was much lower than the stimulation of Ras by classical GAP proteins which is as great as five orders of magnitude and yield apparent turnover numbers of $8.0\ \mathrm{s}^{-1}$

(Ahmadian et al., 1997). By performing assays whereby complex formation is not rate limiting, we have been able to observe greater GTPase stimulation than had been previously demonstrated. From our current estimates, we see approximately 100-fold elevation of the GTPase activity over the Ffh/4.5S RNP's basal rate. The maximal GTPase rate of $0.7\ s^{-1}$ for the Ffh/4.5S $RNP^{GTP}\bullet FtsY^{GTP}$ complex from Figure 6 is much closer to the stimulated activity of Ras ($8.0\ s^{-1}$) than what we have previously thought from studies of the Ffh•FtsY GTPase complex (Miller, et al., 1994; Powers and Walter, 1995).

The five fold difference in the maximal GTPase rate for the Ffh/4.5S $RNP^{GTP}\bullet FtsY^{GTP}$ and $Ffh^{GTP}\bullet FtsY^{GTP}$ complexes has interesting implications as well. One explanation for these findings would posit a conformational change occurring within the complex prior to hydrolysis. Potentially, 4.5S RNA could enhance the kinetics of this conformational change. This would seem a plausible model as conformational changes have been previously identified to occur for the interaction of Ras with one of its GAP proteins (Sydor et al., 1998). In fact, it is entirely possible that the true chemical step for GTP hydrolysis is much faster than can be physically measured due in part to the fact that the rate limiting step is actually the formation and/or subsequent isomerization of the complex.

This model would correlate nicely with our previous observations that 4.5S RNA catalyzes the formation of the $Ffh^{GTP}\bullet FtsY^{GTP}$ complex. In this earlier work, we suggested that the RNA was operating in a catalytic fashion to enable the complex to transition between different conformational states (Peluso et al., 2000). As observed in the present work, 4.5S RNA, in a similar vein, could be enhancing the rate of a conformational change needed to enable efficient GTP hydrolysis to ensue within the complex. By enhancing this conformational change, the RNA would appear to enhance the hydrolysis of GTP by the complex.

Alternatively, the differences in maximal GTPase rates could represent actual differences in catalytic efficiency between the two complexes. While 4.5S RNA clearly enhances the kinetics of association between Ffh and FtsY, it could also serve in a structural fashion to maintain Ffh in an optimal conformation for enhancing FtsY's GTPase activity. In the absence of the RNA, the natural corollary to this model would suggest that Ffh binds to FtsY and maintains locked in a conformation which is not as active with respect to GAP activity. The likeliest target for the RNA would have to be the Ffh protein.

Perhaps the recent crystal structure of the M-domain-4.5S RNA complex can provide insights into how this might come about. In this structure, Arg398, which is absolutely conserved, is pointing out into solution due in part to nearby interactions between 4.5S RNA and adjacent amino acids within the M-domain. Interestingly, this Arg398 is not required for binding to 4.5S RNA (Kurita et al., 1996). Crystal structures of Ras•GAP complexes have shown that the GAP proteins provide key Arg residues to Ras (Scheffzek et al., 1997). This presumably helps to stabilize the pentavalent transition state of the γ-phosphate during the hydrolysis step (Wittinghofer et al., 1997). Perhaps, 4.5S RNA is responsible for properly positioning this residue in order to enhance the GTPase activity within the complex as has been previously speculated. This would break up the inherent structural symmetry seen for the two GTPases (Freymann et al., 1997; Montoya et al., 1997). Yet, while these two proteins possess structurally identical GTPase domains, both Ffh and FtsY have their own unique domains in the M- and A-domains respectively. Perhaps, the counterpart Arg for FtsY lies within the A-domain. In addition, crosstalk between these two domains has recently been shown for FtsY (de Leeuw et al., 2000).

The possibility that the GTPase activity of the Ffh•FtsY complex may be tightly coupled with specific conformational changes would provide a sensible means of regulating this activity within the context of protein targeting. If GTP hydrolysis was used as some sort of proofreading mechanism during protein targeting and translocation, one might expect interplay between the domain which facilitates membrane targeting and the GTPase domain. For Ffh, the two activities converge within the GTPase domain itself (Zopf et al., 1993). It remains to be determined how the various steps in the reaction mechanism of Figure 1 are precisely coordinated in the context of other ligands within the SRP functional cycle, namely the ribosome-nascent chain complexes and the translocation apparatus.

The fact that the Ffh/4.5SRNP•FtsY complex and the Ffh•FtsY complex exhibit different intrinsic GTPase rates argue that 4.5S RNA further affects the conformation of the Ffh-FtsY complex. Taken together 4.5S RNA can be viewed as allosterically altering the Ffh•FtsY complex in a way which increases its dissociation and its catalytic activity as well. One could view 4.5S RNA as evolving into an effector/catalyst which prevents the GTPase complex from becoming kinetically trapped. Perhaps this property is utilized by having changes in the contacts between 4.5S RNA and the Ffh•FtsY complex especially in the context of molecules in the targeting cycle, the ribosome-nascent change complex. It's not too difficult to see how such conformational changes are used to provide ways to block the turnover of GTP . Such a built in gate would provide a means for ensuring fidelity and accuracy in protein targeting and translocation.

Instead of the RNA controlling the activity of the Ffh•Ftsy complex, the regulation could also be coming from the occupancy of Ffh with a signal sequence. At the C-terminus of the GTPase domain resides a methionine rich domain, or M-domain . This M-domain has been previously demonstrated to interact specifically with both the signal sequences and the SRP RNA. In this light, perhaps the properties of the Ffh-FtsY complex described here are providing us with insight into the type of allosteric control which signal sequences impart to the Ffh/4.5S•FtsY complex. Perhaps the occupancy of the M-domain by the signal sequence serves to inhibit the turnover of GTP by the Ffh/4.5S•FtsY. This would also be a sensible way of providing allosteric control for the process and better integrating the GTPase activities into the targeting/translocation process.

FtsY's ability to interact with Ffh/4.5S RNP could potentially be subjected to regulation as well. Interestingly, an the binding of Ffh to the full length FtsY protein has not been observed in the absence of 4.5S RNA (Junutula Jagath, personal communication). In our assays we have used a deletion construct of FtsY whereby the first 45 amino acids of the acidic, or A-domain, has been deleted. From earlier studies, it has been established that the A-Domain is critical for interactions between FtsY and the membrane (Zelazny et al., 1997). More recently, it has been suggested that this unique region provides an interacting domain for lipids. The binding of lipids has been subsequently shown to enhance FtsY's intrinsic GTPase activity (de Leeuw et al., 2000). Perhaps this region serves as a sensor for proper membrane anchoring. In the absence of lipid interactions, this domain could have a negative regulatory role on the interaction between FtsY and Ffh/4.5S RNP. Deletion of this inhibitory domain has therefore enabled us to unmask a subsequent step in the complex set of events governing the interaction between Ffh and FstY.

Here we have characterized how 4.5S RNA serves as a positive effector for the Ffh•FtsY GTPase cycle. Further work will now be directed toward integrating the other effector molecules into the basic enzymological framework. In addition this work has suggested possible ways that biological regulation can be imparted into the system. This should enable us to gain a better understanding of how GTP hydrolysis by the two GTPases is mechanistically coupled to the SRP functional cycle.

REFERENCES

Ahmadian, M.R., U. Hoffmann, R.S. Goody, and A. Wittinghofer. 1997. Individual rate constants for the interaction of Ras proteins with GTPase-activating proteins determined by fluorescence spectroscopy. *Biochem.* 36:4535-4541.

Batey, R.T., R.P. Rambo, L. Lucast, B. Rha, and J.A. Doudna. 2000. Crystal structure of the ribonucleoprotein core of the signal recognition particle. *Science* 287:1232-1239.

Bernstein, H.D., M.A. Poritz, K. Strub, P.J. Hoben, S. Brenner, and P. Walter. 1989. Model for signal sequence recognition from amino-acid sequence of 54k subunit of signal recognition particle. *Nature* 340:482-486.

Brown, S., and M.J. Fournier. 1984. The 4.5S RNA Gene of *Escherichia coli* is Essential for Cell Growth. *J. Mol. Biol.* 178:533-550.

Connolly, T., and R. Gilmore. 1993. GTP Hydrolysis by Complexes of the Signal Recognition Particle and the Signal Recognition Particle Receptor. *J. Cell Biol.* 123:799-807.

de Leeuw, E., K. te Kaat, C. Moser, G. Menestrina, R. Demel, B. de Kruijff, B. Oudega, J. Luirink, and I. Sinning. 2000. Anionic phospholipids are involved in membrane association of FtsY and stimulate its GTPase activity. *EMBO J.* 19:531-541.

Fersht, A. 1985. Enzyme Structure and Mechanism. W.H. Freeman and Co., New York. pp. 150-151.

Freymann, D.M., R.J. Keenan, R.M. Stroud, and P. Walter. 1997. Structure of the conserved GTPase domain fo the signal recognition particle. *Nature* 385:361-364.

Freymann, D.M., R.J. Keenan, R.M. Stroud, and P. Walter. 1999. Functional changes in the structure of the SRP GTPase on binding GDP and Mg2+GDP. *Nat Struct. Biol.* 6:793-801.

Gilmore, R., and Hoffman, K.E. 1988. Guanosine Triphosphate Promotes the Post-translational Integration of Opsin into the Endoplasmic Reticulum Membrane. *J. Biol. Chem.* 263:4381-4385.

Gilmore, R., G. Blobel, and P. Walter. 1982a. Protein translocation across the endoplasmic reticulum. I. Detection in the microsomal membrane of a receptor for the signal recognition particle. *J. Cell Biol.* 95:463-469.

Gilmore, R., P. Walter, and G. Blobel. 1982b. Protein translocation across the endoplasmic reticulum. II. Isolation and characterization of the signal recognition particle receptor. *J. Cell Biol.* 95:470-477.

Jagath, J.R., M.V. Rodnina, G. Lentzen, and W. Wintermeyer. 1998. Interaction of guanine nucleotides with the signal recognition particle from Escherichia coli. *Biochem.* 37:15408-15413.

Jagath, J.R., M.V. Rodnina, and W. Wintermeyer. 2000. Conformational changes in the bacterial SRP receptor FtsY upon binding of guanine nucleotides and SRP. *J. Mol. Biol.* 295:745-753.

John, J., R. Sohmen, J. Feuerstein, R. Linke, A. Wittinghofer, and R.S. Goody. 1990. Kinetics of interaction of nucleotides with nucleotide-free H-ras p21. *Biochem.* 29:6058-6065.

Keenan, R.J., D.M. Freymann, P. Walter, and R.M. Stroud. 1998. Crystal structure of the signal sequence binding subunit of the signal recognition particle. *Cell* 94:181-191.

Kurita, K., K. Honda, S. Suzuma, H. Takamatsu, K. Nakamura, and K. Yamane. 1996. Identification of a region of Bacillus subtilis Ffh, a homologue of mammalian SRP54 protein, that is essential for binding to small cytoplasmic RNA. *J. Biol. Chem.* 271:13140-13146.

Lentzen, G., H. Moine, C. Ehresmann, B. Ehresmann, and W. Wintermeyer. 1996. Structure of 4.5S RNA in the signal recognition particle of Escherichia coli as studied by enzymatic and chemical probing. *RNA* 2:244-253.

Luirink, J., C.M. ten Hagen-Jongman, C.C. van der Weijden, B. Oudega, S. High, B. Dobberstein, and R. Kusters. 1994. An alternative protein targeting pathway in Escherichia coli: studies on the role of FtsY. *EMBO J.* 13:2289-2296.

Lütcke, H., S. High, K. Römisch, A. Ashford, and B. Dobberstein. 1992. The methionine-rich domain of the 54 kDa subunit of signal recognition particle is sufficient for the interaction with signal sequences. *EMBO J.* 11:1543-1551.

Macao, B., J. Luirink, and T. Samuelsson. 1997. Ffh and FtsY in a Mycoplasma mycoides signal-recognition particle pathway: SRP RNA and M domain of Ffh are not required for stimulation of GTPase activity in vitro. *Mol. Microbiol.* 24:523-534.

Miller, J.D., H.D. Bernstein, and P. Walter. 1994. Interaction of E. coli Ffh/4.5S ribonucleoprotein and FtsY mimics that of mammalian signal recognition particle and its receptor. *Nature* 367:657-659.

Miller, J.D., H. Wilhelm, L. Gierasch, R. Gilmore, and P. Walter. 1993. GTP binding and hydrolysis by the signal recognition particle during initiation of protein translocation. *Nature* 366:351-354.

Montoya, G., C. Svensson, J. Luirink, and I. Sinning. 1997. Crystal structure of the NG domain from the signal-recognition particle receptor FtsY. *Nature* 385:365-368.

Moser, C., O. Mol, R.S. Goody, and I. Sinning. 1997. The signal recognition particle receptor of Escherichia coli (FtsY) has a nucleotide exchange factor built into the GTPase domain. *Proc. Natl. Acad. Sci. U. S. A.* 94:11339-11344.

Neidhardt, F.C. 1987 in Escherichia coli and Salmonella Typherium Cellular and Molecular Biology. F.C. Neidhardt, J.L. Ingraham, K.B. Low, B. Magasanik, M. Schaechter, and H.E. Umbarger, eds. American Society for Microbiology, Washington D.C. pp. 4-5.

Peluso, P., D. Herschlag, S. Nock, D.M. Freymann, A.E. Johnson, and P. Walter. 2000. Role of 4.5S RNA in assembly of the bacterial signal recognition particle with its receptor. *Science* 288:1640-1643.

Phillips, G.J., and T.J. Silhavy. 1992. The E. coli *ffh* gene is necessary for viability and efficient protein export. *Nature* 359:744-746.

Poritz, M.A., H.D. Bernstein, K. Strub, D. Zopf, H. Wilhelm, and P. Walter. 1990. An E. coli ribonucleoprotein containing 4.5S RNA resembles mammalian signal recognition particle. *Science* 250:111-1117.

Powers, T., and P. Walter. 1995. Reciprocal Stimulation of GTP Hydrolysis by Two Directly Interacting GTPases. *Science* 269:1422-1424.

Powers, T., and P. Walter. 1997. Co-translational protein targeting catalyzed by the Escherichia coli signal recognition particle and its receptor. *EMBO J.* 16:4880-4886.

Ribes, V., K. Römisch, A. Giner, B. Dobberstein, and D. Tollervey. 1990. E. coli 4.5S RNA Is Part of a Ribonucleoprotein Particle That Has Properties Related to Signal Recognition Particle. *Cell* 63:591-600.

Römisch, K., J. Webb, K. Lingelbach, H. Gausepohl, and B. Dobberstein. 1990. The 54-kD protein of signal recognition particle contains a methionine-rich RNA binding domain. *J. Cell Biol.* 111:1793-1802.

Sambrook, J., E. F. Fritsch, T. Maniatis. 1989. Molecular Cloning: A Laboratory Manual, 2nd Edition. Cold Spring Harbor Laboratory Press. p. 7.28.

Scheffzek, K., M.R. Ahmadian, W. Kabsch, L. Wiesmuller, A. Lautwein, F. Schmitz, and A. Wittinghofer. 1997. The Ras-RasGAP complex: structural basis for GTPase activation and its loss in oncogenic Ras mutants. *Science* 277:333-338.

Siegel, V., and P. Walter. 1988. Each of the activities of signal recognition particle (SRP) is contained within a distinct domain: analysis of biochemical mutants of SRP. *Cell* 52:39-49.

Sydor, J.R., M. Engelhard, A. Wittinghofer, R.S. Goody, and C. Herrmann. 1998. Transient kinetic studies on the interaction of Ras and the Ras-binding domain of c-Raf-1 reveal rapid equilibration of the complex. *Biochem.* 37:14292-14299.

Walter, P. 1996. Signal Sequence Recognition and Protein Targeting to the Endoplasmic Reticulum Membrane. *In* The Harvey Lectures, Series 91. Wiley-Liss, Inc. 115-131.

Walter, P., and G. Blobel. 1981. Translocation of proteins across the endoplasmic reticulum. III. Signal recognition protein (SRP) causes signal sequence and site specific arrest of chain elongation that is released by microsomal membranes. *J. Cell Biol.* 91:557-561.

Walter, P., and G. Blobel. 1982. Signal recognition particle contains a 7S RNA essential for protein translocation across the endoplasmic reticulum. *Nature* 299:691-698.

Walter, P., I. Ibrahimi, and G. Blobel. 1981. Translocation of proteins across the endoplasmic reticulum I. Signal Recognition Protein (SRP) binds to in vitro assembled polysomes synthesizing secretory protein. *J. Cell Biol.* 91:545-550.

Walter, P., and A.E. Johnson. 1994. Signal Sequence Recognition and Protein Targeting to the Endoplasmic Reticulum Membrane. *Ann. Rev. Cell Biol.* 10:87-119.

Walter, P., R. Keenan, and U. Schmitz. 2000. Perspectives: structural biology. SRP--where the RNA and membrane worlds meet. *Science* 287:1212-1213.

Wittinghofer, A., K. Scheffzek, and M.R. Ahmadian. 1997. The interaction of Ras with GTPase-activating proteins. *FEBS Lett.* 410:63-67.

Zelazny, A., A. Seluanov, A. Cooper, and E. Bibi. 1997. The NG domain of the prokaryotic signal recognition particle receptor, FtsY, is fully functional when fused to an unrelated integral membrane polypeptide. *Proc. Natl. Acad. Sci. U. S. A.* 94:6025-6029.

Zopf, D., H.D. Bernstein, A.E. Johnson, and P. Walter. 1990. The methionine-rich domain of the 54 kd protein subunit of the signal recognition particle contains an RNA binding site and can be crosslinked to a signal sequence. *EMBO J.* 9:4511-4517.

Zopf, D., H.D. Bernstein, and P. Walter. 1993. GTPase domain of the 54kD subunit of the mammalian signal recognition particle is required for protein translocation but not for signal sequence binding. *J. Cell Biol.* 120:1113-1121.

Figure 4-1 Model depicting a simple reaction scheme of GTP hydrolysis by the Ffh-FtsY complex. The symmetrical model implies that both GTPases, Ffh and FtsY, each have a basal rate of hydrolysis (upper cycles, steps 1, 2 and 6 for Ffh and steps 1′, 2′, and 6′ for FtsY), and then exhibit stimulated GTP hydrolysis upon complex formation (steps 3, 4 and 5). Ffh can participate in this reaction by itself, or can be complexed with 4.5S RNA to form Ffh/4.5S RNP, a stable ribonucleoprotein (as indicated by the "± R").

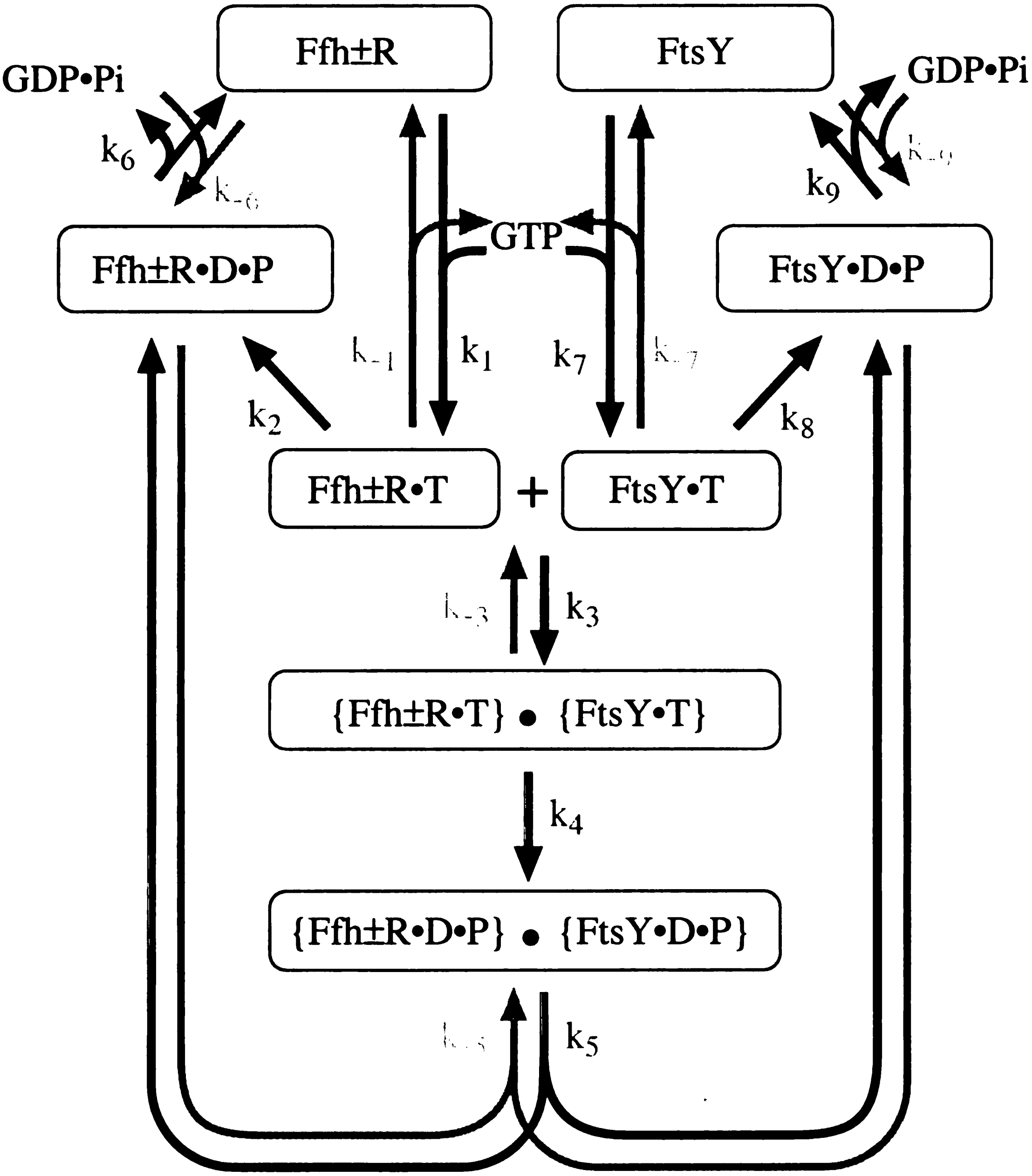
Ffh±R
FtsY
GDP•Pi
GDP•Pi
k6
k-6
k9
k-9
GTP
Ffh±R•D•P
FtsY•D•P
k-1
k1
k7
k-7
k2
k8
Ffh±R•T
+
FtsY•T
k-3
k3
{Ffh±R•T} • {FtsY•T}
k4
{Ffh±R•D•P} • {FtsY•D•P}
k-5
k5

Figure 4-2: **Time course of GTP hydrolysis of Ffh-FtsY and Ffh/4.5S RNP-FtsY complexes.** GTP hydrolysis was measured in reactions containing 1 μM Ffh and 35 μM FtsY(■), 1 μM Ffh-4.5S RNP + 35 μM FtsY (●), and 35 μM FtsY alone (▲). Assays were performed at 25° C in Buffer E. Reactions were initiated by the addition of 500 μM GTP with a stoichiometric amount of Mg^{2+}. Linear fits of the data yielded GTP hydrolysis rates of 0.21 GTP hydrolyzed per Ffh/4.5S RNP-FtsY complex per second and 0.028 GTP hydrolyzed per Ffh-FtsY complex per second. The rate of GTP hydrolysis by FtsY alone was much lower giving a value of 0.0006 GTP hydrolyzed per FtsY per second.

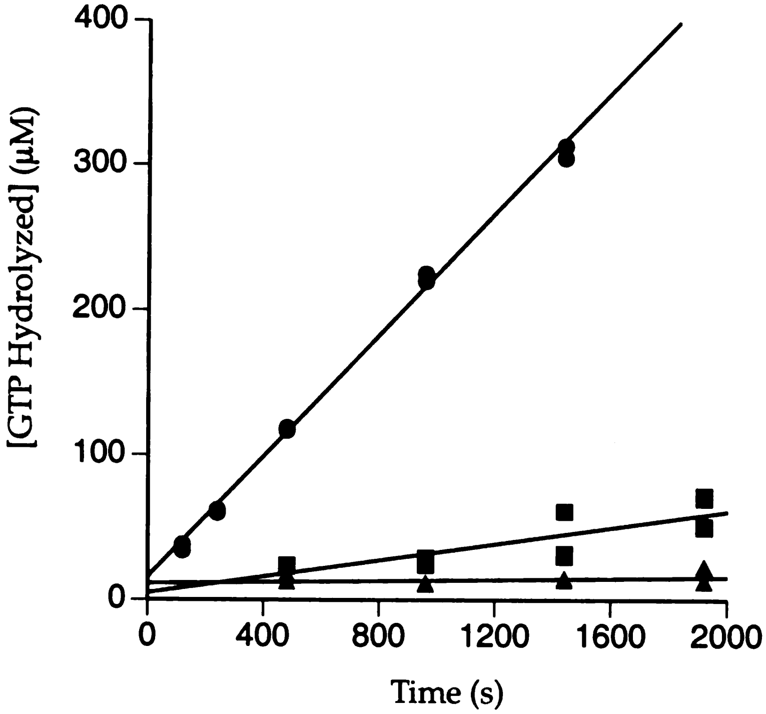
[GTP Hydrolyzed] (μM)
400
300
200
100
0
0
400
800
1200
1600
2000
Time (s)

Figure 4-3: **Measurement of $K_{1/2}$ and k_{chem} for Ffh, Ffh/4.5S RNP, and FtsY.** GTP hydrolysis was assayed in reactions containing varying concentrations of either Ffh (Panel A), Ffh-4.5S RNP (Panel B), or FtsY (Panel C). The concentration of GTP was 5 nM for the reactions containing Ffh and Ffh-4.5S RNP, and 33 nM for the reactions containing FtsY. The time courses were fit with single exponential functions, and the thus derived exponential rate constants were plotted as a function of the enzyme concentrations. The plots were fit to the equation: rate = ([enzyme] / ([enzyme] + $K_{1/2}$)) * k_{chem}. The values obtained were for Ffh: $k_{chem} = 1.6 (\pm 0.02) \times 10^{-3}$ sec^{-1} and $K_{1/2} = 0.3 (\pm.02)$ μM, for Ffh/4.5S RNP $k_{chem} = 2.4 (\pm 0.3) \times 10^{-3}$ sec^{-1}, and $K_{1/2} = 1.8 (\pm 0.4)$ μM, and for k_{chem} = FtsY $4.0 (\pm 0.3) \times 10^{-4}$ sec^{-1} and $K_{1/2} = 20 (\pm 6.0)$ μM.

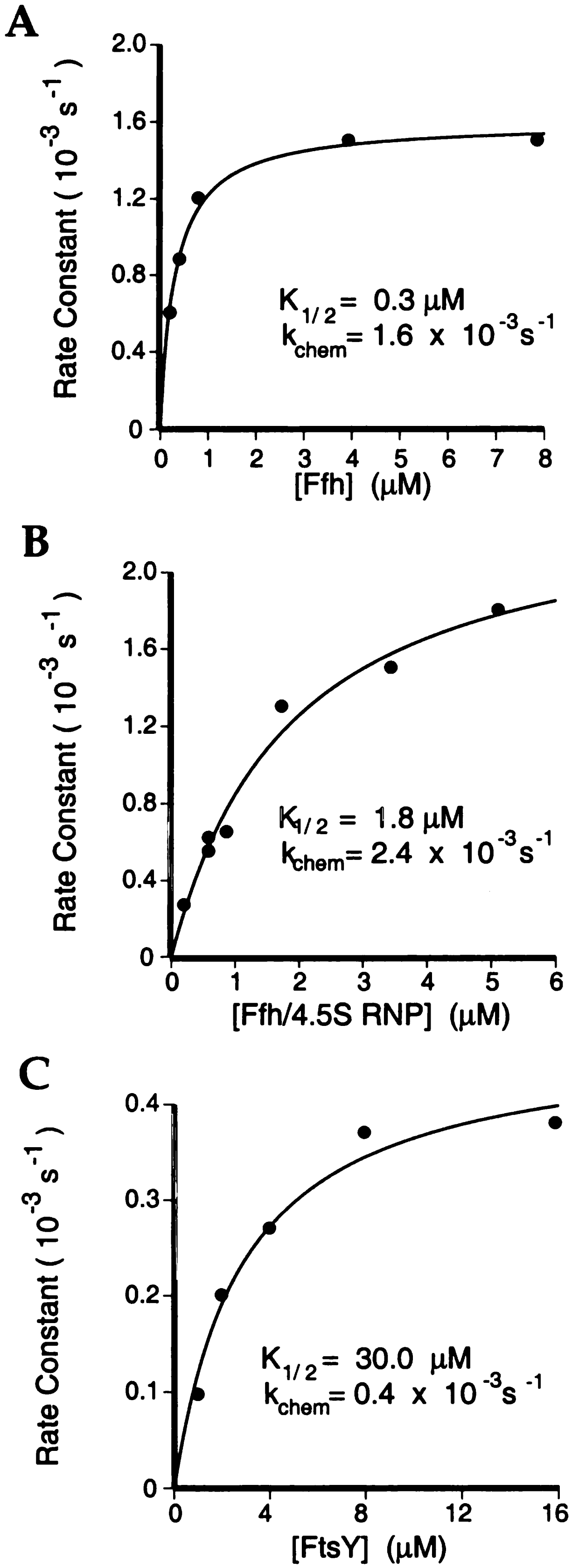
A
Rate Constant (10^{-3} s^{-1})
2.0
1.6
1.2
0.8
0.4
0
0
1
2
3
4
5
6
7
8
[Ffh] (μM)
$K_{1/2}$ = 0.3 μM
k_{chem} = 1.6 x $10^{-3}$$s^{-1}$
B
Rate Constant (10^{-3} s^{-1})
2.0
1.6
1.2
0.8
0.4
0
0
1
2
3
4
5
6
[Ffh/4.5S RNP] (μM)
$K_{1/2}$ = 1.8 μM
k_{chem} = 2.4 x $10^{-3}$$s^{-1}$
C
Rate Constant (10^{-3} s^{-1})
0.4
0.3
0.2
0.1
0
0
4
8
12
16
[FtsY] (μM)
$K_{1/2}$ = 30.0 μM
k_{chem} = 0.4 x $10^{-3}$$s^{-1}$

Figure 4-4: Association Kinetics for Ffh•FtsY and Ffh/4.5S RNP•FtsY complexes in the presence of GTP. Binding of 0.5 μM FtsY to 9.1 μM Ffh (A) and 9.1 μM Ffh/4.5S RNP (B) were monitored by measuring changes in tryptophan fluorescence over time. The time courses were fit to single exponential curves yielding k_{obs} of 0.145 (± 0.001) s^{-1} and 15.67 (± 0.44) s^{-1}, respectively. Plots of k_{obs} against varying concentrations of Ffh or Ffh/4.5S RNP were generated in (C) and (D) from different experiemnts performed in a similar to those in (A) and (B). The Plots in (C) and (D) were fit to the equation $k_{obs} = k_{on}[\text{Ffh}\pm 4.5\text{S RNA}] + k_{off}$. From the slopes of the curve fits, k_{on} values of 5.6 (± 0.3) x 10^3 $M^{-1}s^{-1}$ and 1.8 (± 0.1) x 10^6 $M^{-1}s^{-1}$ were obtained for the formation of the Ffh•FtsY and Ffh/4.5S RNP•FtsY complexes respectively.

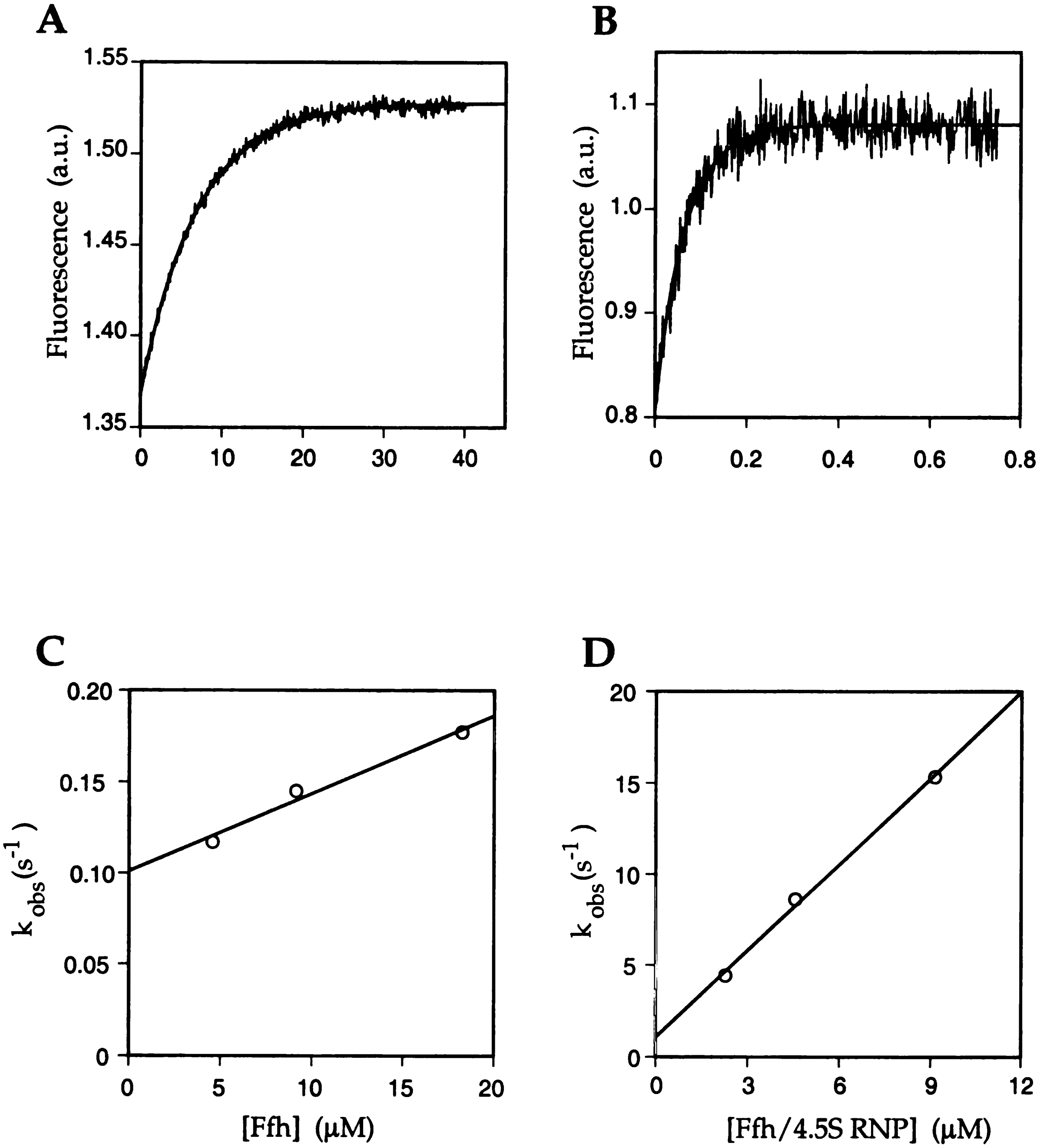
A
Fluorescence (a.u.)
1.55
1.50
1.45
1.40
1.35
0
10
20
30
40
B
Fluorescence (a.u.)
1.1
1.0
0.9
0.8
0
0.2
0.4
0.6
0.8
C
$k_{obs}(s^{-1})$
0.20
0.15
0.10
0.05
0
0
5
10
15
20
[Ffh] (μM)
D
$k_{obs}(s^{-1})$
20
15
10
5
0
0
3
6
9
12
[Ffh/4.5S RNP] (μM)

Figure 4-5: Dissociation kinetics of the Ffh•FtsY and Ffh/4.5S RNP•FtsY complexes. In a two-step mixing process, 1.0 μM FtsY was first mixed with either 1.6 μM Ffh (A) or 1.6 μM Ffh/4.5S RNP (B) in the presence of 30 μM GTP•Mg^{2+} followed by mixing with a 50-fold excess of GDP•Mg^{2+} after complex formation had reached steady state in both cases. The decays in tryptophan fluorescence were fit to single exponential curves which yielded dissociation rates of 0.15 (± 0.01) s^{-1} and 0.72 (± 0.01) s^{-1} for the Ffh•FtsY and Ffh/4.5S RNP•FtsY complexes respectively. Similar rates were observed at different protein concentrations and the 50-fold excess GDP was determined to be sufficient to yield the maximal rate constants (data not shown).

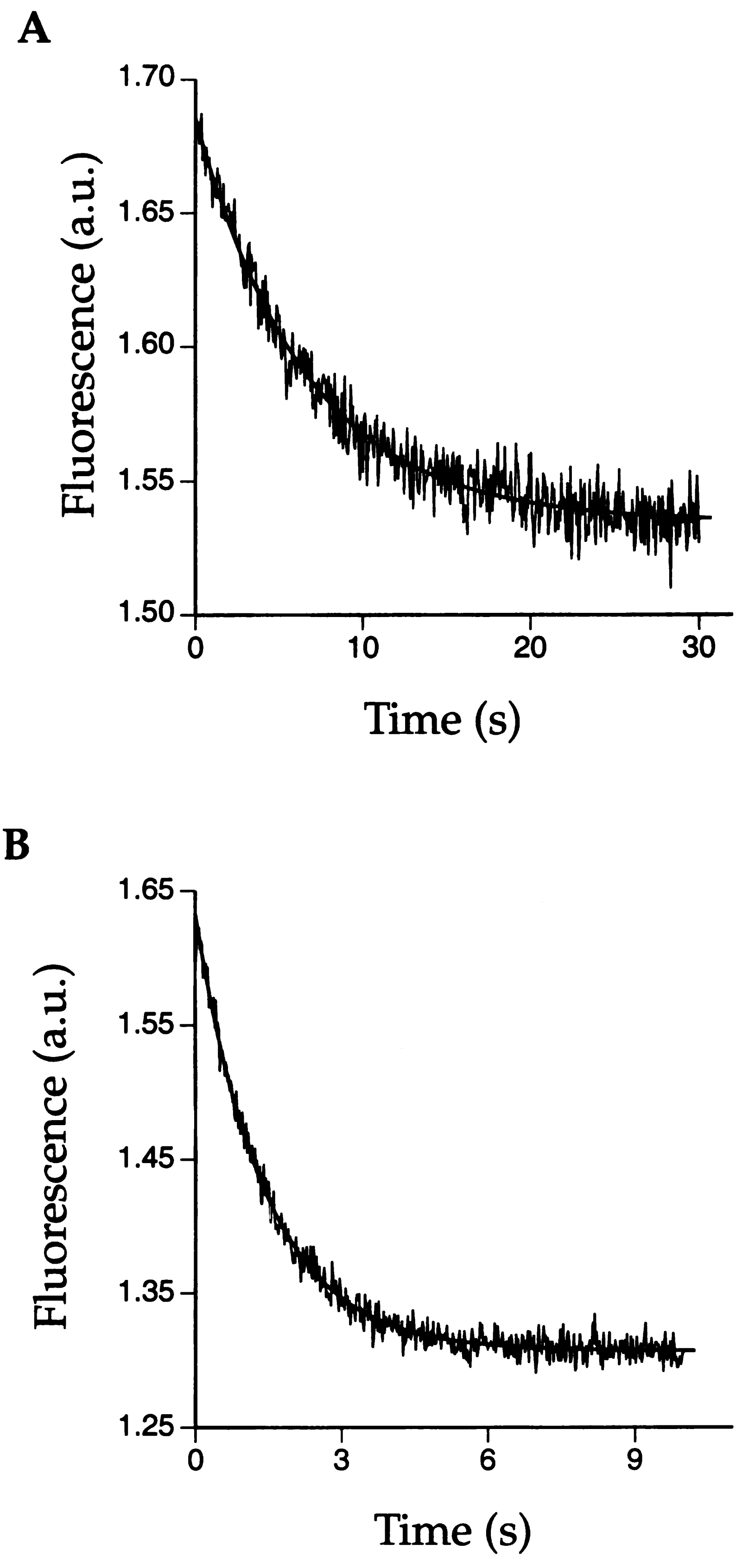
A
Fluorescence (a.u.)
1.70
1.65
1.60
1.55
1.50
0
10
20
30
Time (s)
B
Fluorescence (a.u.)
1.65
1.55
1.45
1.35
1.25
0
3
6
9
Time (s)

Figure 4-6: Determination of the maximal GTPase rates for the Ffh•FtsY and Ffh/4.5S RNP•FtsY complexes. 0.5 μM Ffh (A) and 0.1 μM Ffh/4.5S RNP (B) were assayed for GTPase activity in the presence of varying concentrations of FtsY. Reactions were initiated by the addition of GTP to a final concentration of 1mM with a stoichiometric amount of Mg^{2+}. This concentration was determined to be sufficient for yielding maximal steady state rates (data not shown). For each assay condition, a GTPase time course was carried out, requiring multiple rounds of turnover by each enzyme molecule, and the steady state rate was determined from a linear fit. These linear rates were plotted versus FtsY concentration as shown above. The data was fit to the equation GTPase velocity $= (([\mathrm{FtsY}]/([\mathrm{FtsY}] + K_m)) \times V_{max}$. From the fits, V_{max} values of 0.12 GTP hydrolyzed complex^{-1}s^{-1} and 0.71 GTP hydrolyzed per complex^{-1}s^{-1} were obtained for the Ffh•FtsY and Ffh/4.5S RNP•FtsY complexes respectively. In addition, K_m values of 11 μM and 1.6 μM were obtained for the Ffh•FtsY and Ffh/4.5S RNP•FtsY complexes.

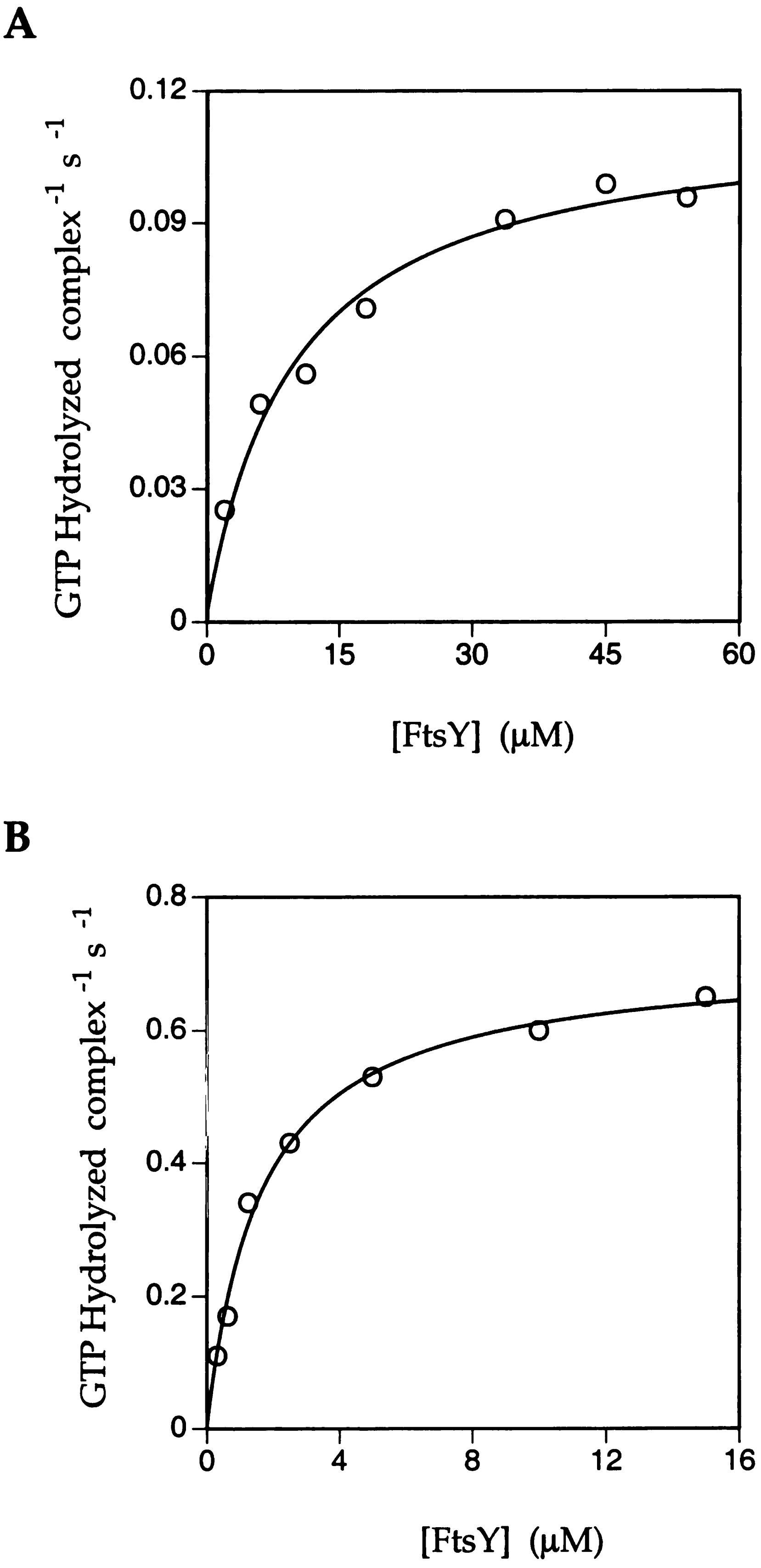
A
GTP Hydrolyzed complex $^{-1}$ s $^{-1}$
0.12
0.09
0.06
0.03
0
0
15
30
45
60
[FtsY] (μM)
B
GTP Hydrolyzed complex $^{-1}$ s $^{-1}$
0.8
0.6
0.4
0.2
0
0
4
8
12
16
[FtsY] (μM)

Figure 4-7: Initial velocity measurements for the Ffh^{GTP}•FtsY^{GTP} complex. 20 μM Ffh and 79 μM FtsY were assayed under standard conditions in the presence of 250 μM GTP with a stoichiometric amount of Mg^{2+} present in order to obtain an accurate determination of the initial velocity for the complex. The concentration of GTP hydrolyzed is plotted versus time for the time courses monitored. From a linear fit to the initial portion of the time course, a velocity of 0.03 GTP complex^{-1} s^{-1} was extrapolated.

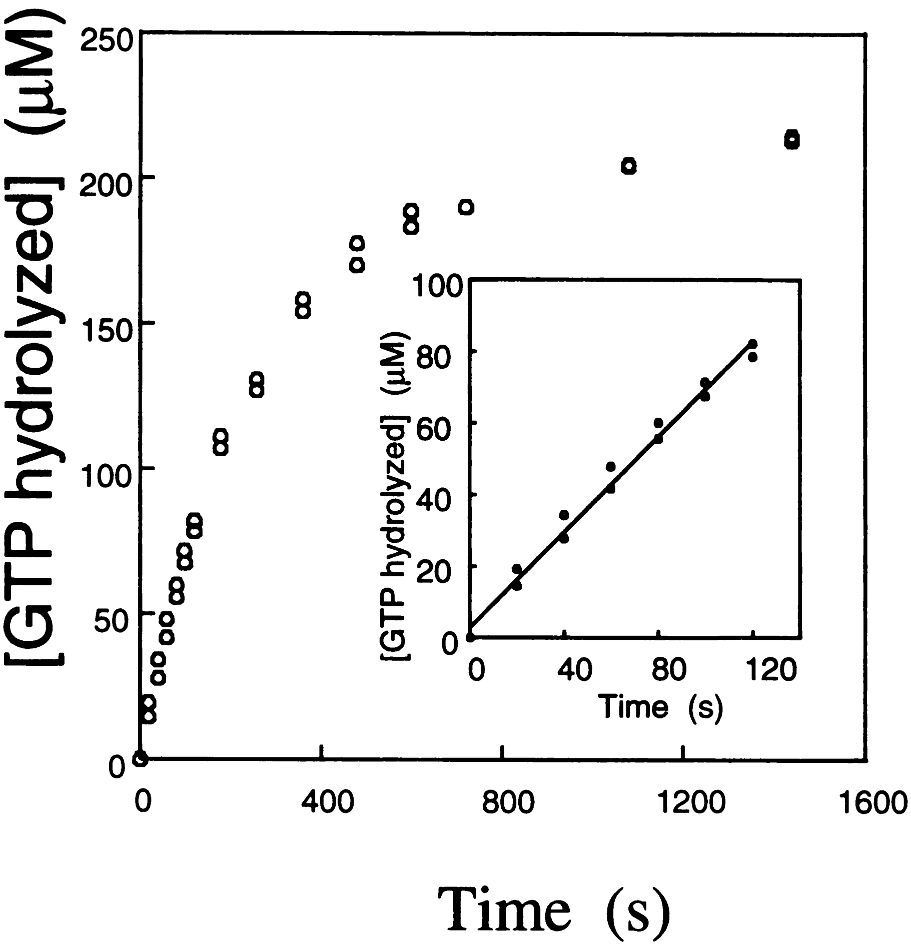
[GTP hydrolyzed] (μM)
250
200
150
100
50
0
0
400
800
1200
1600
Time (s)
[GTP hydrolyzed] (μM)
100
80
60
40
20
0
0
40
80
120
Time (s)

Figure 4-8: GDP inhibition of Ffh's basal GTPase is similar both in the presence and absence of 4.5S RNA. For these experiments, Ffh and Ffh/4.5S RNP were assayed at 50 nM with 5 nM GTP. Time courses were carried out at various concentrations of GDP. For each condition, the single turnover rate was determined as a single exponential fit. These rate constants were then compared to determine the relative inhibition resulting from increasing levels of GDP. The percentage inhibition was plotted versus concentration of GDP above. These curves were fit to a binding equation : $f(x) = (x / (x + K_i)) * (100\%$ inhibition$)$. From these fits, K_i of 203 (± 100) nM and 322 (± 78 nM) were determined for Ffh and Ffh/4.5S RNP, respectively.

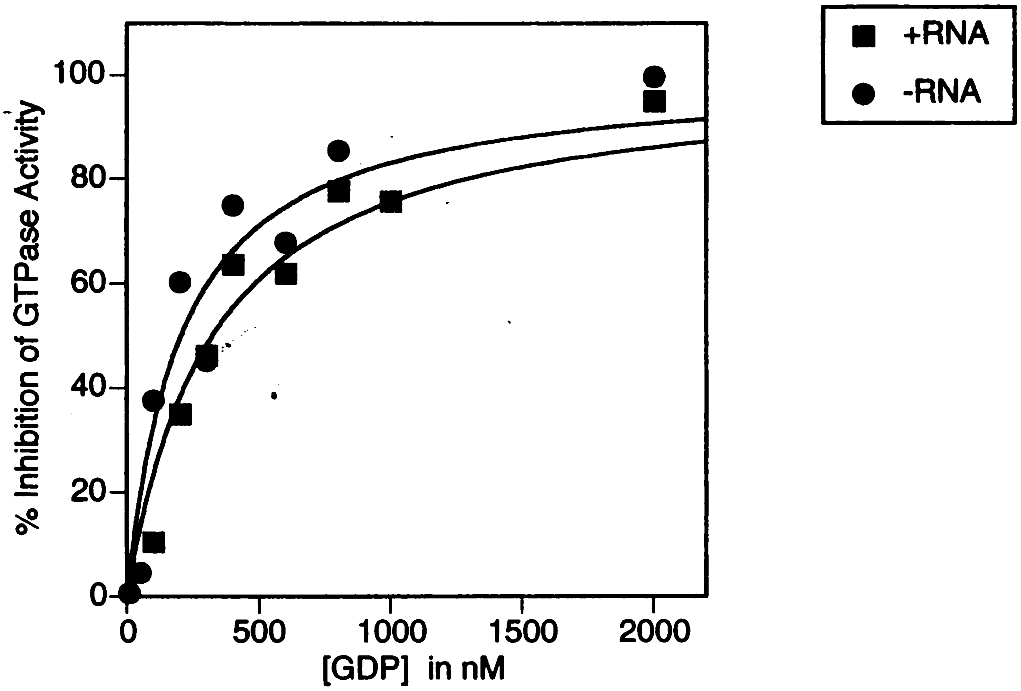
% Inhibition of GTPase Activity
100
80
60
40
20
0
0
500
1000
1500
2000
[GDP] in nM
■ +RNA
● -RNA

Appendix A. Fluoresence Studies to Monitor Ffh/4.5S RNP Interactions With the Ribosome

Abstract

In this section, we describe our efforts to characterize a fluorescence-based assay which we had hoped to employ in looking at the interactions between the Ffh/4.5S RNP and the ribosome. The assay utilized a 4.5S RNA which was specifically labelled at the 3′ end with a fluorescein derivative. Monitoring the fluorescence anisotropy of the 3′-fluorescein-4.5S RNA, a dramatic 3-fold increase was observed upon the addition of Ffh. The addition of salt-washed ribosome and 50S subunits caused a decrease in the anisotropy of the Ffh/3′-fluorescein-4.5S RNP. We describe here our initial characterization of the assay, in collaboration with Dr. Arthur Johnson's laboratory. Furthermore, we describe how additional experiments led to the invalidation of the assay as we learned that the anisotropy changes observed were due to an aggregation effect due in part to the low ionic conditions used in the assay.

Introduction

Fluorescence techniques have long been established as a means of quantifying interactions between biomolecules under equilibrium conditions. Previous use of these techniques had been employed to study the assembly of the mammalian SRP (Janiak et al., 1992). Using a specifically fluorescently-labeled SRP RNA, the binding of the various protein subunits was directly quantified. From these studies, it was demonstrated that the SRP9/SRP14 and SRP68/SRP72 bound non-cooperatively to the RNA (Janiak et al., 1992).

With the ability to specifically label 4.5S RNA at the 3′ end, it seemed reasonable to test whether interactions between the RNA and other biomolecules could be detected via fluorescence techniques. The first obvious candidate was, of course, the Ffh protein. As it was known that Ffh and 4.5S RNA formed a tight complex in *E. coli (Poritz et al., 1990)*, functioning as the bacterial SRP (Phillips and Silhavy, 1992; Ribes et al., 1990), it seemed likely that binding of Ffh to the RNA might be observable via fluorescence. Of course, as SRP is known to interact with ribosomes during the targeting cycle, it was of interested to investigate whether an *in vitro* interaction between the two particles could be monitored via fluorescence as well. We were motivated to probe this interaction by the hypothesis that perhaps the 4.5S RNA was an essential component of SRP because it could provide interaction contacts with the ribosome through direct RNA-RNA contacts with the rRNA.

The data in this appendix describes efforts started by our collaborator, Dr. Arthur Johnson, utilizing a 3′labeled 4.5S RNA, which was labeled with fluorescein. The measurement of the dye's fluorescence anisotropy exhibited dramatic increase upon addition of Ffh to the RNA. Moreover, addition of ribosomes, caused an equally dramatic decrease in the anisotropy of the dye. This appeared to offer a means of providing an assay to map the interaction between the bacterial SRP and the ribosome.

In collaboration with the Johnson lab, we set out to probe the interaction between the ribosome and the Ffh/4.5S RNP. Described in the following sections is our efforts toward this goal. Unfortunately as the data will demonstrate, we discovered that the assay was not monitoring formation of a specific RNP complex between Ffh and 4.5S RNA and subsequent interactions with the ribosome. Rather, the fluorescence changes reflected the formation of larger order Ffh-4.5S RNA aggregates which are of no physiological relevance. This was due specifically in part to the low ionic strength of the conditions initially employed in setting up the assay. Furthermore, we determined that the anisotropy decreases caused by the ribosome were due to the fact that ribosomes solubilized the aggregates.

Results

As seen in Figure 1, the steady state anisotropy measurements of the fluorescein-4.5S RNA appeared to be useful for monitoring Ffh association with the RNA. In the absence of Ffh, the RNA exhibited an anisotropy of approximately 0.08. Upon addition of increasing amounts of Ffh, the anisotropy increased to an apparent maximum of 0.240. This would be consistent with the binding of Ffh decreasing the mobility of the RNA molecule thereby increasing the observed anisotropy of the dye.

The plot of anisotropy versus [Ffh] exhibited characteristics of a binding curve. However, we were initially surprised that the plot saturated at approximately 3-fold molar excess Ffh to 4.5S RNA. This was surprising because earlier filter binding studies (L-S Kahng, unpublished observations) had estimated the K_d to be approximately 5 nM. One would expect the profile to exhibit characteristics more like a titration and saturate at 7 nM Ffh. However, we did not have a sense at the time what percentage of our Ffh protein was actually active. We therefore did not become completely dissuaded by this observation.

As a way of validating the fluorescence observation by demonstrating reversibility of the anisotropy measurement, we devised an experiment to correlate this reversibility with dissociation of Ffh from 3′-fluorescein-4.5S RNA. As shown in Figure 2, upon addition of a 30-fold excess non-fluorescent 4.5S RNA to preformed Ffh/3′-fluorescein-4.5S RNP, we observed a slow decrease in the anisotropy approaching a value close to that of the free 3′-fluorescein-4.5S RNA. Forcing this curve to fit to a single exponential, yielded a rate constant of 3 X 10^{-5} s^{-1}. This seemed reasonable with respect to earlier observations made from the filter binding studies (L-S Kahng, unpublished results).

Salt washed 70S ribosomes had been demonstrated to cause a decrease in the measured fluorescence anisotropy of the Ffh/3′-fluorescein-4.5S RNP (A. Johnson, unpublished results). This seemed counterintuitive since one would assume the rotational diffusion of the Ffh/4.5S RNP to become vastly slower upon binding to the ribosome. Rather, one would expect an even larger increase in the fluorescence anisotropy measured. However, since the measurements described here were steady state measurements, they reflected the composite of both global rotation as well as localized movement about molecular bonds as well as potential domain flexibility within the RNA, particularly at the 3′ end. It was conceivable, therefore, that the binding to the ribosome caused increased flexibility within 4.5S RNA. Alternatively, we speculated about the possibility of

4.5S RNA becoming displaced from Ffh during this interaction with the ribosome.

To further map the interaction in terms of the ribosomal subunits, we next asked which subunit on its own could interact with the Ffh/3′-fluorescein-4.5S RNP to cause the same fluorescence change. As seen in Figure 3, the 50S subunit caused a decrease in the fluorescence anisotropy similar to the one seen for the ribosome. The smaller 30S subunit did not cause as dramatic a change when added to the bacterial SRP (data not shown).

Feeling confident that we had at least mapped the SRP binding site to the large subunit, we went ahead and performed a large scale chemical probing study to localize the binding site to its precise location within the 23S rRNA. Following the methods established by the Noller lab (Moazed et al., 1986), we probed the RNA with DMS and kethoxal with the hope of identifying which bases of the rRNA were providing the binding site for the Ffh/4.5S RNP. These chemical probing studies failed to locate an obvious potential binding site within the 23S rRNA (data not shown).

At around the same time as we were probing the 23S rRNA, a paper was published by another group who also monitored the interaction between 4.5S RNA and Ffh using a 3′-fluorescein-conjugated RNA (Lentzen et al., 1994). In this work, interestingly, only a modest change in fluorescence intensity was observed for the dye upon binding of Ffh to the RNA. In this study, the binding of Ffh to the RNA did not result in an increase in the fluorescence anisotropy. Upon seeing these results, we went back and further questioned what our results were in fact actually representing. One difference in this other study was that the buffer conditions used were of higher ionic strength, in general.

As we had been able to footprint Ffh on the 4.5S RNA under higher ionic strength conditions, we decided to see whether we could observe the same increase in anisotropy in response to Ffh addition at both low and high KOAc levels, i.e., 50 mM as compared to 500 mM. As shown in Figure 4, the increase in anisotropy was very sensitive to [KoAc]. At 500 mM KOAc, a condition at which we were certain that Ffh bound to the RNA as evidenced from both filter binding studies and chemical footprinting results (see Chapter 2 of this thesis, and L-S Kahng and P Walter, unpublished results).

As an alternative means of monitoring the interaction between Ffh/4.5S RNP and the 50S subunits, we set up an assay which utilized a ^{32}P-radiolabeled 4.5S RNA. Using centrifugation over a 15% sucrose cushion as a means of separating free Ffh/^{32}P-labeled-4.5S RNP from 50S-bound Ffh/^{32}P-labeled-4.5S RNP, we tried to quantify association of the bacterial SRP with the 50S subunit under identical conditions to those of the fluorescence-based assay. Similarly as for the fluorescence assay, we reconstituted the RNA with excess Ffh and then added 50S subunits to the sample. Assays were performed at 50 mM KOAc as had been previously established for the spectroscopic studies.

As Figure 5 shows, in the absence of 50S subunits, the Ffh/^{32}P-labeled-4.5S RNP was already large enough to pellet through the sucrose cushion. The free ^{32}P-labeled-4.5S RNA in the presence of the 50S subunits, in contrast, remained in the supernatant. Interestingly, addition of the 50S subunits to the Ffh/4.5S RNP increased recovery of the labeled RNA in the supernatant. This observation, in conjunction with the data in Figure 4, suggested to us that perhaps the anisotropy measurements were in fact monitoring a much larger aggregate of Ffh/4.5S RNA. This would also explain the superstoichiometric plateau for the Ffh titration obtained in Figure 1. Moreover, the ribosomes would then appear to be acting to solubilize this aggregate.

When we increased the concentration of material while maintaining the ratio of Ffh:4.5S RNA, we could visualize the increase in turbidity within the sample (data not shown). In fact, examining the samples under EM clearly showed the formation of higher order aggregates due to the low ionic conditions of the buffer (data not shown).

Conclusion

From the data presented in this section of the thesis, it is clear that the manipulation of Ffh and 4.5S RNA in low ionic strength buffers presents problems for *in vitro* work. This was perhaps the most practical lesson learned from this data. As a result of this work, we moved our assay conditions away from those original established for the GTPases assays (Miller et al., 1994; Miller et al., 1993). Moreover, in all future work, we were especially careful not to have the Ffh present in molar excess over the RNA unless the buffer was of sufficiently high enough ionic strength (≥ 250 mM KOAc or ≥150 mM NaCl). Having excess 4.5S RNA over Ffh, however, counteracts aggregation. The earlier work whereby a two-fold excess of RNA was typically reconstituted with the Ffh avoided this misfortune even though the asays were performed at very low [KOAc] (25 – 50 mM).

Clearly, the anisotropy measurements were not reflecting physiologically relevant interactions. However, from the invalidation of this spectroscopic assay and the failure to observe any footprint on the ribosomal RNA from the Ffh/4.5S RNP, we abandoned our effort to probe the interaction between the bacterial SRP and the ribosome. Upon changing directions we moved from the work in Chapter 2 to the studies in Chapters 3 & 4 which were centered around the enzymology of the Ffh•FtsY GTPase complex.

References

Janiak, F., P. Walter, and A.E. Johnson. 1992. Fluorescence-detected assembly of the signal recognition particle: binding of the two SRP protein heterodimers to SRP RNA is noncooperative. *Biochem*. 31:5830-5840.

Lentzen, G., B. Dobberstein, and W. Wintermeyer. 1994. Formation of SRP-like particle induces a conformational change in E. coli 4.5S RNA. *FEBS Lett*. 348:233-238.

Miller, J.D., H.D. Bernstein, and P. Walter. 1994. Interaction of E. coli Ffh/4.5S ribonucleoprotein and FtsY mimics that of mammalian signal recognition particle and its receptor. *Nature* 367:657-659.

Miller, J.D., H. Wilhelm, L. Gierasch, R. Gilmore, and P. Walter. 1993. GTP binding and hydrolysis by the signal recognition particle during initiation of protein translocation. *Nature* 366:351-354.

Moazed, D., S. Stern, and H.F. Noller. 1986. Rapid chemical probing of conformation in 16 S ribosomal RNA and 30 S ribosomal subunits using primer extension. *J. Mol. Biol.* 187:399-416.

Phillips, G.J., and T.J. Silhavy. 1992. The E. coli *ffh* gene is necessary for viability and efficient protein export. *Nature* 359:744-746.

Poritz, M.A., H.D. Bernstein, K. Strub, D. Zopf, H. Wilhelm, and P. Walter. 1990. An E. coli ribonucleoprotein containing 4.5S RNA resembles mammalian signal recognition particle. *Science* 250:111-1117.

Ribes, V., K. Römisch, A. Giner, B. Dobberstein, and D. Tollervey. 1990. E. coli 4.5S RNA Is Part of a Ribonucleoprotein Particle That Has Properties Related to Signal Recognition Particle. *Cell* 63:591-600.

Figure A-1: Binding of Ffh to 4.5S RNA can be monitored by fluorescence anisotropy. 7.0 nM 3′fluorescein-4.5S RNA was titrated with varying amounts of Ffh in the following buffer: 50 mM Hepes (pH 7.5), 50 mM KOAc, 2.5 mM $Mg(OAc)_2$, 0.01% Nikkol, and 1 mM DTT. Fluorescence measurements were made in a photoncounting SLM-Aminco 8100 Spectrofluoromoter. The samples were excited with 490 nm and emission at 520 nm was measured. The excitation and emission light was polarized with GlanThompson calcite polarizers. For each concentration of Ffh, emission intensities were made at the following polarizer combinations: $I_{(0^\circ,0^\circ)}$, $I_{(0^\circ,I90^\circ)}$, $I_{(90^\circ,90^\circ)}$,and $I_{(90^\circ,0^\circ)}$. Fluorescence anisotropy (r) values were calculated from these mesasurements in the following manner:

$$r = \left(I_{(0^\circ,0^\circ)} - G^*I_{(0^\circ,90^\circ)} \right) / \left(I_{(0^\circ,0^\circ)} + 2^*G^*I_{(0^\circ,90^\circ)} \right)$$

$$\text{where } G = I_{(90^\circ,0^\circ)} / I_{(90^\circ,90^\circ)}$$

Measurements were taken after addition of Ffh, followed by a 20 min incubation period. Measurements were made after an additional 10 min for the first three points to verify that equilibrium had been reached for the measurement (data not shown).

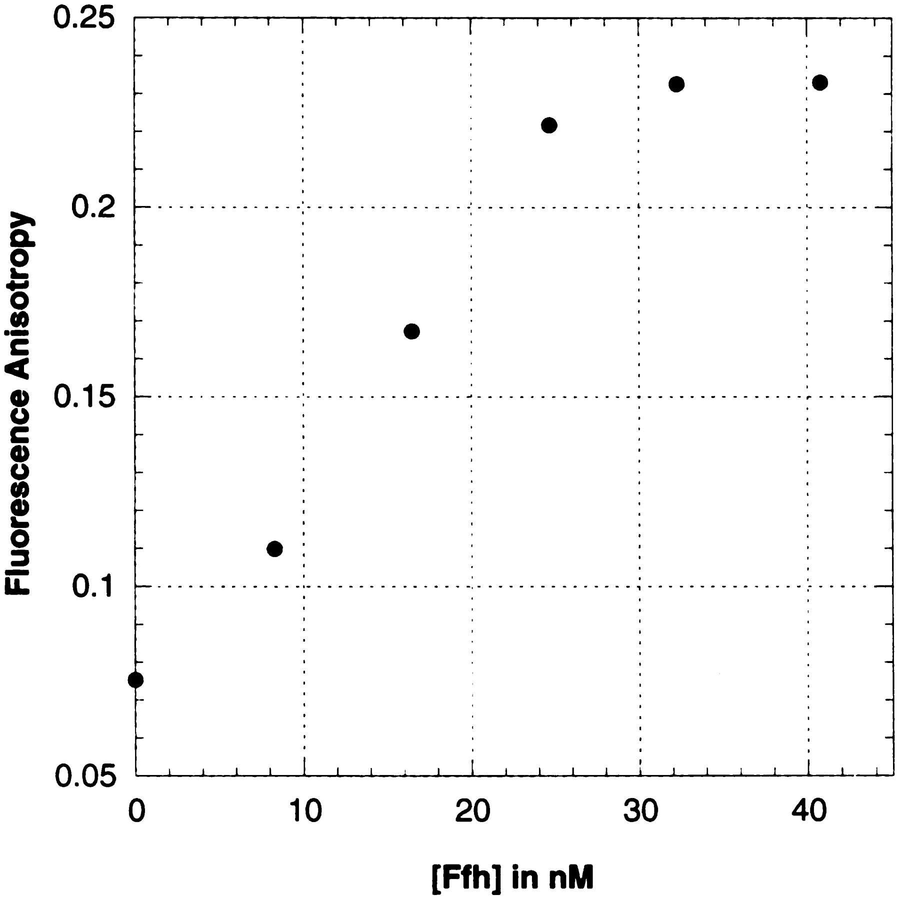
Fluorescence Anisotropy
0.25
0.2
0.15
0.1
0.05
0
10
20
30
40
[Ffh] in nM

Figure A-2: **Dissociation of Ffh from 3′-fluorescein-4.5S RNA results in a decrease in fluorescence anisotropy.** All assay conditions and measurements were made as described in the legend of Figure 1. Initially 40 nM Ffh was mixed with 7 nM 3′-fluorescein-4.5S RNA and anisotropy measurements were made to verify that the value of 0.245 was attained to reflect formation of the Ffh/3′-fluorescein-4.5S RNP. Nonfluorescent 4.5S RNA was then added to the sample to a final concentration of 250 nM to trap dissociating Ffh from the fluorescently-labeled RNA. Measurements were performed over the time period indicated. The data was fit to a single exponential equation and yielded a rate constant of $3 \times 10^{-5}\ s^{-1}$. A sample without addition of nonfluorescent RNA was also monitored over the same time interval and showed no decrease in fluorescence anisotropy (data not shown).

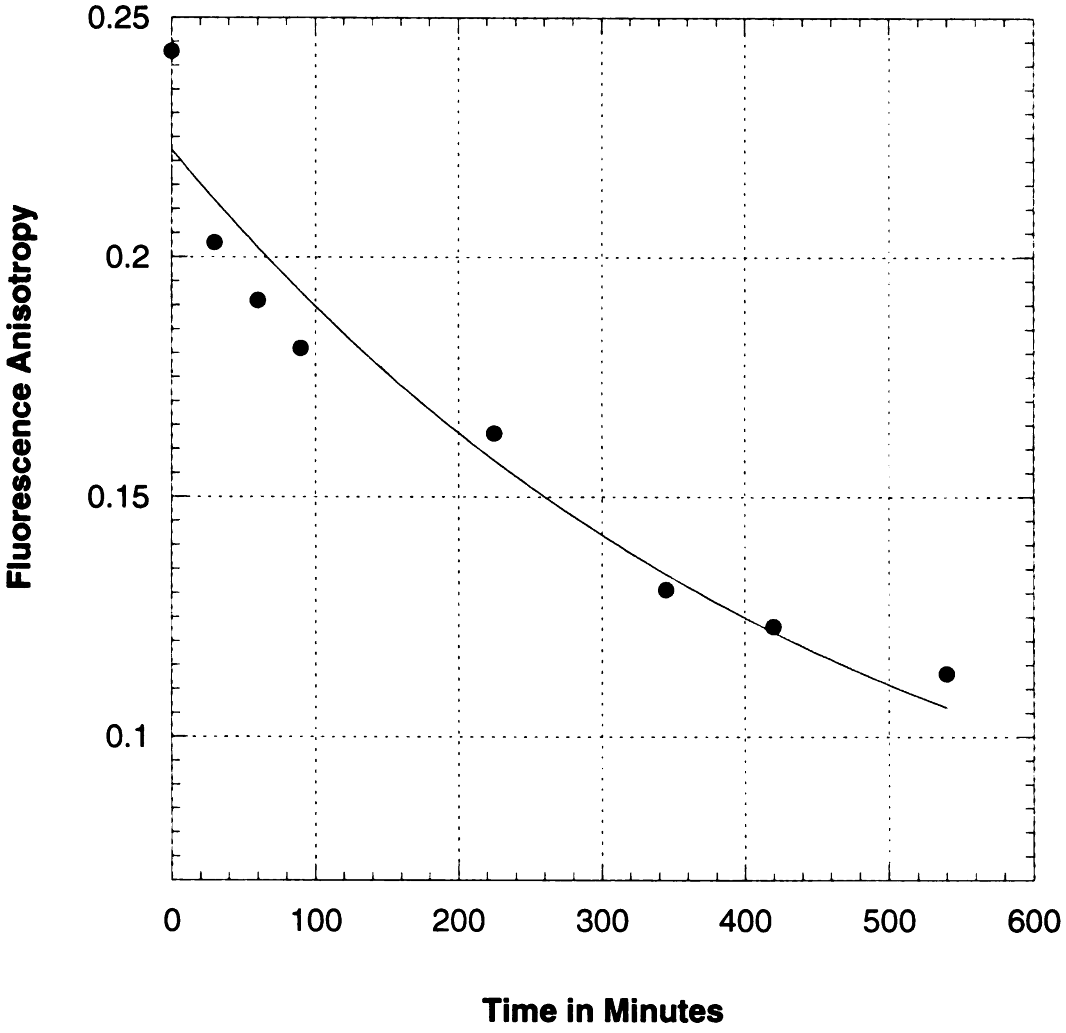
0.25
0.2
0.15
0.1
0
100
200
300
400
500
600
Fluorescence Anisotropy
Time in Minutes

Figure A-3: **Addition of 50S ribosomal subunits to Ffh/ 3′-fluorescein-4.5S RNP results in a cocncentration dependent decrease in fluorescence anisotropy.** Assay conditions and fluorescence measurements were as described in the legend of Figure 1. Fluorescence anisotropy measurements were carried out at various concentrations of 50S subunits. The fluorescence anisotropy measurements versus 50S subunit concentration are plotted in Figure 3. The profile suggests an affinity in the 10^{-9} M range.

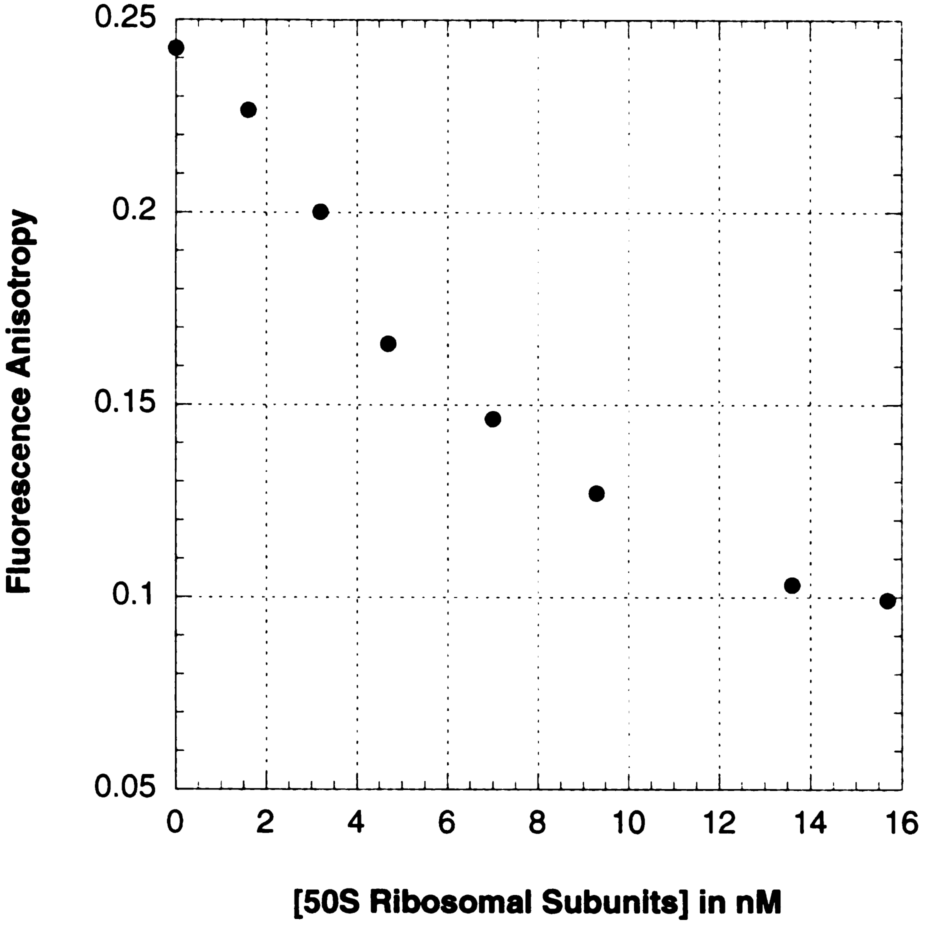
Fluorescence Anisotropy
0.25
0.2
0.15
0.1
0.05
0
2
4
6
8
10
12
14
16
[50S Ribosomal Subunits] in nM

Figure A-4: Fluorescence anisotropy change from Ffh is sensitive to KOAc concentration.

Assay conditions and fluorescence measurements were as described in Figure 1. However, this time the KOAc concentration was varied. Assay were performed in the typical buffer, but at two different levels of KOAc. One assay set was performed at the standard condition where the KOAc concentration was 50 mM (data plotted in red) and the other (plotted in green) was performed in a buffer whereby the KOAc was 500 mM. Plots of measured fluorescence anisotropy versus assay conditions are shown. As can be clearly seen, the typical change in fluorescence anisotropy upon addition of Ffh does not occur when the assay was performed at the higher KOAc concentration.

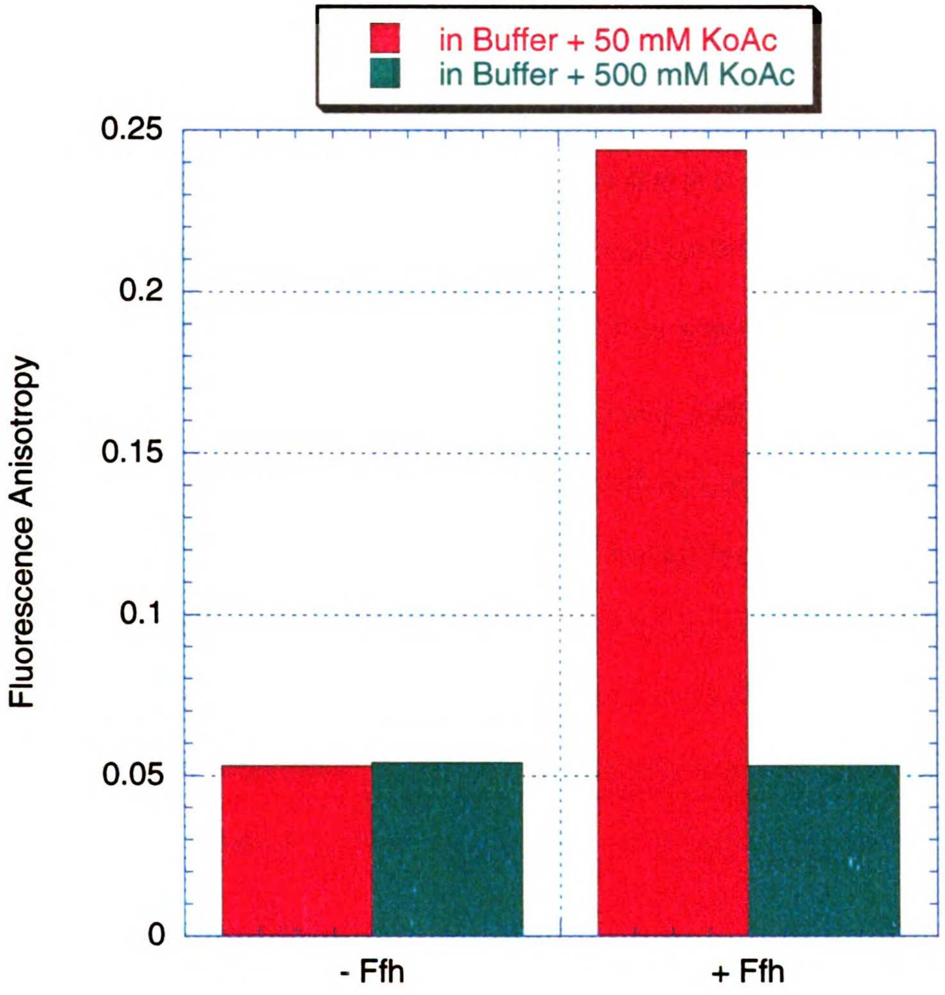

in Buffer + 50 mM KoAc
in Buffer + 500 mM KoAc
Fluorescence Anisotropy
0.25
0.2
0.15
0.1
0.05
0
- Ffh
+ Ffh

Figure A-5: ^{32}P-labeled 4.5S RNA forms large aggregates upon addition of Ffh which the 50S subunits appear to solubilize. Assays were performed in the following buffer: 50 mM Hepes (pH 7.5), 50 mM KOAc, 2.5 mM $Mg(OAc)_2$, 0.01% Nikkol, and 1 mM DTT. The 100 μl samples were layered over a 1 ml assay buffer + 15% sucrose cushion. The samples were centrifuged in a TLS-55 rotor at 55,000 rpm for 1 h in order to achieve suitable separation of the 50S subunits from the Ffh/^{32}P-4.5S RNP. After centrifugation, the top 200 μl was fractionated off as the supernatants while the remainder was considered the "pellet" fraction. The percentage of RNA recovered in either the supernatant (red) versus the pellet (green) is shown in Figure 5. For the 3 conditions tested the total recovery of counts was estimated to be greater than 90% (data not shown). As seen above, in the absence of ribosomal subunits addition of Ffh to the 4.5S RNA leads to the formation of a rather large pelleting molecular species. Interestingly, addition of 50S subunits to this mixture appears to decrease the apparent size of the ^{32}P-labeled 4.5S RNA containing species. Meanwhile, in the absence of Ffh, the ^{32}P-4.5S RNA remains in the soluble fraction even in the presence of 50S subunits.

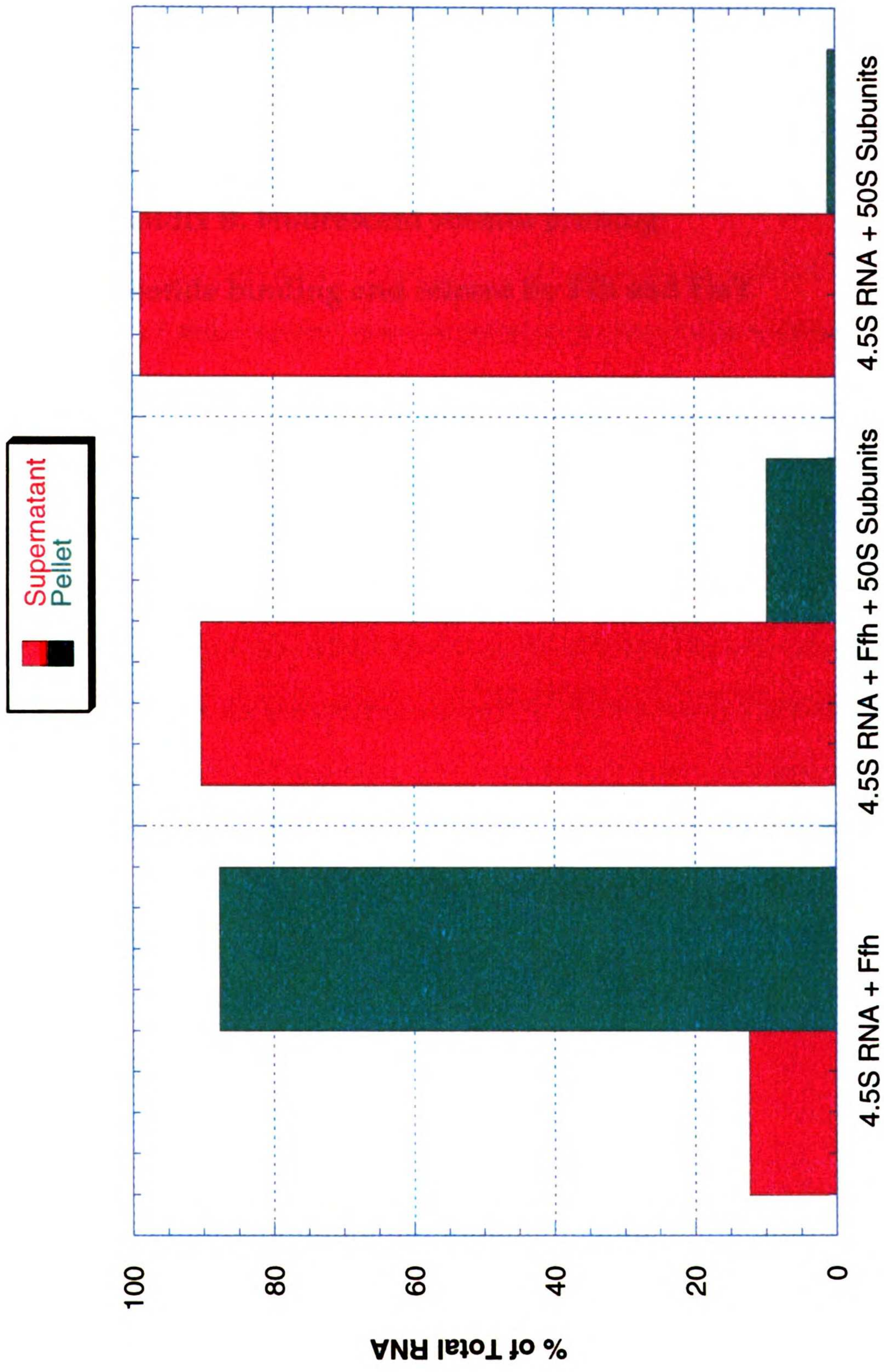
Supernatant
Pellet
% of Total RNA
100
80
60
40
20
0
4.5S RNA + Ffh
4.5S RNA + Ffh + 50S Subunits
4.5S RNA + 50S Subunits

Appendix B. Fluorescent studies probing nucleotide binding and release by Ffh and FtsY

Abstract

In this section, I will briefly describe our efforts to quantify the kinetics of nucleotide binding and release for Ffh and FtsY. Using (2′ or 3′)–(N-methylanthraniloyl)-nucleotide derivatives, or MANT-nucleotide derivatives, we were able observe binding of Ffh and FtsY in real time by monitoring the change in MANT fluoresence. From our analysis, we were able to determine k_{on} and k_{off} values for the binding of various nucleotides to both Ffh and FtsY. Our observations were in close agreement with similar measurements made independently by others. Upon monitoring the release of MANT-GDP from both Ffh and Ffh/4.5S RNP, we were surprised to find two dramatically different dissociation traces which varied in rate constants by at least two orders in magnitude. As our synthesized MANT-nucleotide derivatives were mixtures of 2′-MANT-nucleotides and 3′-MANT-nucleotides, we postulate that the two dissociating species is likely due to this heterogeneity in labeling. This suggests that direct interactions between Ffh and the fluorophore could be affecting the release rates, and hence, the affinity of Ffh for the nucleotide.

Introduction

We were interested in determining the kinetics of nucleotide binding and release for Ffh and FtsY as part of our goal to fully characterize the mechanism of the Ffh•FtsY GTPase complex (see Chapter 4). From earlier published work, we reasoned that the binding and release of nucleotides would be fast for both Ffh and FtsY (Miller et al., 1994; Miller et al., 1993). In order to monitor occupancy of Ffh, FtsY, and their mammalian homologues, a crosslinking approach had to be employed. While affinities for GTP were derived from these crosslinking assays, the assays suffer from not representing true equilibrium. In addition, interpretation of crosslinking results can become difficult due to the fact that the extent of crosslinking can be influenced by two factors: one being the occupancy of the active site by the nucleotide and the other being the chemical efficiency of crosslinking which can be sensitive to any structural changes that might occur.

We were motivated to develop a fluorescence-based assay to monitor nucleotide binding for three primary reasons. First, assays could be carried out at true equilibrium conditions. Second, assays could potentially performed in real time. This offered the potential of extracting true rate constants for the various interactions being studied. Third, we were interested in developing fluorescence methods to confirm the crosslinking results which argued for stabilization of the nucleotide-free state of Ffh upon binding of signal sequences to the M-domain (Miller et al., 1994; Miller et al., 1993). We hoped to ultimately develop fluorescence resonance energy transfer techniques to demonstrate the whether or not there was co-occupancy of both nucleotide and signal sequence within Ffh.

As a starting point we employed a strategy which had been developed by others to analyze binding of nucleotides via fluorescent-derivatives (Hiratsuka, 1983; John et al., 1990) (N-methylanthraniloyl)- or MANT- derivatives of nucleotides were generated synthesized and purified as previously described (Hiratsuka, 1983). One main advantage to this strategy was that the same fluorescent-derivatives could be generated for all the nucleotides of interest to us:

GTP, GDP, and 5'guanylylimidodiphosphate (GppNHp). With these fluorescent-nucleotides, we proceeded to monitor the nucleotide binding rate constants of Ffh (with and without 4.5S RNA) and FtsY.

Results

In all cases examined, we found the MANT fluorescence to increase dramatically upon binding of either Ffh, Ffh/4.5S RNP, and FtsY to the various MANT-nucleotide derivatives. Typically, the fluorescence intensity monitored at 440 nm would increase from 30% - 40% upon binding of all the MANT-nucleotide molecules by the different proteins. The results shown in Figure 1 represent a typical kinetic trace observed for the binding of MANT-GTP. In this case, 1 μM MANT-GTP was mixed with 36 μM FtsY. For this particular experiment, the change in fluorescence could be fit to a single exponential, which yielded an apparent rate of 1.08 s^{-1} ± 0.014 s^{-1}.

In order to derive a value for the k_{on} of the association of FtsY with MANT-GTP, assays similar to the one in Figure 1 were performed at varying FtsY concentrations. The apparent rates from single exponential fits to the various assays were plotted against their respective FtsY concentrations as shown in Figure 2. From a linear fit of this plot we were able to use the slope to determine a k_{on} of $6.1 \times 10^5\ M^{-1}\ s^{-1} \pm 4.6 \times 10^4\ M^{-1}\ s^{-1}$.

At around the same time we were performing these kinetic studies, another group was investigating the nucleotide binding properties of FtsY by monitoring FtsY's tryptophan fluorescence (Moser et al., 1997). From this work, they offered kinetic arguments for the existence of multiple steps during the binding of nucleotides to FtsY. In our studies using MANT-GTP, we were unable to come to any similar conclusions. There are several reasons to account for this. First each study utilized a different fluorescence probe. We monitored the nucleotide directly with the MANT probe, whereas Moser, et al., were monitoring the tryptophan signal within FtsY which is very sensitive to the protein's conformation. Second, the two studies used different constructs of FtsY. We have been using a form of FtsY which is missing only its first 45 amino acids while they were using a much smaller construct representing just the core NG-domain of FtsY. Our attempts to make a similar construct have proved difficult in terms of obtaining soluble protein (T. Powers and P. Walter, unpublished). We and others (Jagath et al., 2000) have been unable to observe as dramatic a change in tryptophan fluorescence with larger forms of FtsY. The shorter FtsY NG form could be more unstructured than the larger FtsY form used in our studies.The complex kinetics and larger fluorescence changes could result from protein reordering upon binding of nucleotide.

Ffh appeared to bind nucleotides with a rate constant approximately 10-fold faster than FtsY. When looking at the binding of Ffh to MANT-GppNHp, as shown in Figure 3, we determined a value of k_{on} for this reaction to be approximately $1.1 \times 10^{6}\ M^{-1}\ s^{-1} \pm 6.4 \times 10^{4}\ M^{-1}\ s^{-1}$. This faster association rate constant is not all that surprising when one considers the fact that Ffh exhibits a 0.3 μM K_m for GTP while FtsY exhibits a weaker K_m of approximately 30.0 μM (see Chapter 4 of this thesis).

We were interested in looking at the release of nucleotides from Ffh and FtsY. Our hope was to use real-time fluorescence measurements to quantify the kinetics of nucleotide release from the two proteins. There were various issues we hoped to address with these studies. From previous studies, we expected nucleotide release to be very rapid (Miller et al., 1994; Miller et al., 1993) and therefore hoped to demonstrate this directly. Secondly, we suspected that formation of the $Ffh^{GTP} \bullet FtsY^{GTP}$ and Ffh/4.5S $RNP^{GTP} \bullet FtsY^{GTP}$ complexes resulted in occlusion of the GTPase active sites slowing the release of GTP from one or both of the proteins (Miller et al., 1994; Miller et al., 1993; Peluso et al., 2000). Again, we hoped from stopped flow studies to directly quantify this effect.

The first nucleotide dissociation we monitored was that of FtsY and MANT-GDP. In order to monitor the off rate we needed to trap the dissociating complexes. This was achieved by mixing preformed FtsY•MANT-GDP complex with an 8000-fold excess of non-fluorescent GDP. As shown in Figure 4, we were able to monitor the dissociation of MANT-GDP from FtsY. From a single exponential curve fit to the fluorescence decay, we determined a k_{off} of 19.7 (±0.5) s^{-1}. This was approximately 10-fold faster than the published k_{off} of 3.7 determined for FtsY NG domain as analyzed by tryptophan fluoresence. Despite the difference, in both cases the release was found to be markedly faster than what has been seen for Ras, where fluorescence studies have determined a koff of 1.8 x 10^{-5} s^{-1} for GDP (John et al., 1990).

We looked at the dissociation of MANT-GDP from both Ffh and Ffh/4.5S RNP using the same assay set up as we used for FtsY. As shown in Figure 5, we were able to determine k_{off} values of 23.5 (± 0.4) s^{-1} and 19.4 (± 0.6) s^{-1} for Ffh and Ffh/4.5S RNP respectively. These rates were similar to the koff independently measured by others using the same MANT-GDP analogue where a k_{off} of 13.7 (± 0.6) s^{-1} was observed for Ffh. We were not surprised to find similarly rapid k_{off} values for Ffh•MANT-GDP and Ffh/4.5S RNP•MANT-GDP as had been seen for FtsY•MANT-GDP. Both proteins are structurally identical to each other possessing a unique motif which has been termed the insertion box domain, or IBD which is unique to this subfamily of GTPases (Bernstein et al., 1989; Freymann et al., 1997; Montoya et al., 1997; Römisch et al., 1989).

We were surprised to make an additional observation for the release of MANT-GDP from Ffh and Ffh/4.5S RNP. When looking at longer time windows of approximately 10 - 30 seconds, we found a slow linear fluorescence decay which appeared to follow the initial rapid exponential decay which we believed to represent the release of MANT-GDP (data not shown). Upon performing longer time traces on the order of 10 minutes we observed the existence of a second much slower exponential decay in fluorescence as shown in Figure 6. When fit to a single exponential curve, a rate constant of 5.00 (± 0.02) s^{-1} was obtained. This rate is approximately 5000 times slower than the initial decay (Figure 6, inset). In addition, the magnitude in fluorescence change was similar for both the fast and slow decays.

To further investigate the nature of this slower fluorescence decay. We performed tests to determine whether this slower decay was due to photobleaching or the absence of 4.5S RNA. Control studies showed photobleaching to be linear over the same time window with only a 5% reduction in fluorescence signal as compared with the approximate 20% decrease observed during this slow exponential decay (data not shown). We also observed the slow decay for the release of MANT-GDP from Ffh/4.5S RNP as shown in Figure 7. This ruled out the possibility that the second decay was due to some unique equilibrium of Ffh conformations due to the absence of 4.5S RNA.

Discussion

The work presented in this appendix describes our initial efforts to measure the kinetics of nucleotide binding and release by Ffh and FtsY. Our initial findings suggested that these reactions occurred rapidly. This was in close agreement with previous work which had to rely on uv-crosslinking in order to trap the interactions between nucleotides and Ffh and FtsY as well as their mammalian homologues (Miller et al., 1994; Miller et al., 1993).

The rapid release initially seen for MANT-GDP was interesting as it is much faster than what had been previously shown for Ras using similar techniques (John et al., 1990). At the time we and others (Jagath et al., 1998; Moser et al., 1997) were making these observations, x-ray crystallographic structures were solved for the nucleotide-free and GDP-bound forms of Ffh which helped explain these kinetic observations at the molecular level (Freymann et al., 1997; Freymann et al., 1999). Residues within the IBD were seen to form salt-bridges with residues of the active site which would normally be interacting with the substrate (Freymann et al., 1999). This would explain why nucleotide-free forms of these proteins can be obtained (Freymann et al., 1997; Montoya et al., 1997) rather easily as compared to the Ras-like GTPases (Feuerstein et al., 1987).

The discovery of two dramatically different fluorescent decay events, however, suggested that perhaps there were serious issues with this method which will need to be addressed if this method is going to be applied to this GTPase system in future studies. It is unlikely that the two fluorescent decays represent steps which are linked in the same pathway for nucleotide release. If this were true, then a rate limiting step of 10^{-3} s^{-1} should exist within the GTPase reaction pathway due to the fact that GDP release should be the rate limiting step. In our assays probing the activity of the $Ffh^{GTP} \bullet FtsY^{GTP}$ and Ffh/4.5S $RNP^{GTP} \bullet FtsY^{GTP}$ complexes we see much faster steady state rates. It is also unlikely that the two fluorescent decay species represent GDP release from to distinct conformational forms of Ffh due to the absence of 4.5S RNA as similar results were obtained for the Ffh/4.5S RNP.

A simpler interpretation for our unexpected results for MANT-GDP release stems from the fact that our labeled nucleotides are all mixtures of 2'-MANT-GDP and 3'-MANT-GDP. In all of our labeling reactions we used ribonucleotides which have 2' and 3' hydroxyl groups. Both hydroxyl groups can be labeled with the MANT-derivative. The simplest interpretation for our observations for MANT-GDP release would argue that the 2'-MANT-GDP and 3'-MANT-GDP forms interact differently with Ffh and Ffh/4.5S RNP due to interactions between the dye molecule and the protein. One could dissociate much slower than the other from Ffh's active site due to these differences.

Upon seeing these inherent problems with the MANT-GDP, we decided to focus our attentions on the functional GTPase assys in order to determine the affinities of Ffh and FtsY for GTP. As we describe in Chapter 4 in greater detail, the GTPase activity assay enabled us to determine a Km value for Ffh, Ffh/4.5S RNP and FtsY. Moreover using competition assays we were able to determine the affinity of Ffh for GDP and further show that 4.5S RNA did not affect this affinity. Clearly, the results from our MANT-nucleotide work remain unresolved. Further work will require use of deoxynucleotide forms to synthesize pure isomeric forms of the MANT-nucleotide derivatives in order to determine the nature of these bizarre kinetics for MANT-GDP release.

References

Bernstein, H.D., M.A. Poritz, K. Strub, P.J. Hoben, S. Brenner, and P. Walter. 1989. Model for signal sequence recognition from amino-acid sequence of 54k subunit of signal recognition particle. *Nature* 340:482-486.

Feuerstein, J., R.S. Goody, and A. Wittinghofer. 1987. Preparation and characterization of nucleotide-free and metal ion-free p21 "apoprotein". *J. Biol. Chem.* 262:8455-8458.

Freymann, D.M., R.J. Keenan, R.M. Stroud, and P. Walter. 1997. Structure of the conserved GTPase domain fo the signal recognition particle. *Nature* 385:361-364.

Freymann, D.M., R.J. Keenan, R.M. Stroud, and P. Walter. 1999. Functional changes in the structure of the SRP GTPase on binding GDP and Mg2+GDP. *Nat. Struct. Biol.* 6:793-801.

Hiratsuka, T. 1983. New ribose-modified fluorescent analogs of adenine and guanine nucleotides available as substrates for various enzymes. *Biochim. Biophys. Acta.* 742:496-508.

Jagath, J.R., M.V. Rodnina, G. Lentzen, and W. Wintermeyer. 1998. Interaction of guanine nucleotides with the signal recognition particle from Escherichia coli. *Biochem.* 37:15408-15413.

Jagath, J.R., M.V. Rodnina, and W. Wintermeyer. 2000. Conformational changes in the bacterial SRP receptor FtsY upon binding of guanine nucleotides and SRP. *J. Mol. Biol.* 295:745-753.

John, J., R. Sohmen, J. Feuerstein, R. Linke, A. Wittinghofer, and R.S. Goody. 1990. Kinetics of interaction of nucleotides with nucleotide-free H-ras p21. *Biochem.* 29:6058-6065.

Miller, J.D., H.D. Bernstein, and P. Walter. 1994. Interaction of E. coli Ffh/4.5S ribonucleoprotein and FtsY mimics that of mammalian signal recognition particle and its receptor. *Nature* 367:657-659.

Miller, J.D., H. Wilhelm, L. Gierasch, R. Gilmore, and P. Walter. 1993. GTP binding and hydrolysis by the signal recognition particle during initiation of protein translocation. *Nature* 366:351-354.

Montoya, G., C. Svensson, J. Luirink, and I. Sinning. 1997. Crystal structure of the NG domain from the signal-recognition particle receptor FtsY. *Nature* 385:365-368.

Moser, C., O. Mol, R.S. Goody, and I. Sinning. 1997. The signal recognition particle receptor of Escherichia coli (FtsY) has a nucleotide exchange factor built into the GTPase domain. *Proc. Natl. Acad. Sci. U. S. A.* 94:11339-11344.

Peluso, P., D. Herschlag, S. Nock, D.M. Freymann, A.E. Johnson, and P. Walter. 2000. Role of 4.5S RNA in assembly of the bacterial signal recognition particle with its receptor. *Science* 288:1640-1643.

Römisch, K., J. Webb, J. Herz, S. Prehn, R. Frank, M. Vingron, and B. Dobberstein. 1989. Homology of the 54K Protein of signal recognition particle, docking protein, and two E. coli proteins with putative GTP-binding domains. *Nature* 340:478-482.

__Figure B-1:__ **Binding of FtsY to MANT-GTP as monitored in real time with a stopped flow.** MANT-GTP and FtsY were rapidly mixed to final concentrations of 1.0 μM and 36μM respectively. The the change in fluorescence over time was monitored in a KinTec stopped flow apparatus. Reactions were performed at 25°C in the following Buffer: (50 mM Hepes, pH 7.5, 150 mM KOAc, 1.5 mM $Mg(OAc)_2$, 0.01% Nikkol and 1 mM DTT). From a single exponential fit to the fluorescence trace, a rate constant of 1.08 (± 0.014) s^{-1} was calculated.

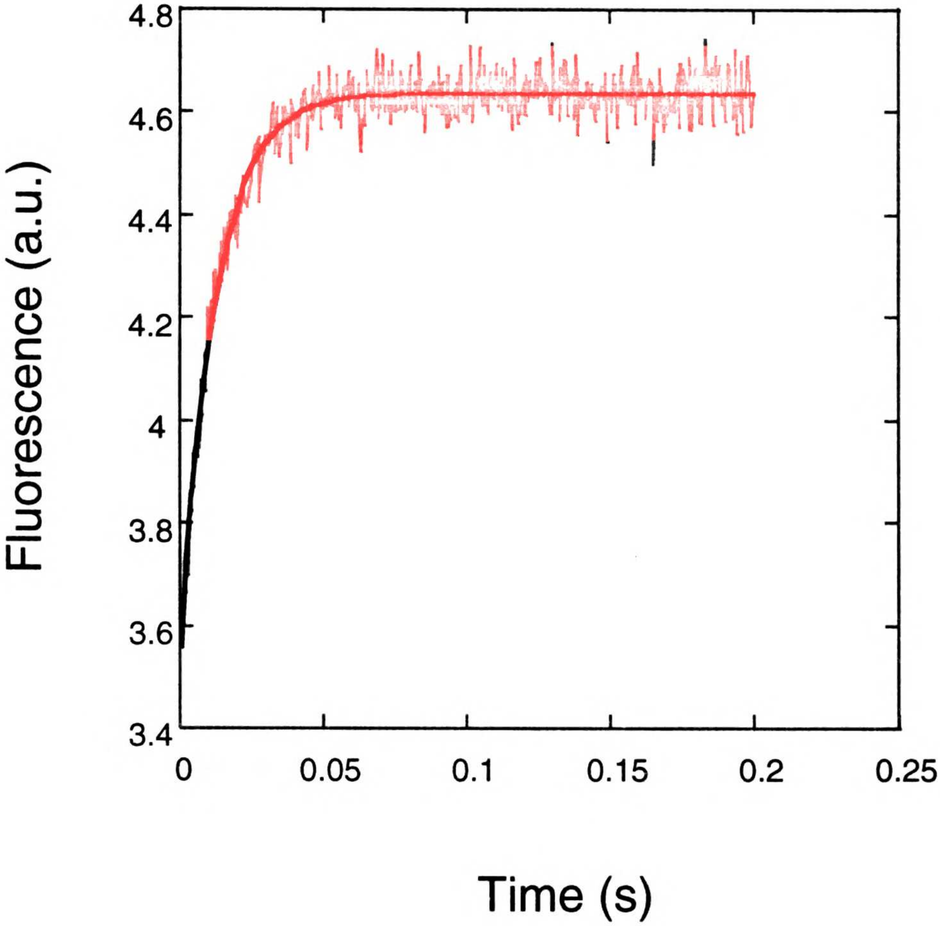

Fluorescence (a.u.)
4.8
4.6
4.4
4.2
4
3.8
3.6
3.4
0
0.05
0.1
0.15
0.2
0.25
Time (s)

Figure B-2: Determination of the k_{on} for the association of FtsY with MANT-GTP. Reactions similar to the one in Figure 1 were performed at varying concentrations of FtsY. Rate constants were obtained for each reaction from single exponential curve fits to each time trace. These observed rate constants were plotted against their respective FtsY concentrations. The data was fit with the equation $k_{obs} = k_{on} \times [FtsY] + k_{off}$ to yield a k_{on} of 6.1 (± 0.5) x 10^{-5} M^{-1} s^{-1}.

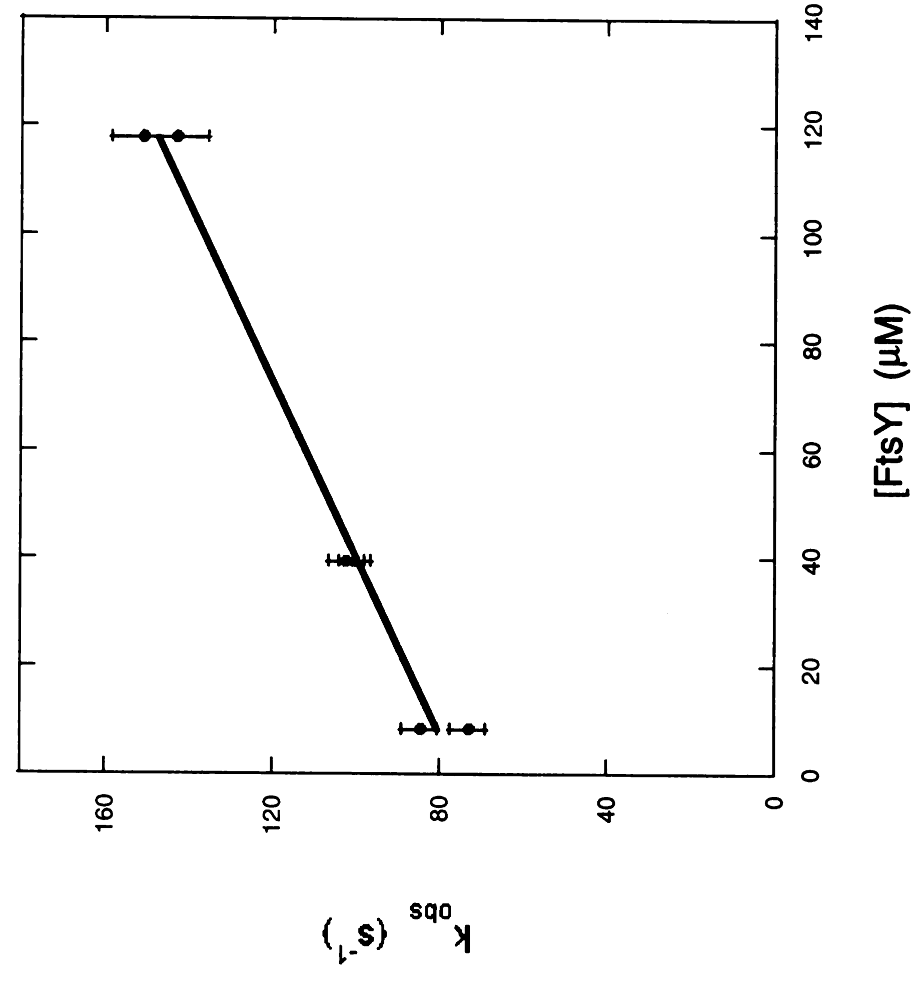
k
obs
(s-1)
160
120
80
40
0
0
20
40
60
80
100
120
140
[FtsY] (μM)

Figure B-3: Determination of the k_{on} for the association of Ffh with MANT-GppNHp. Binding of Ffh to MANT-GppNHp was assayed as described for FtsY in Figure 1. Assays were performed at various concentrations of Ffh. For each reaction a observed rate constant was determined from a single exponential curve fit to the fluorescence time trace. From the above plot of these observed rate constants versus their respective Ffh concentrations, a kon was derived by fitting the plot with the following equation: $k_{obs} = k_{on} \times [\mathrm{Ffh}] + k_{off}$. From this fit a k_{on} of 1.1 (± 0.1) x $10^{6}\ M^{-1}\ s^{-1}$ was determined.

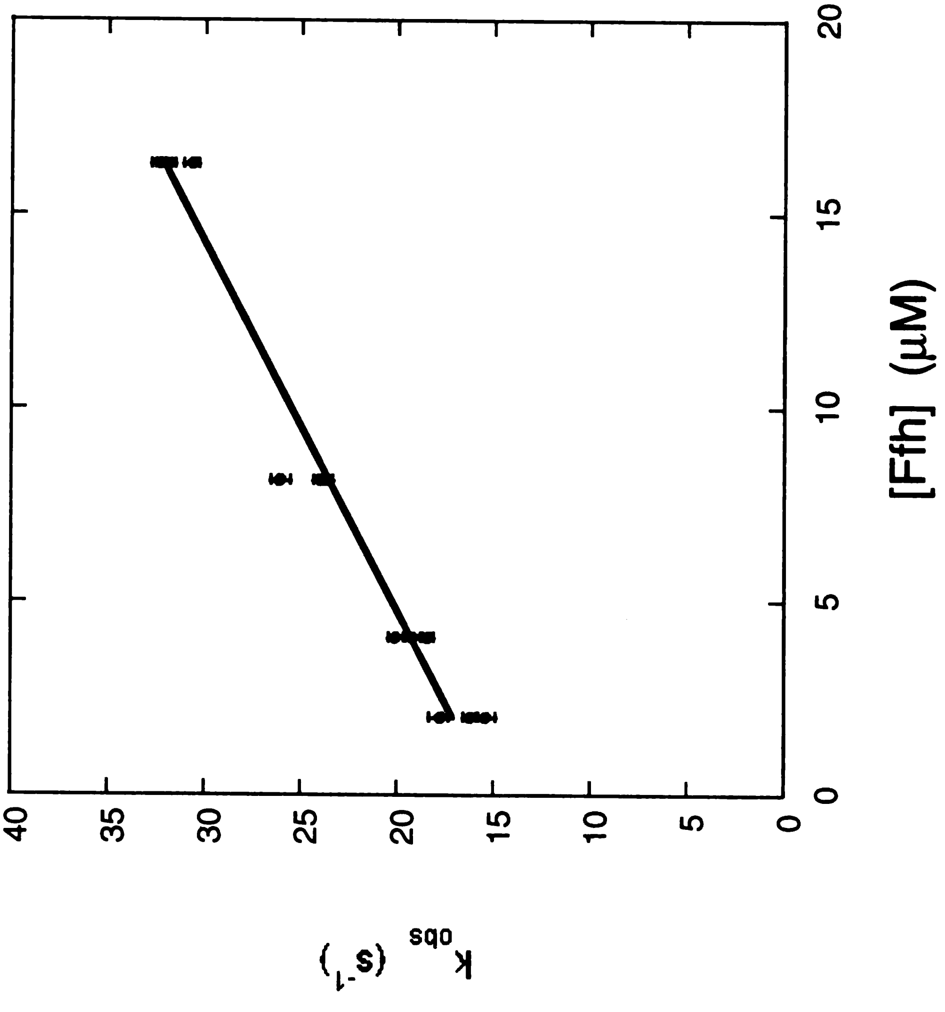

k_obs (s^-1)
40
35
30
25
20
15
10
5
0
0
5
10
15
20
[Ffh] (µM)

Figure B-4: Measuring the release rate of FtsY for MANT-GDP. 1μM MANT-GDP was premixed with 40 μM FtsY. The dissociation reaction was initiated by addition of 2 mM GDP. The reaction was performed in a KinTek stopped flow apparatus under similar conditions as described in Figure 1 legend. From a single exponential fit to the fluorescence time trace a k_{off} of 19.7 (± 0.5) s^{-1} was determined.

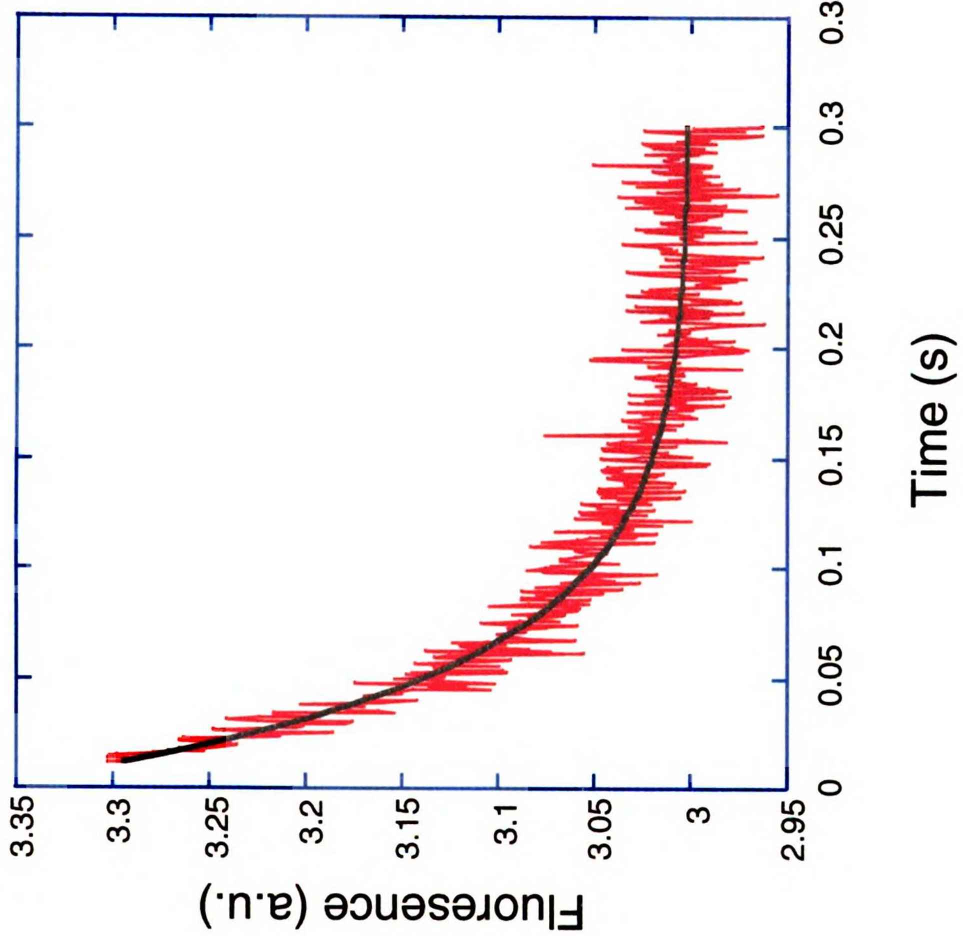
Fluoresence (a.u.)
3.35
3.3
3.25
3.2
3.15
3.1
3.05
3
2.95
0
0.05
0.1
0.15
0.2
0.25
0.3
0.35
Time (s)

Figure B-5: **Determination of the k_{off} of MANT-GDP for Ffh and Ffh/4.5S RNP.** (A) 8.5 μM Ffh was premixed with 10 μM MANT-GDP. The dissociation reaction was initiated by the addition of an equal volume of 8.2 mM GDP. From a single exponential curve fit to the fluorescence trace a k_{off} of 23.5 (± 0.4) s^{-1} was determined. (B) 1 μM MANT-GDP was premixed with 4 μM Ffh/4.5S RNP. The dissociation reaction was initiated by the addition of an equal volume of 5 mM GDP. From a single exponential curve fit to the fluorescence trace, a k_{off} of 19.4 (± 0.6) s^{-1} was determined.

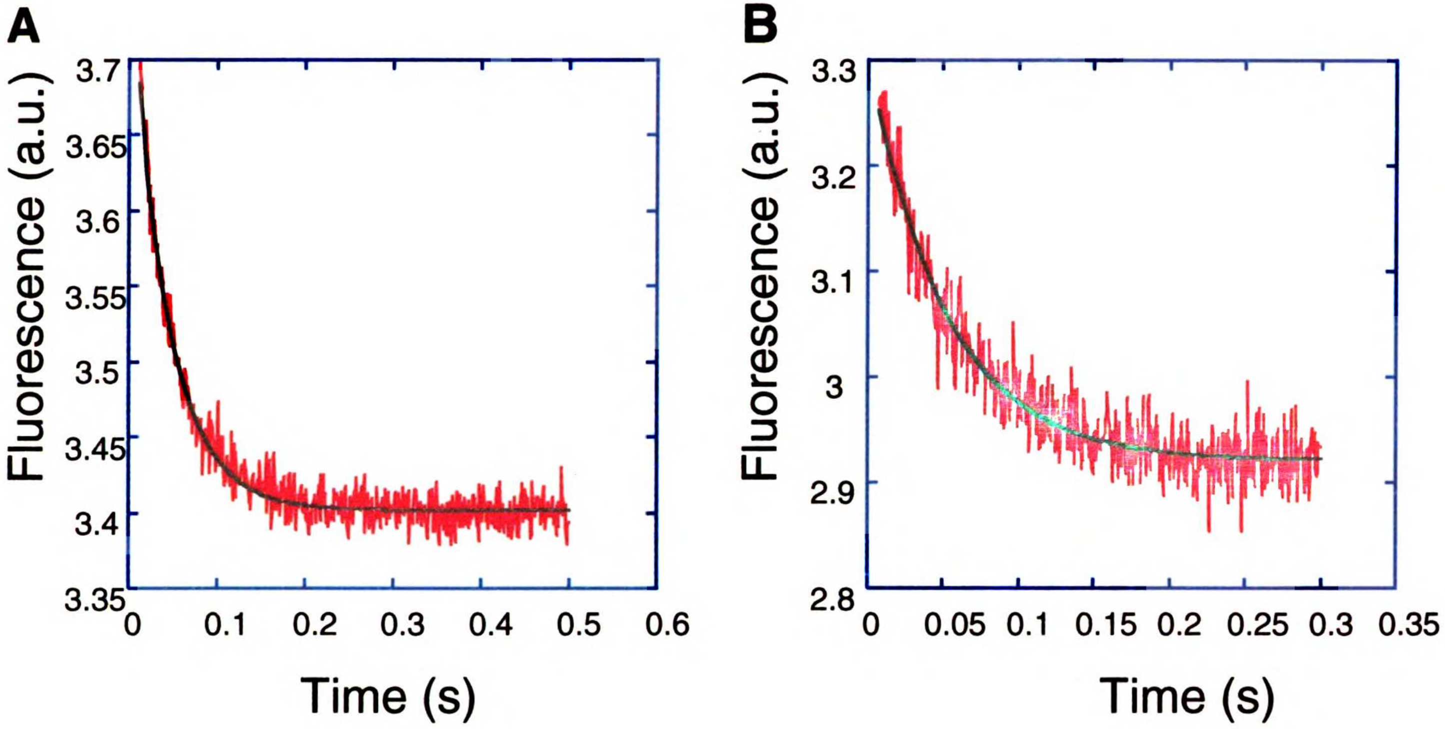
A
Fluorescence (a.u.)
3.7
3.65
3.6
3.55
3.5
3.45
3.4
3.35
0
0.1
0.2
0.3
0.4
0.5
0.6
Time (s)
B
Fluorescence (a.u.)
3.3
3.2
3.1
3
2.9
2.8
0
0.05
0.1
0.15
0.2
0.25
0.3
0.35
Time (s)

Figure B-6: Dissociation of MANT-GDP from Ffh exhibits two fluorescence decays with dramatically different rate constants. 8.5 μM Ffh was premixed with 10 μM MANT-GDP. The dissociation was initiated by the addition of 8.2 mM GDP as in Figure 5A. Fluorescence changes were monitored simultaneously over two time durations. The shorter duration shown in the inset was for 500 msec while the longer was for 600 sec. Single exponential curve were fit to each trace yielding observed rate constants of 23 (± 0.4) s^{-1} and 6.0 (± 0.02) s^{-1} resepectively.

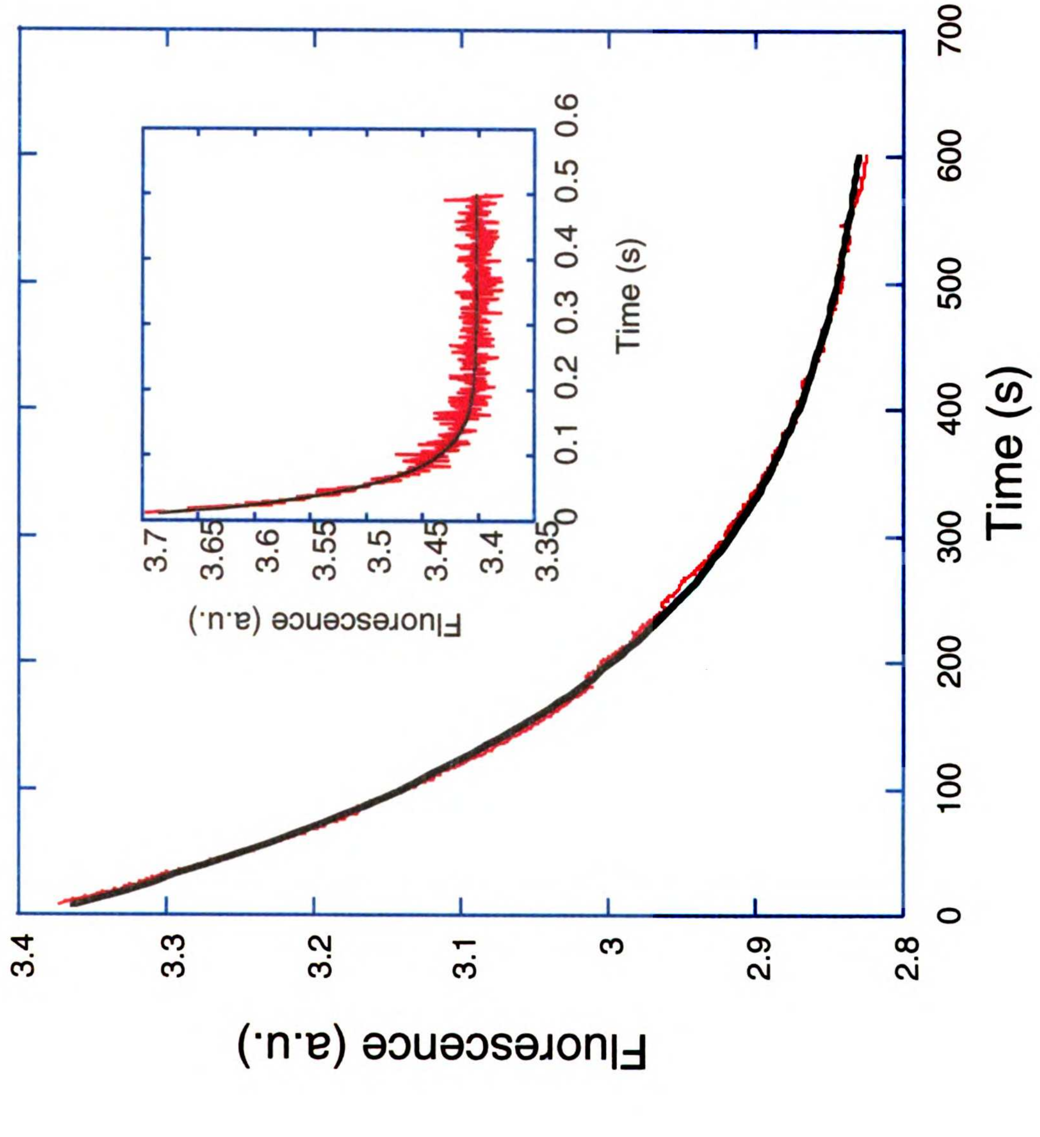
Fluorescence (a.u.)
3.4
3.3
3.2
3.1
3
2.9
2.8
Time (s)
0
100
200
300
400
500
600
700
Fluorescence (a.u.)
3.7
3.65
3.6
3.55
3.5
3.45
3.4
3.35
Time (s)
0
0.1
0.2
0.3
0.4
0.5
0.6

Figure B-7: Dissociation of MANT-GDP from Ffh/4.5S RNP exhibits two fluorescence decays with dramatically different rate constants. 4 μM Ffh/4.5S RNP was premixed with 1 μM MANT-GDP. The dissociation was initiated by the addition of 5.0 mM GDP as in Figure 5B. Fluorescence changes were monitored simultaneously over two time durations. The shorter duration shown in the inset was for 500 msec while the longer was for 600 sec. Single exponential curve were fit to each trace yielding observed rate constants of 19 (± 0.6) s^{-1} and 8.0 (± 0.02) s^{-1} resepectively.

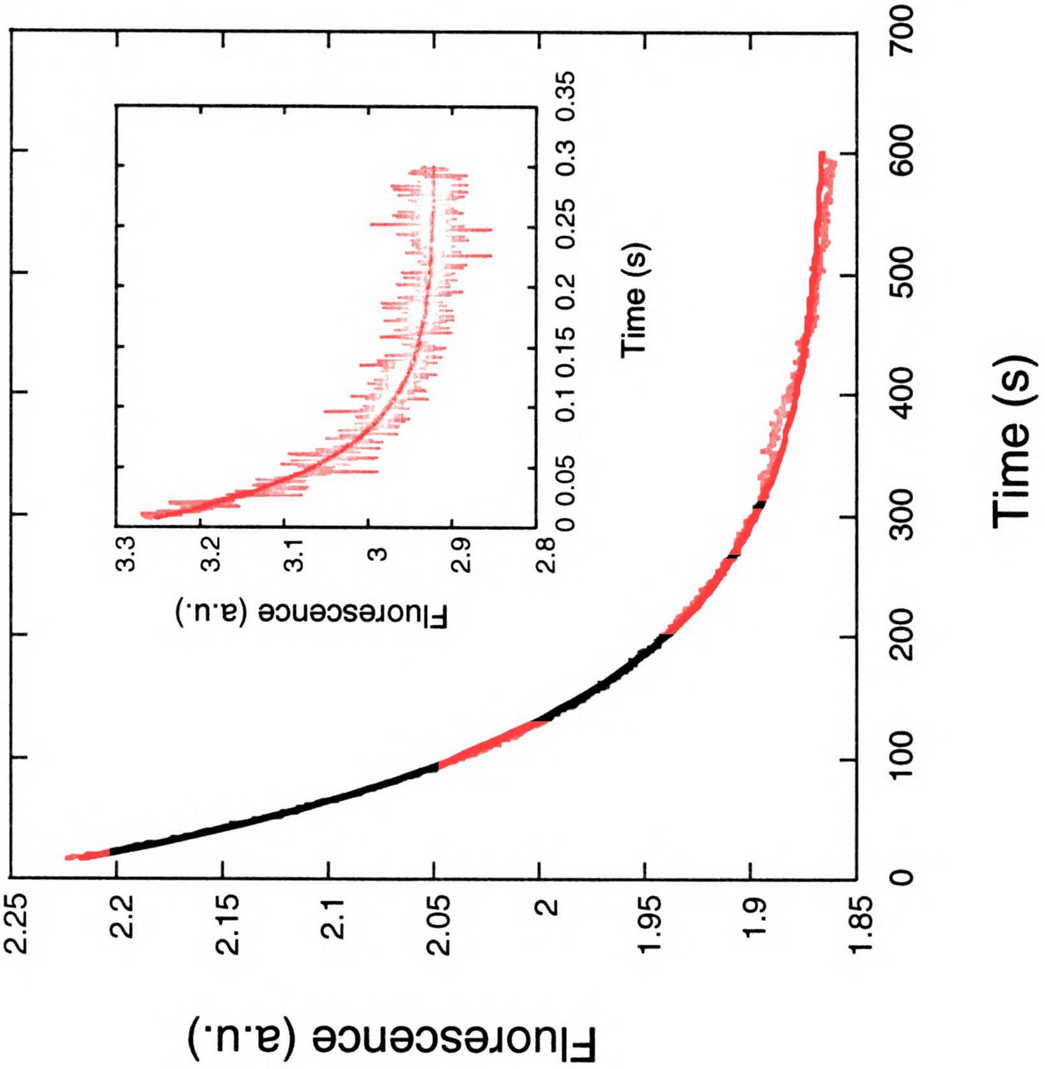
Fluorescence (a.u.)
2.25
2.2
2.15
2.1
2.05
2
1.95
1.9
1.85
Time (s)
0
100
200
300
400
500
600
700
Fluorescence (a.u.)
3.3
3.2
3.1
3
2.9
2.8
Time (s)
0
0.05
0.1
0.15
0.2
0.25
0.3
0.35

Conclusion and Future Directions

Conclusion:

From the work detailed in this thesis, we have clearly identified a functional role for 4.5S RNA during the SRP targeting cycle. Through the use of a variety of techniques, we have gained a mechanistic understanding of how the RNA modulates the interaction between Ffh and FtsY. While this work has been able to answer some important questions in this vein, many questions still remain to be answered while a few new ones have arisen since the observations detailed in this thesis.

It is clear from this work that the interaction between Ffh and FtsY is extremely complex. The proteins most likely undergo conformational changes upon binding to each. 4.5S RNA's catalytic role in this process was surprising to us as we had assumed at the outset that the RNA was more likely to increase the affinity between the two proteins. However, this novel catalytic property described in Chapter 3 taken together with the in depth kinetic studies of Chapter 4 suggests that the RNA is probably assisting the proteins to undergo the necessary conformational changes. The results in Chapter 4 would further argue that the conformational changes are directly liked to the GTPase activity of the complex.

One major challenge which now follows is to physically observe these conformational changes with the hope of gaining a better mechanistic understanding for how they directly impact upon the GTPase activity of the complex. While the kinetics would strongly argue for the existence of conformational changes preceding the GTPase step ion the enzymatic cycle, we have unfortunately no direct physical evidence to conclusively demonstrate this.Future efforts will require developing novel probes which might shed insight into the intricate structure of this complex.

While the tryptophan fluorescence assay has open new doors for us, it is problematic in certain respects. Because of filtering from the nucleotides and RNA, the signal is very weak and limits the concentration regimes that can be successfully assayed. Secondly, the probe is specific to FtsY. Therefore, it would be useful to have probes specific to Ffh for several reasons. This strategy would perhaps identify functional effects of the RNA with respect to Ffh's structure. Alternatively, a probe which could respond to FtsY binding could allow one to perform complementary kinetic analyses to the ones presented in Chapters 3 and 4. As FtsY is inherently more soluble than Ffh, such a kinetic analysis would be able to cover a broader concentration range and perhaps be able to convincingly demonstrate any potential first order steps to the formation of the $\mathrm{Ffh}^{\mathrm{GTP}} \bullet \mathrm{FtsY}^{\mathrm{GTP}}$ complex which have thus far eluded our efforts.

The discrepancies which have arisen between our work and that reported for the full-length FtsY may prove interesting from a biological perspective. As the full length FtsY possesses the A-domain which has recently been reported to a target for interactions with lipids which effect the GTPase activity of FtsY, perhaps this domain serve some sort of regulatory function. The simplest model would be to suggest that this domain serves an inhibitory role to the interaction between Ffh/4.5S RNP and FtsY. Lipids and/or other membrane components could counter this inhibitory role. Future work will be needed to shed further light on the functional role of FtsY's A-domain.

Now that we have established a detailed kinetic framework for the Ffh-FtsY GTPase cycle, characterizing mutant forms of these proteins in light of this framework should enable us to identify key amino acid residues which are critical for enzymatic function. It will be particularly interesting to see if mutants can be generated which can no longer perform the GAPing activity. Perhaps this activity can be uncoupled from basal hydrolysis. The assays detailed in this thesis should serve useful in characterizing and identifying such a mutant. This will enable us to get a better understanding of how these two proteins communicate with each other during their enzymatic cycle.

Future work will be required in order to integrate other components into this mechanistic puzzle. The signal sequence is an obvious primary component of interest. The proximity of the RNA's tetraloop to the signal sequence binding pocket and the recent demonstration of a role for the tetraloop in the Ffh-FtsY interaction would suggest potential cross-talk between these various components. With the kinetic framework for the Ffh-FtsY interaction established in this thesis, one can begin to probe for effects of signal sequences on the various steps which comprise the GTPase enzymatic pathway. Perhaps, a novel allosteric role for the signal sequence awaits being uncovered.

Finally, the Ffh/4.5S RNP-ribosome interaction remains an unanswered question. From the elegant genetic work in *E. coli* and *S. Cerevisaie,* it is very likely that this interaction is governed by many factors such as the conformational state of the ribosome or even the Ffh/4.5S RNP for that matter. Our initial strategy in attacking this problem likely suffered from its simplicity. Future work in this direction may require intricate strategies in order to successfully map this interaction. One technical advance, which has arisen since this earlier thesis work, may prove useful in ultimately tackling this problem. The use of tethered Fe-EDTA mediated hydroxy radical cleavage has proven rather useful in much of the most recent ribosomal work. This may prove useful here as well. However, the major challenge will be to identify the interaction and the components required to establish it. Perhaps, locking ribosomes into specific translating states with displayed signal sequences will be required to achieve this. We may then be able to determine whether 4.5S RNA plays functional roles in both of the major interactions of the SRP functional cycle, the interaction with the receptor as well as the one with the ribosome.

UC
San Francisco
LIBRARY
UNIVERSITY OF CALIFORNIA

For reference

Not to be taken from the room.

7063418

3 1378 00706 3418